DISSERTATION

Differential roles of G protein-coupled receptors GPR55 and CB_1 in colorectal cancer

submitted by

CARINA HASENOEHRL, BSC MSC

for the Academic Degree of

Doctor of Philosophy (PhD)

at the

Medical University of Graz

Institute of Experimental and Clinical Pharmacology

under the supervision of

Assoc.-Prof. Dr. Rudolf Schicho

2017

STATUTORY DECLARATION

I hereby declare that this thesis is my own original work and that I have fully acknowledged by name all of those individuals and organizations that have contributed to the research for this thesis. Due acknowledgement has been made in the text to all other material used. Throughout this thesis and in all related publications I followed the “Standards of Good Scientific Practice and Ombuds Committee at the Medical University of Graz”.

Graz, 29 August 2017

DISCLOSURES

Part of this thesis has been published in Hasenoehrl C, Feuersinger D, Sturm EM, Bärnthaler T, Heitzer E, Graf R, Grill M, Pichler M, Beck S, Butcher L, Thomas D, Ferreirós N, Schuligoi R, Schweiger C, Haybaeck J, and Schicho R. *G protein-coupled receptor GPR55 promotes colorectal cancer and has opposing effects to cannabinoid receptor 1.* Int J Cancer **2017**. Accepted August 22, 2017.

The following authors have actively contributed to results reported in this thesis:

David Feuersinger
Institute of Experimental and Clinical Pharmacology, Medical University of Graz

Ricarda Graf
Institute of Human Genetics, Medical University of Graz

Martin Pichler
Department of Internal Medicine, Division of Oncology, Medical University of Graz

Lee Stirling
UCL Cancer Institute, University College London, United Kingdom

Nerea Ferreirós
Institute of Clinical Pharmacology, Goethe University, Frankfurt/Main, Germany

Harald Höger
Div. Laboratory Animal Science and Genetics, Medical University of Vienna

All of the above mentioned have explicitly agreed to the use of their data in this thesis. Permission to reproduce figures published in (1) has been obtained from Wiley.

ACKNOWLEDGEMENTS

First of all, I would like to thank Prof. Rudolf Schicho for welcoming me in his lab and enabling this work. I am very grateful for the amount of freedom I was given while conducting my research, for profiting from his expertise and for his guidance throughout my PhD studies.

Secondly, I would like to thank the head of the Institute of Experimental and Clinical Pharmacology, Prof. Akos Heinemann, for creating such a pleasant working environment where the knowledge is shared among several research groups and collaborations are established easily.

My gratitude goes to all collaborators that contributed to this research project. Foremost, I want to thank the OncoTrack consortium for providing me with DNA methylation and mRNA expression data of colorectal cancer patients. I really appreciate Dr. Lee Stirling's effort in extracting and analyzing the data concerning the methylation status of patient samples. Furthermore, I want to thank Prof. Martin Pichler for performing the survival analysis of colorectal cancer patients using the publicly available data set R2, and Prof. Ellen Heitzer and Ricarda Graf for facilitating the bisulfite sequencing. My appreciation goes to Dominique Thomas and Nerea Ferreirós for performing the mass spectrometry analysis, and to Prof. Höger for performing the xenograft experiments.

Very special thanks go to David Feuersinger for his effort during his master's thesis where he investigated GPR55 signaling in colon cancer cell lines. I also really want to thank Veronika Pommer for her help with various experiments. I am very grateful to Prof. Eva Sturm for helping me with the flow cytometry, and my lab mates Thomas, Magdalena, Sanja, Markus, Lisa, Miriam, Anna, David, Geraldine, Eva, and Athina for inspiring conversations and consolations when necessary.

Furthermore, I would like to thank my thesis committee, Prof. Rufina Schuligoi and Prof. Johannes Haybäck, for their invaluable advice and support during my studies. My appreciation goes to the Austrian Science Fund (grants P25633 and KLIF 521-B31) and the Medical University for funding my research through the PhD Program Molecular Medicine (MolMed).

Last but not least, I would like to thank my family for their infinite support.

TABLE OF CONTENTS

ABBREVIATIONS

1-AG	1-arachidonoylglycerol
2-AG	2-arachidonoylglycerol
5-Aza	5-Aza-2'-deoxycytidine
5'-UTR	5'-untranslated region
ABC	avidin-biotin complex
ABHD6/12	α/β domain-containing hydrolase 6/12
AEA	arachidonoylethanolamide
ANOVA	analysis of variance
AOM	azoxymethane
Apc	adenomatous polyposis coli
APC	allophycocyanin
BSA	bovine serum albumine
BV	brilliant violet
Ca^{2+}	calcium ions
CAC	colitis-associated colorectal cancer
CB_1	cannabinoid receptor 1
CB_2	cannabinoid receptor 2
CBD	cannabidiol
CCL2	CC-chemokine ligand 2
CD	cluster of differentiation
COX-2	cyclooxygenase-2
CRC	colorectal cancer
DAGL	diacylglycerol lipase
DMSO	dimethyl sulfoxide
DSS	dextran sulfate sodium
ECL	enhanced chemiluminescence
EDTA	ethylenediaminetetraacetic acid
EET	epoxyeicosatrienoic acid
ELISA	enzyme-linked immunosorbent assay
ERK1/2	extracellular signal-related kinase 1/2
ESI	electrospray ionization

FAAH	fatty acid amide hydrolase
FBS	fetal bovine serum
FITC	fluorescein isothiocyanate
FSC	forward scatter
GAPDH	glyceraldehyde 3-phosphate dehydrogenase
GPCR	G protein-coupled receptor
GPR55	G protein-coupled receptor 55
HA	hemagglutinin
HBSS	Hank's balanced salt solution
HCl	hydrochloric acid
HEPES	4-(2-hydroxyethyl)-1-piperazineethanesulfonic acid
HETE	hydroxyeicosatetraenoic acid
hg19	human genome 19
HPETE	hydroperoxyeicosatetraenoic acid
HPLC	high-performance liquid chromatography
Hprt	hypoxanthine-guanine phosphoribosyltransferase
IBD	inflammatory bowel disease
IL	interleukin
i.p.	intraperitoneal
LC-MS/MS	liquid chromatography-mass spectrometry
LPI	L-α-lysophosphatidylinositol
MCP-1	monocyte chemoattractant protein-1
MDSC	myeloid-derived suppressor cell
MGL	monoglyceride lipase
NAAA	N-acyl ethanolamine amino hydrolase
NAGly	N-arachidonoylglycine
NAla	N-arachidonoylalanine
NAPE	N-arachidonoyl phosphatidyl ethanol
NAPE-PLD	N-arachidonoyl phosphatidyl ethanol-preferring phospholipase D
NFAT	nuclear factor of activated T cells
NF-κB	nuclear factor κ-light chain enhancer of activated B cells
n.s.	not significant
OEA	oleoylethanolamide
PBS	phosphate buffered saline

PCR	polymerase chain reaction
PE	phycoerythrin
PEA	palmitoylethanolamide
pERK1/2	phosphorylated extracellular signal-related kinase 1/2
PG	prostaglandin
PGD_2	prostaglandin D_2
PGE_2	prostaglandin E_2
$PGF_{2\alpha}$	prostaglandin $F_{2\alpha}$
PGH_2	prostaglandin H_2
PI3K	phosphoinositide 3-kinase
PPAR	peroxisome proliferator-activated receptor
P/S	penicillin / streptomycin
pSTAT3	phosphorylated signal transducer and activator of transcription 3
qRT-PCR	quantitative real time polymerase chain reaction
RIPA	radioimmunoprecipitation assay
RP	reversed phase
RPKM	reads per kilobase per million mapped reads
SCID	severe combined immunodeficiency
SD	standard deviation
SDS	sodium dodecyl sulfate
SEM	standard error of the mean
SSC	side scatter
STAT3	signal transducer and activator of transcription 3
TBST	Tris-buffered saline / Tween 20
TGF-β	transforming growth factor-β
THC	Δ^9-tetrahydrocannabinol
TRPV1	transient receptor potential vanilloid type-1
TSS	transcription start site
TXA_2	thromboxane A_2
TXB_2	thromboxane B_2
UICC	union international contre le cancer
WT	wild-type

LIST OF FIGURES

ABSTRACT

Colorectal cancer (CRC) is a common malignancy in the Western world that is not only linked to lifestyle factors such as diet, smoking, and alcohol consumption but also to inflammatory bowel disease. Although tremendous advances have been made in detection and treatment of the disease, it is still the third most leading cause of cancer death in the United States. In recent years, the endocannabinoid system has become of interest in cancer research since several of its constituents have been observed to be differentially expressed under many pathophysiological conditions including cancer. While the cannabinoid receptor 1 (CB_1) has been reported to suppress intestinal tumor growth, the role of lysophospholipid and atypical cannabinoid receptor GPR55 in the development of gastrointestinal cancers is not yet elucidated.

GPR55 is involved in many physiological and pathological processes of the gastrointestinal tract and has been shown to play a tumor-promoting role in various cancers. It has recently been reported to exert a pro-inflammatory role in gastrointestinal inflammation via mechanisms involving leukocyte infiltration. This thesis aims at elucidating the hitherto unknown functions of GPR55 in the development and progression of colorectal cancer. Additionally, the involvement of CB_1 in colorectal carcinogenesis has been investigated.

Using azoxymethane and dextran sulfate sodium-driven CRC mouse models, GPR55 was found to play a tumor-promoting role that is likely based on alterations of leukocyte populations, i.e. myeloid-derived suppressor cells and T lymphocytes, within the tumor microenvironment. Concomitantly, the expression levels of tumor promoting factors cyclooxygenase-2 and signal transducer and activator of transcription 3 were reduced in tumor tissue of GPR55 knockout ($GPR55^{-/-}$) mice, indicating reduced presence of tumor-promoting factors in the microenvironment. By employing the experimental CRC models to CB_1 knockout ($CB_1^{-/-}$) and CB_1/GPR55 double knockout ($CB_1^{-/-}GPR55^{-/-}$) mice, it was further observed that GPR55 plays an opposing role to CB_1. Furthermore, GPR55 and CB_1 mRNA expression were differentially regulated in the experimental models and in a cohort of 86 CRC patients. Epigenetic methylation of *CNR1* (the gene coding for CB_1) and

GPR55 was also differentially regulated in human CRC tissue compared to control samples.

Collectively, the data presented in this thesis suggest that GPR55 and CB_1 play opposing roles in colorectal carcinogenesis where the former seems to act as oncogene and the latter as tumor suppressor. These findings are of importance when developing strategies to target the endocannabinoid system for the therapy of CRC.

ZUSAMMENFASSUNG

Kolorektale Karzinome sind Tumorerkrankungen, die besonders in der westlichen Welt häufig auftreten. Als Risikofaktoren für kolorektale Karzinome gelten entzündliche Erkrankungen des Darms und Lebensstile, die den übermäßigen Konsum von rotem Fleisch, Tabak und Alkohol beinhalten. Obwohl bereits große Fortschritte bei der Erkennung und Behandlung von kolorektalen Karzinomen erzielt wurden, stellt die Erkrankung in den USA den dritthäufigsten Grund für krebsbedingtes Ableben dar. In den letzten Jahren ist das Forschungsinteresse am Endocannabinoidsystem in der Krebsforschung erwacht, da einige Komponenten dieses Systems unter pathologischen Bedingungen anders exprimiert werden als unter physiologischen. Der Cannabinoid Rezeptor 1 (CB_1) scheint ein Tumorsuppressor zu sein, wohingegen die Funktion des atypischen Cannabinoid Rezeptors GPR55 in gastrointestinalen Tumorerkrankungen noch relativ unerforscht ist.

GPR55 spielt in vielen physiologischen und pathologischen Prozessen des Gastrointestinaltrakts eine Rolle und wirkt in einigen Krebsarten wachstumsfördernd. Außerdem fördert der Rezeptor die entzündungsbedingte Einwanderung von Leukozyten in das Kolon. Das Ziel dieser Dissertation war es daher, bisher unbekannte Funktionen von GPR55 in der Entstehung und Fortschreitung des Kolonkarzinoms aufzuklären. Zusätzlich sollte untersucht werden, welche Funktion CB_1 in kolorektaler Karzinogenese ausübt.

Mittels chemisch induzierter Krebsmodelle in Mäusen wird in dieser Arbeit gezeigt, dass GPR55 eine tumorfördernde Rolle spielt, die wahrscheinlich darauf basiert, dass bestimmte Leukozyten – insbesondere myeloide Suppressorzellen und T-Zellen – in die Tumoren rekrutiert werden. Außerdem wurde herausgefunden, dass die tumorfördernden Moleküle Cyclooxygenase-2 und STAT3 im Tumorgewebe von GPR55 knockout ($GPR55^{-/-}$) Mäusen in geringerem Ausmaß vorhanden waren. GPR55 dürfte daher die Zusammensetzung des Tumorgewebes dahingehend beeinflussen, dass mehr tumorfördernde Faktoren vorhanden sind. Die Anwendung der chemisch induzierten Krebsmodelle auf CB_1 knockout ($CB_1^{-/-}$) und Doppelknockout ($CB_1^{-/-}GPR55^{-/-}$) Mäuse hat weiters ergeben, dass GPR55 eine

entgegengesetzte Rolle zu CB_1 spielt. Expressionsanalysen der beiden Rezeptoren haben gezeigt, dass ihre mRNA Levels sowohl in Mausgeweben als auch in Biopsien von Patienten unterschiedlich reguliert werden. Die epigenetische Methylierung von *CNR1* (dem Gen, das für CB_1 kodiert) und *GPR55* in den Patientenproben war auch jeweils unterschiedlich reguliert.

Insgesamt weisen die hier präsentierten Daten darauf hin, dass GPR55 und CB_1 in der kolorektalen Karzinogenese entgegengesetzte Funktionen ausüben, wobei ersterer Rezeptor als Onkogen und letzterer als Tumorsuppressor agiert. Diese Erkenntnis ist von großer Bedeutung, falls das Endocannabinoidsystem in der Zukunft als therapeutischer Angriffspunkt zur Behandlung des kolorektalen Karzinoms genützt wird.

1. INTRODUCTION

1.1 Discovery of the endocannabinoid system

Preparations of the marijuana plant *Cannabis sativa* have been used for both recreational and medicinal purposes for thousands of years, although the constituents and their mode of action remained largely unknown. Discovery of the main psychoactive component of *Cannabis*, i.e. Δ^9-tetrahydrocannabinol (THC) in the 1960s (2), and the discovery, cloning, expression and imaging of the first cannabinoid receptor in 1990 (3), however, boosted research in this field. In 1992, the first endogenous cannabinoid, i.e. arachidonoylethanolamide (AEA, named "anandamide"), was identified. The identification of another cannabinoid receptor, i.e. CB_2 (4), as well as the discovery of the endocannabinoid 2-arachidonoylglycerol (2-AG) followed shortly (5).

1.2 Components of the endocannabinoid system

1.2.1 Classical components of the endocannabinoid system

In the classical sense, the endocannabinoid system is now described as consisting of the two cannabinoid receptors CB_1 and CB_2, endogenous lipid ligands (called endocannabinoids), and synthesizing and degrading enzymes of the endocannabinoids.

The cannabinoid receptors CB_1 and CB_2 are G protein-coupled receptors (GPCRs) that show 68% amino acid homology in the transmembrane domains and 44% overall homology (4). Upon activation, both receptors primarily couple to G proteins of the G_i and G_o classes, which cause inhibition of adenylyl cyclases and activation of several mitogen-activated protein kinases (6). Cannabinoid receptor activation modulates diverse aspects of cell physiology, including synaptic function, gene transcription, and cell motility (6). CB_1 is mainly expressed in the central nervous system, but it has also been shown to be expressed in several peripheral tissues, e.g. spleen, adipose tissue and the gastrointestinal tract, albeit at much lower

densities than in the brain (7). CB_2 expression is largely restricted to immune and hematopoietic cells, and it has been found to be present under certain pathophysiological conditions in various organs (7,8).

Endocannabinoids are synthesized from precursor molecules that are present in lipid membranes. This process is typically induced by the activation of certain G protein-coupled receptors or by depolarization (9). Endocannabinoids are, thus, produced on demand and released into the extracellular space upon which they bind to the respective receptors (7,9–11). Inactivation of endocannabinoids is achieved by enzymatic degradation after cellular reuptake via (a yet to be identified) endocannabinoid membrane transporter or passive diffusion (7,12). Degradation typically occurs rapidly, resulting in the fact that endocannabinoids are short-lived bioactive lipid mediators (12–14).

The two most extensively studied endocannabinoids, AEA and 2-AG, both contain arachidonic acid but their routes of synthesis and degradation *in vivo* are mediated by different enzymes. AEA can be synthesized via different pathways but most of it appears to be produced from N-arachidonoyl phosphatidyl ethanol (NAPE). Hydrolysis of NAPE by N-arachidonoyl phosphatidyl ethanol-preferring phospholipase D (NAPE-PLD) yields AEA and phosphatidic acid (9). Degradation of AEA is primarily performed by fatty acid amide hydrolase (FAAH) but N-acyl ethanolamine amino hydrolase (NAAA) has also been described to be expressed in several tissues (9,15). 2-AG is produced from 2-arachidonoyl-containing phospholipids with inositol head groups by diacylglycerol lipase (DAGL). Degradation of 2-AG is achieved by the actions of monoglyceride lipase (MGL), or α/β domain-containing hydrolase 6 (ABHD6) or 12 (ABHD12) (9,12). Additionally, endocannabinoids can be further metabolized by enzymes that have very little to do with endocannabinoid targets. Cyclooxygenase-2 (COX-2), for instance, can oxidize AEA and 2-AG, giving rise to prostamides and prostaglandin glycerol esters that can act as prostaglandin precursors (9,12). Arachidonic acid arising from the degradation of AEA and 2-AG also serves as precursor for eicosanoid production, making it an important link between endocannabinoid and eicosanoid signaling. There are three major pathways through which arachidonic acid can be metabolized to eicosanoids: the cyclooxygenase, the lipoxygenase, and the cytochrome P450

monooxygenase pathways (16). In the cyclooxygenase pathway, arachidonic acid is metabolized to prostaglandin (PG) H_2 (PGH_2), which is sequentially metabolized to prostanoids, including PGE_2, PGD_2, $PGF_{2\alpha}$, and thromboxane A_2 (TXA_2). Lipoxygenases convert arachidonic acid into leukotrienes and hydroxyeicosatetraenoic acids (HETEs) while P450 metabolizes arachidonic acid into epoxyeicosatrienoic acids (EETs), HETEs, and hydroperoxyeicosatetraenoic acids (HPETEs) (16,17).

Next to AEA and 2-AG, other endocannabinoids having little known functions have been described, e.g. virodhamine (O-arachidonoyl ethanolamide), noladin ether (2-arachidonoyl glyceryl ether), and N-arachidonoyl-dopamine (10,18).

1.2.2 The expanded endocannabinoid system

Endocannabinoids, however, do not just bind to the classical cannabinoid receptors CB_1 and CB_2. In fact, several non-cannabinoid receptors have been found to be responsive to endocannabinoids and/or plant-derived cannabinoids. The transient receptor potential vanilloid type-1 (TRPV1), for instance, has been shown to be responsive to AEA, but not to 2-AG (19). TRPV1 is a non-selective cation channel that is activated by heat (>42°C), low pH (<6.0), and capsaicin, the pungent constituent of hot chili peppers (19). The stimulatory effects of AEA on TRPV1 and the subsequent desensitization of the receptor are now believed to represent one of the most important mechanisms by which AEA exerts its biological functions (19,20). Peroxisome proliferator-activated receptors (PPARs) have also been shown to mediate some of the gastrointestinal, anti-inflammatory, and anti-tumor effects of certain cannabinoids (21). Importantly, cannabidiol (CBD), a non-psychoactive constituent of *Cannabis* with low affinity for CB_1 and CB_2, has been shown to have potent anti-inflammatory effects in intestinal inflammation that are exerted via PPAR activation (22,23).

Besides ligand-sensitive ion channels (i.e. TRPV1) and nuclear receptors (i.e. PPARs), GPCRs other than CB_1 and CB_2 have also been found to be responsive to certain cannabinoids. G protein-coupled receptor 55 (GPR55), for instance, has

recently been proposed as a new cannabinoid receptor after it was found to be responsive to a variety of natural and synthetic cannabinoids, including AEA, virodhamine, and THC (24–27). GPR55, however, has no significant sequence similarity with CB_1 or CB_2 (28) and is rather related (with ~30% similarity) to the purinergic receptor P2Y5, as well as to GPR23 and GPR92, which have been shown to be lysophosphatidic acid receptors (29–31). GPR55 does not possess the typical "cannabinoid binding pocket" but rather exhibits a deep vertical binding pocket for long, thin inverted L- or T-shaped ligands (32) and, accordingly, its endogenous ligand was found to be a lysophospholipid, namely L-α-lysophosphatidylinositol (LPI) (33). In particular, it is believed that LPI carrying an arachidonic acid moiety is the most potent endogenous agonist of GPR55 (34–36).

GPR55 is highly expressed in the central nervous system, and at moderate levels in adrenal glands and spleen, as well as on immune cells, endothelial cells and in the intestine (26,37–41). Contrary to CB_1 and CB_2, GPR55 signals through $G_{\alpha 12/13}$ and G_q, thereby initiating excitatory rather than inhibitory effects, such as activation of phospholipase C and RhoA, phosphorylation of extracellular signal-related kinase 1/2 (ERK1/2), Ca^{2+} release from intracellular stores, and activation of transcription factors such as nuclear factor of activated T cells (NFAT) and nuclear factor κ-light chain enhancer of activated B cells (NF-κB) (24,25,35). Recently, it has been shown that plant-derived cannabinoids like Δ^9-tetrahydrocannabivarin, cannabidivarin, and cannabigerovarin non-competitively inhibited the effects of LPI on GPR55 (42). Since those cannabinoids acted as GPR55 agonists when applied alone, it was suggested that GPR55 possesses an orthosteric and an allosteric ligand binding site (42).

GPR55 is also able to form heteromers with other GPCRs, which affects down-stream signaling pathways. When CB_1 and GPR55 were co-expressed in HEK293 cells, GPR55 signaling was inhibited in the presence of CB_1, but was restored upon co-stimulation of both receptors with specific agonists since CB_1 was internalized after activation. CB_1 signaling in turn was enhanced in the presence of GPR55 (43). CB_1-GPR55 receptor heteromers were observed when both GPCRs were co-expressed in HEK293 cells, but receptor internalization was not affected by heteromerization (43). CB_1-GPR55 heteromers have also been observed in rat and

monkey striatum (44). Furthermore, GPR55 has been reported to form heteromers with CB_2 in human glioblastoma cells that endogenously express both receptors, and in human neutrophils (45,46). Overall, GPR55 signaling appears to be rather complex and modulated by several other factors including allostery, receptor heteromerization, as well as interactions with membrane lipids (47). Since GPR55 is sensitive to certain cannabinoids, but its endogenous ligand is a non-cannabinoid lipid, the discussion on whether GPR55 should be named the 'third cannabinoid receptor' is still ongoing (48,49).

Recently, several putative GPR55 antagonists have been tested for their selectivity towards GPR55 (39,50). The compound CID16020046 was reported to selectively antagonize GPR55 and had no effect on CB_1 signaling. LPI-induced ERK1/2-phosphorylation was selectively inhibited by CID16020046 while CB_1/CB_2-mediated ERK1/2-phosphorylation was unaffected. In addition, pretreatment with CID16020046 prevented GPR55 internalization and the mechanism was suggested to be non-competitive antagonism (39).

Chemically, AEA belongs to the family of N-acylethanolamides, i.e. it is the amide of arachidonic acid (20:4 ω-6) and ethanolamine. Structural relatives of AEA, such as palmitoylethanolamide (PEA, 16:0) and oleoylethanolamide (OEA, 18:1) do not contain highly unsaturated fatty acids, and do not show high affinities for cannabinoid receptors (51). They are, however, able to interfere with classical endocannabinoids since they share several synthesizing and degrading enzymes (51). Other so-called endocannabinoid-like compounds include N-arachidonoylglycine (NAGly), N-arachidonoylalanine (NAla), and N-arachidonoylserine (52). Even though endocannabinoid-like compounds generally do not activate CB_1 or CB_2, they can activate other cannabinoid-responsive receptors, e.g. GPR55 or TRPV1, that mediate their effects in physiological and pathological conditions (12,53). Additionally, endocannabinoid-like compounds can also potentiate the actions of endocannabinoids, a property known as the 'entourage' effect (54,55). The isomer of 2-AG that has the arachidonic acid moiety in the *sn*1-position, i.e. 1-arachidonoylglycerol (1-AG), is thermodynamically more stable than the 2-AG isomer and found to be present in several tissues (56). In fact, it has been reported that 1-AG may act either as a weak competitive antagonist of

2-AG, but its effect can also be additive to that of 2-AG, depending on the ratio in which the two isomers are present (56).

Together, the classical cannabinoid receptors, endocannabinoids, metabolic enzymes, and 'atypical cannabinoid receptors' as well as endocannabinoid-like compounds make up a complex system best described as the 'endocannabinoidome' (12).

1.3 General actions of the endocannabinoid system

1.3.1 Physiologic roles of the endocannabinoid system

Initially, the endocannabinoid system was found to play a role in the inhibition of neurotransmitter release in the brain. CB_1 expression in the brain is up to 50-fold higher than expression levels of other GPCRs, such as dopamine and opioid receptors, making it the most abundant GPCR in the brain (11). Endogenous CB_1 agonists have been shown to serve as retrograde synaptic messengers in the central nervous system (9). Suppression of synaptic transmission is achieved by the production of AEA and 2-AG in postsynaptic neurons upon certain stimuli. The endocannabinoids are then released into the synaptic cleft and activate CB_1 receptors located at the presynaptic terminal. Activation of CB_1 consequently leads to the suppression of glutamate release (9,57).

Research of the last 25 years has now established a key role of the endocannabinoid system in several physiological and pathological mechanisms, in both central and peripheral tissues. Of note for the present study is its function in modulating the immune system, and more importantly, its role in the gastrointestinal tract. Involvement of the endocannabinoid system in cardiovascular, respiratory, and reproductive functions, as well as in bone formation and energy metabolism has also been proposed (18).

1.3.2 Endocannabinoids and the immune system

Endocannabinoids modulate immune functions in an autocrine and paracrine fashion, mostly through the activation of CB_2 expressed on cells of the adaptive immune system. Activation of CB_2 initiates a cascade of signal transduction events that converge at the transcriptional level to inhibit the migratory activity of diverse immune cell types. Additionally, endocannabinoids have been reported to modulate the release of cytokines and chemokines from immune cells. In human monocytes, for instance, AEA diminished the production of interleukin (IL)-6 and IL-8. In activated human peripheral T lymphocytes, AEA suppressed the release of IL-2, tumor necrosis factor α, and interferon γ. Endocannabinoid mediated effects that occurred independent of CB_1/CB_2 activation have also been observed (15,58).

1.3.3 The role of the endocannabinoid system in the intestine

In the gastrointestinal tract, CB_1 receptors can be found in the enteric nervous system (59) and the epithelial lining (60). Furthermore, CB_1 was also reported to be expressed by plasma cells, and in smooth muscle cells of blood vessels within the colonic wall (61). CB_2 receptors are mainly expressed by immune cells, myenteric plexus neurons, and under pathophysiological conditions (60,61) while GPR55 expression was localized to epithelial cells and the enteric nervous system (41).

Under physiological conditions, the endocannabinoid system is believed to control various aspects of gut homeostasis, such as gastrointestinal motility, gastric and intestinal secretion, and mucosal integrity (14,15,62). An involvement of the endocannabinoid system in the regulation of food intake, satiety, nausea and emesis, as well as immune function, visceral pain, intestinal inflammation, and cell proliferation has also been implicated (63–66).

Under pathophysiological conditions, e.g. in intestinal inflammation, a dysregulation of several constituents of the endocannabinoid system has been observed. Inflammatory bowel disease (IBD) is a chronic relapsing-remitting disorder that occurs in two major forms, ulcerative colitis and Crohn’s disease. The etiology of IBD is not yet known, but it is thought to originate from a disturbed interaction of the

gut microbiota (or their products) with the epithelial barrier causing misdirected attacks of the immune system at gut components (67,68). Preclinical evidence suggests that the endocannabinoid system could be a valuable therapeutic target for treating IBD. Using mouse models of chemically induced mucosal inflammation it was observed that endocannabinoid signaling was strongly enhanced under inflammatory conditions (22). In particular, CB_1, CB_2, and AEA expression were up-regulated (69,70) and the AEA-degrading enzyme FAAH was found to be expressed to a lesser extent in the initial stage of experimental colitis (71). Pharmacological strategies to further enhance endocannabinoid levels by means of inhibiting their metabolizing enzymes ameliorated the inflammation (72,73). Accordingly, it was also found that activation of CB_1 and CB_2 with synthetic agonists or THC protected rodents from intestinal inflammation (70,74,75). These findings prompted the investigation of other non-psychoactive constituents of *Cannabis* and it was observed that CBD, cannabigerol, and cannabichromene also showed beneficial effects in colitis models (75–82). Atypical cannabinoid receptor GPR55 was found to play a pro-inflammatory role in murine colitis since genetic ablation, and treatment with the antagonists CID16020046 or ML-191 alleviated intestinal inflammation (83,84). Expression levels of endocannabinoid-like compounds PEA and OEA were increased under inflammatory conditions, and reported to exert beneficial effects (85,86). Taken together, preclinical data suggest that the enhanced endocannabinoid signaling observed under inflammatory conditions of the gastrointestinal tract is a response to disturbances of the homeostatic system and is aimed at restoring its balance (22,87,88).

1.4 Inflammation and colorectal cancer (CRC)

Chronic inflammatory conditions of the gut have been identified as a risk factor for the development of CRC (89). About 20% of IBD patients develop colitis-associated colorectal cancer (CAC) within 30 years of disease onset (90). During persisting colonic inflammation recruited immune cells produce reactive oxygen and nitrogen species that can cause DNA damage and alter cell proliferation and survival, which then promotes carcinogenesis (91). Immune cells that infiltrate preneoplastic lesions

and/or tumors produce cytokines and chemokines that, in addition to causing a localized inflammatory response, can enhance the growth and survival of premalignant cells, e.g. through NF-κB signaling (92).

CRC can be traced back to a familial basis such as adenomatous polyposis in some cases, but the majority of incidences are sporadic and likely caused by environmental components (93,94). CRC is the third most common cancer in the world, and despite benefits from early screening, it remains the third most leading cause of cancer death in the United States (95). Although CAC and CRC development are seemingly of different origin, they exhibit common genetic and signaling pathways that are altered, such as those involving Wnt, β-catenin, K-ras, p53, transforming growth factor (TGF)-β, and the DNA mismatch repair proteins (89). CAC and CRC also have the main and essential stages of cancer development in common. The progression in both malignancies usually follows the transformation of epithelial cells into aberrant crypt foci, which then progress to early and advanced adenomas and finally to adenocarcinomas (94). Interestingly, even colorectal tumors that are not associated with IBD show robust signs of inflammation, i.e. infiltration of immunocytes and expression of pro-inflammatory cytokines (89). The involvement of leukocytes, inflammatory mediators and their receptors within the tumor microenvironment is currently being uncovered and recent studies indicate that immunotherapy might become a valuable treatment option in addition to traditional chemotherapy (96).

Importantly, molecules known for their role in inflammation, such as COX-2-derived mediators and the transcription factor signal transducer and activator of transcription 3 (STAT3), are now regarded as driving factors in colorectal carcinogenesis (89). COX-2 is overexpressed in a majority of CRCs and the role of pro-inflammatory prostaglandins has been studied extensively (97). Thus, molecules involved in gastrointestinal homeostasis appear to also play a critical role in the development of gastrointestinal cancers. In this context, studying the endocannabinoid system is of great interest as it plays a prominent role in physiological and pathophysiological processes of the gastrointestinal tract.

1.5 The endocannabinoid system in CRC

Few studies have investigated the endocannabinoid system in patients with CRC so far. Ligresti *et al.* were the first to report that AEA and 2-AG levels were increased (threefold and twofold, respectively) in CRC lesions as compared to normal colonic mucosa (98). A more recent study then reported overall increased endocannabinoid metabolism in CRC (99). Here, AEA and the synthesizing enzyme NAPE-PLD were upregulated twofold, and mRNA and activity levels of the degrading enzyme FAAH were increased. Probably as a consequence of increased FAAH activity, elevated levels of arachidonic acid were also detected (99). Another study reported the 2-AG degrading enzyme MGL to also be increased in CRC specimens (100).

Examination of CB_1 expression revealed a down-regulation of mRNA and protein levels in colon cancer samples as compared to adjacent non-neoplastic colon mucosa (101,102). The reason for the down-regulation was found to be DNA hypermethylation of CpG islands in the promoter region of *CNR1* (the gene coding for CB_1) (101). A comprehensive study describing the correlation between receptor immunoreactivity and patient outcome, however, found no differences in overall survival between patients with high or low CB_1 expressing carcinomas (103). Yet another study reported that high CB_1 immunoreactivity even correlated with poorer disease-free survival in stage II microsatellite stable CRC patients (104). Reduced overall survival has also been reported for patients who were either homo- or heterozygous for a single nucleotide exchange polymorphism in the *CNR1* gene, i.e. 1359 G/A, although it is not yet resolved how this polymorphism affects CB_1 signaling (105). Interestingly, CB_2 mRNA expression was only observed in 28.6% of CRC samples – where it was strongly expressed by epithelial cells – but correlated significantly with tumor growth and lymph node involvement (106). Overall, studies on human biopsies indicate increased endocannabinoid activity while the role of cannabinoid receptors remains less clear.

Animal models used for studying colorectal carcinogenesis generally include chemically induced models of CRC or mice with a germline mutation of the adenomatous polyposis coli (*Apc*) gene. $Apc^{Min/+}$ mice spontaneously develop multiple polyps in the intestine and additional knockout of *Cnr1* or inhibition of CB_1

with a specific antagonist strongly increased tumor burden (101). Genetic deletion of *Cnr2* in this strain of mice, however, did not affect polyp growth (101). Chemically, CRC can be induced by multiple applications of the carcinogen azoxymethane (AOM), which was reported to increase AEA and 2-AG levels in precancerous lesions of the colon (107). Inhibition of FAAH with N-arachidonoyl-serotonin reduced the development of precancerous lesions in this model, and the non-selective CB_1/CB_2 agonist HU210 was able to mimic the effect (107). Similar effects were also observed with non-psychotropic cannabinoids. Application of e.g. CBD or cannabigerol reduced aberrant crypt foci formation, polyps, and tumors in the colon (108–110). In yet another model in which colitis-associated colorectal cancer (CAC) was induced by application of AOM and dextran sulfate sodium (DSS), the atypical cannabinoid O-1602 showed anti-tumorigenic properties (111). Here, treatment with O-1602 reduced the number and area of tumors by 30% and 50%, respectively, and activation of the oncogenic transcription factor STAT3 was reduced (111). Perhaps surprisingly, one study found that antagonism of CB_1 with SR141716 (rimonabant; a drug approved for the treatment of metabolic syndrome, but later withdrawn from the market due to psychotropic side-effects) also reduced aberrant crypt foci formation in AOM-treated mice (112).

Potential applications of cannabinoids or related substances have also been studied in xenograft models. The hexahydrocannabinol analogue LYR-8 reduced tumor growth in xenografts derived from HT-29 cells (113), while CB13 (a CB_2 agonist) inhibited the growth of DLD-1 derived tumors (102). Cannabigerol was reported to even halt the growth of HCT116 xenografts (110).

The anti-carcinogenic effects of cannabinoids are believed to be mediated by a reduction of cancer cell proliferation and induction of apoptosis, as well as inhibition of angiogenesis and metastasis (114,115). The molecular mechanisms underlying the induction of apoptosis upon CB_1/CB_2 receptor activation include *de novo* synthesis of the pro-apoptotic sphingolipid ceramide (102), and the down-regulation of the apoptosis inhibitor survivin (101). Furthermore, the inhibition of PI3K/Akt signaling (116), and the induction of endoplasmic reticulum stress leading to autophagy-mediated cell death have been reported (117). Notably, even cannabinoids with low or no affinity to CB_1 or CB_2, e.g. CBD or O-1602, exert anti-

proliferative effects, although the underlying mechanism is not well understood yet (108,109,111). LYR-8, for instance, decreased angiogenesis in a chick chorioallantoic membrane xenograft model and, concomitantly, modulated factors involved in shaping the tumor microenvironment, such as vascular endothelial growth factor, COX-2, and hypoxia-inducible factor 1α (113). Inhibition of MGL attenuated the invasion of colon cancer cells (100) suggesting an involvement of the endocannabinoid system in CRC progression. Taken together, the literature to date suggests that components of the endocannabinoid system are differentially expressed under neoplastic conditions. Promising preclinical data concerning the effects of cannabinoids on tumor growth warrant further exploration on the cause of the dysregulation of the endocannabinoid system in colorectal carcinogenesis. Investigating known and hitherto unknown constituents of the endocannabinoid system in more detail to better understand the complexity of cannabinoid receptor signaling should thus be of prime interest.

1.6 Atypical cannabinoid receptor GPR55 in cancer

GPR55 is structurally related to other cancer-relevant GPCRs, such as GPR35, GPR92, and GPR23 (118) and signals through α-subunits that are known to contribute to proliferation, migration and invasion (119). A role for GPR55 in carcinogenesis has, therefore, been postulated. To date, the role of GPR55 has been investigated in several different cancers, but its role in colorectal cancer has not been elucidated so far.

GPR55 expression levels were found to be up-regulated in human squamous cell carcinomas, breast and pancreatic cancer, and in glioblastomas, positively correlating with aggressiveness (120,121). *In vivo*, GPR55 promoted carcinogenesis in a mouse model of skin cancer (120). Here, $GPR55^{-/-}$ mice were more resistant to papilloma and carcinoma formation than wild-type littermates (120). Xenografts derived from glioblastoma or skin carcinoma cells exhibited significantly reduced growth when GPR55 was knocked down (120,121).

The main signaling pathway through which GPR55 exerts its proliferative effects in cancer cells was identified to be ERK1/2-phosphorylation (121). Since LPI was found to be the endogenous agonist of GPR55 (33) and since GPR55 had been reported to be expressed in various cancer types in an aggressiveness-related manner (122), a role for the LPI/GPR55 axis in cancer was recently postulated (123). GPR55 expression has been demonstrated in several types of cancer cell lines, such as breast, prostate, ovarian, glioblastoma, and colon cancer cells (121,124,125). Overexpression of GPR55 enhanced, whereas silencing reduced the proliferation of breast cancer, glioblastoma, and skin carcinoma cells (120,121). Furthermore, LPI is believed to act in an autocrine manner, since it was reported that in prostate cancer cells, LPI is synthesized by cytosolic phospholipase A_2 and pumped out of the cell by an ATP-binding cassette transporter (124). Ovarian cancer cells have also been observed to produce and secrete LPI (126). Correspondingly, increased levels of LPI were found in blood and ascites fluids of patients with ovarian cancer (127). Increased levels of serum LPI were also observed in colon cancer patients (125).

Recently, a role for cancer cell-derived LPI in angiogenesis has been suggested (126). In a chick chorioallantoic membrane assay, LPI stimulated the proliferation, network formation, and migration of human endothelial colony-forming cells(126). This effect was abolished after treatment with the GPR55 antagonist CID16020046 (126), indicating that the LPI/GPR55 axis plays a role in shaping the tumor microenvironment.

Other tumor-promoting functions identified for the LPI/GPR55 axis include migration, invasion, and metastasis. Highly metastatic breast cancer cells MDA-MD-231, for instance, exhibited robust migration towards LPI, whereas MCF-7 cells (which express low GPR55 levels) did not migrate (128). Overexpression of GPR55 in MCF-7 cells, however, caused a strong migratory and invasive response to serum factors, which was further enhanced by LPI (128). In an *in vivo* model of metastasis, MDA-MB-231 cells formed significantly more metastases when cells were pretreated with LPI while ablation of GPR55 expression in these cells strongly inhibited metastasis formation (129). GPR55-driven pro-metastatic signaling was

identified to be achieved via coupling to $G_{q/11}$ and subsequent phosphorylation of ERK1/2 (129).

Thus, a tumor-promoting role is proposed for GPR55 via multiple mechanisms in a variety of cancers. For cholangiocarcinoma, however, it was found that activation of GPR55 with AEA or O-1602 inhibited cancer cell growth both *in vitro* and *in vivo* (130,131). AEA and O-1602 have been reported to exert off-target effects on several receptors of the expanded endocannabinoid system but since the effect on cholangiocarcinoma cells was abolished after GPR55 knockdown, the authors concluded that the observed effect was mediated by GPR55 (130).

1.7 The role of GPR55 in CRC

Previous work of Dr. Schicho's group had revealed that GPR55 promoted the migration and adhesion of the colon cancer cell line HCT116 (125) suggesting that GPR55 might also play a role in colorectal cancer. In this study, HCT116 migration towards serum complemented with LPI, and adhesion to endothelial cells was reduced after pretreatment with GPR55 antagonist CID16020046. Interestingly, LPI did not enhance the migration of native HCT116 cells towards serum. LPI did, however, enhance the migration of GPR55-overexpressing HCT116 cells, and this effect was abolished after pretreatment with CID16020046. In a mouse model of metastasis where HCT116 cells arrest in the liver after intrasplenic inoculation, *in vivo* treatment with CID16020046 led to a significantly reduced number of arrested cells (125).

1.8 Aim of the thesis

The aim of this thesis was to elucidate the role of atypical cannabinoid receptor GPR55 in colorectal carcinogenesis. Because of the receptor's potentially pro-carcinogenic behavior and its actions within the endocannabinoid system contrary to those of CB_1, the goal was to explore the systemical actions of GPR55 in a model

of AOM and DSS-induced CRC using GPR55 knockout ($GPR55^{-/-}$) mice and wild-type littermates. The main question to be addressed was whether GPR55 promotes tumor growth. Additionally, I aimed to further investigate the role of CB_1 in colon cancer tumorigenesis and to elucidate the regulation and function of these two receptors with common ligands. The acquired knowledge should improve our understanding of mechanisms exerted by the expanded endocannabinoid system during pathophysiologic conditions in the colon.

2. MATERIALS AND METHODS

Since parts of this thesis have previously been published as an original research article in the International Journal of Cancer (1), the Materials and Methods section has been partially adapted from there and similarities with regards to content and wording are to be expected.

2.1 Patient data

2.1.1 Survival analysis

A publicly available data set of 557 CRC patients (R2: microarray analysis and visualization platform, http://r2.amc.nl) was used to analyze the influence of GPR55 expression on CRC patient clinical outcome. Relapse-free survival, i.e. the time from surgery to the first recurrence, was the endpoint. Analysis was done according to the Kaplan-Meier method, and differences between survival distributions were assessed with the log-rank test. This survival analysis has also been reported in an original research article (1).

2.1.2 DNA methylation status and mRNA levels

As part of the OncoTrack project (http://www.oncotrack.eu), biopsies were collected from CRC patients. The cohort used for analysis in this study was the same as described in detail previously (132). The methylation status of *CNR1* and *GPR55* in CRC samples and adjacent healthy mucosa was assessed using the Illumina 450K Infinium Human Methylation BeadChip. mRNA expression of CB_1 and GPR55 was assessed according to standardized procedures. Normalization was done using the RPKM method (133). Written informed consent was obtained from all patients and ethical approval was granted by the ethics committee of the Medical University of Graz (23-015 ex 10/11). The collection of these data has previously been described (1).

2.2 Mouse models

2.2.1 Breeding

GPR55$^{-/-}$ mice were acquired from the Mutant Mouse Resource & Research Centers (USA) and bred in house. CB$_1^{-/-}$ breeding pairs were kindly provided by A. Zimmer. CB$_1$/GPR55 double knockout (CB$_1^{-/-}$GPR55$^{-/-}$) mice were created by crossing the two strains. Experimental procedures were approved by the Austrian Federal Ministry of Science, Research and Economy (protocol number: BMWF-66.010/0112-WF/II/3b/2014), performed in strict accordance with international guidelines, and have been described previously (1).

2.2.2 Mouse model of colitis-associated CRC (CAC)

2.2.2.1 Induction of CAC in C57BL/6 mice

CAC was induced in 5-7 weeks old, gender-matched CB$_1^{-/-}$, GPR55$^{-/-}$, and CB$_1^{-/-}$GPR55$^{-/-}$ mice, and respective wild-type littermates on a C57BL/6 background as described (134), with minor modifications. On day one, mice were injected i.p. with 10 mg/kg azoxymethane (AOM; Sigma, Vienna, Austria). Subsequently, dextran sulfate sodium (DSS; MP Biomedicals, Illkirch, France) was supplied *ad libitum* in the drinking water in three cycles: 1.2% on days 8-12, 1.5% on days 22-26, and 1.5% on days 50-54. On day 80, mice were sacrificed, tumor burden was evaluated with a caliper under the microscope, and tumor as well as non-tumor tissue was collected. A schematic overview of the protocol is given in **Figure 1**. Colon tissue was also collected from age-matched healthy mice.

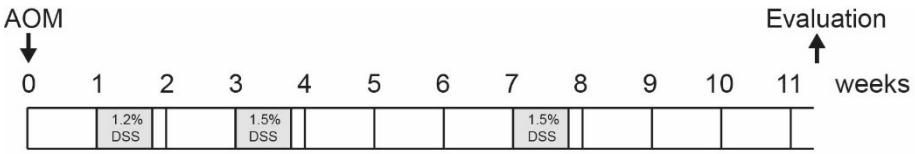

Figure 1. *Schematic overview of the CAC protocol for evaluation of tumor burden and tissue collection in C57BL/6 mice.*

For the analysis of leukocytes recruited into the tumors of GPR55$^{-/-}$ mice and wild-type littermates, the protocol was slightly different (**Figure 2**). The dose of the second cycle of DSS was reduced to 1.2%, and mice were sacrificed on day 108. These changes were applied in order to reduce mortality rates, increase tumor sizes and to obtain a sufficient amount of leukocytes.

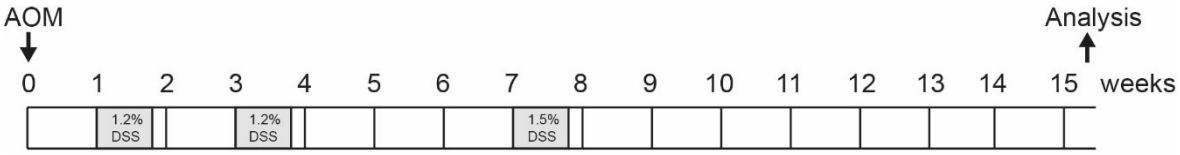

Figure 2. *Schematic overview of the CAC protocol for leukocyte extraction from tumors of GPR55$^{-/-}$ mice and wild-type littermates.*

2.2.2.2 Induction of CAC in CD1 mice

For the pharmacological approach, male CD1 mice were obtained from Charles River (Germany) and the experiment was started as soon as mice weighed 20 g. After AOM injection (10 mg/kg i.p.), DSS was administered as follows: 2% on days 8-15 and 30-36. Additionally, either 5 mg/kg CID16020046 (GPR55 antagonist; ChemDiv, San Diego, USA) or DMSO (vehicle control; VWR, Vienna, Austria) diluted in PBS (Pan-Biotech, Aidenbach, Germany) were applied s.c. on days 22-28 and 38-46. Tumor burden was evaluated on day 100 (**Figure 3**).

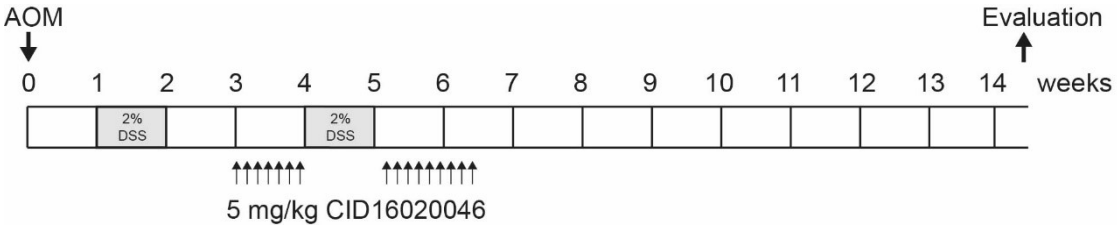

Figure 3. *Schematic overview of the CAC protocol in CD1 mice.*

2.2.3 Mouse model of spontaneous tumor progression

Spontaneous tumor progression was induced in 5-7 weeks old $CB_1^{-/-}$ and $GPR55^{-/-}$ mice and gender-matched C57Bl/6 wild-type littermates by repeated administration of 10 mg/kg AOM i.p. (134). For $CB_1^{-/-}$ mice, only male mice were used and tumors were evaluated six months after the sixth AOM injection. For $GPR55^{-/-}$ mice, male and female mice were used and tumors were evaluated eight months after the sixth AOM injection (**Figure 4**).

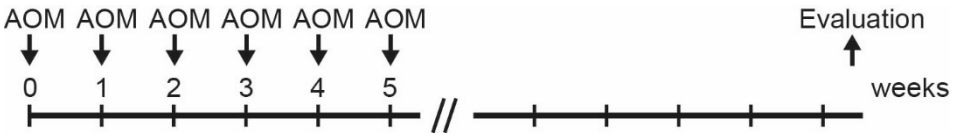

Figure 4. *Schematic overview of the mouse model of spontaneous tumor progression.*

2.2.4 Xenograft tumor model

Female SCID mice were injected subcutaneously into the right flank with $6x10^6$ HCT116 cells in 100 µL PBS. As soon as the tumors were palpable, mice were assigned to different treatment groups with equal mean ± SD of tumor volume. Mice were injected peritumoral daily for 14 days with CID16020046, WIN55,212-2, or JWH133 (Tocris, Bristol, UK) or combinations thereof as indicated. Mice were sacrificed one day after the last injection and tumor weight and volume (length × width × height / 2) were measured. This experimental procedure was approved by the Ethics-Commission of the Medical University of Vienna (UWGZ 66.009/0114-WF/V/3b/2015).

2.3 Cell culture assays and tissue analysis

2.3.1 Cell lines and cell culture

Colon cancer cell lines HCT116, SW480, SW620, HT29, and DLD-1 were obtained from Interlab Cell Line Collection (Genova, Italy), CaCo-2 from ATCC (Manassas, VA, USA). HCT116 and HT29 were maintained in McCoy's 5A, SW480, SW620, DLD-1, and CaCo-2 in DMEM, both supplemented with 10% FBS (all Life

Technologies, Vienna, Austria), 2 mM L-glutamine, and 1% penicillin/streptomycin ("P/S"; both PAA Laboratories, Pasching, Austria), at 37°C, 5% CO_2 in a humidified atmosphere. Routine culture of colon cancer cells has also been described elsewhere (1).

2.3.2 Stable overexpression of GPR55 in colon cancer cells

Colon cancer cell lines stably overexpressing GPR55 were generated by transfecting HCT116 and SW480 cells with a pcDNA3.1 construct coding for GPR55 with an N-terminal hemagglutinin tag (3xHA-GPR55), as described (1,35). Lipofectamine 2000 was used as transfection reagent according to the manufacturer's protocol. Forty-eight hours after transfection, transfected cells were selected with 4 mg/ml G418 (Life Technologies). After cells had grown to confluence, they were harvested with 0.02% EDTA (in PBS), and blocked in PBS containing 1% bovine serum albumin (BSA) and 1% goat serum for 30 min at 4°C. Cells were then incubated with anti-HA antibody (Covance #MMS-101P, 1:1000) for 60 min at 4°C, and consequently stained with an Alexa Fluor 488-conjugated goat anti-mouse antibody (Thermo Scientific #A-21121, 1:4000, 45 min, 4°C). Subsequently, cells were sorted on a FACSAria (BD Biosciences, Franklin Lakes, USA) and maintained in their respective media supplemented with 0.5 mg/ml G418 as HCT116-GPR55 (HCT55) and SW480-GPR55 (SW55).

2.3.3 Cell viability assays

For comparison of native and GPR55-overexpressing HCT116 and SW480, cells were seeded at $7.5x10^4$ cells/ml in 96-well plates. Mitochondrial activity was assessed after 24, 48, and 72 hours using the CellTiter 96® Aqueous Non-Radioactive Cell Proliferation Assay (Promega, Madison, WI, USA). For treatment with CID16020046 or LPI (Sigma), cells were seeded at $1.5x10^5$ cells/ml. After letting them adhere overnight, they were starved in McCoy's 5A without serum for 24 hours. Substances were then added as indicated and cell viability was measured after 24, 48 and 72 hours.

2.3.4 RNA extraction, reverse transcription to cDNA, and qRT-PCR

RNA extraction from tissue was performed using TRIzol (Life Technologies) according to the manufacturer's protocol. RNA from cultured cells was extracted with RNeasy Kit (Qiagen, Hilden, Germany). Isolated RNA preparations were treated with DNA-free DNA Removal Kit (Life Technologies) for the removal of genomic DNA. RNA concentrations were determined on a Nanodrop® spectrophotometer (peqLab Biotechnology, Erlangen, Germany) and 2000 ng of total RNA were reverse transcribed to cDNA using High-Capacity cDNA Reverse Transcription Kit (Applied Biosystems, Carlsbad, USA). Thermal cycling conditions (Mastercycler gradient, Eppendorf, Hamburg, Germany) were as recommended by the manufacturer: 25°C (10 min), 37°C (120 min), 85°C (5 min), 4°C (∞).

Quantification of gene expression was done by real-time PCR (CFX Connect Real-Time System, Bio-Rad, Vienna, Austria) using SsoAdvanced Universal SYBR Green Supermix (Bio-Rad). Primers were obtained from Bio-Rad: Gpr55 (mouse, ID: qMmuCID0007644), Cnr1 (mouse, ID: qMmuCED0037834), Hprt (mouse, ID: qMmuCED0045738); GPR55 (human, ID: qHsaCED0001676), GAPDH (human, ID: qHsaCED0038674), HPRT1 (human, ID: qHsaCID0016375) and relative gene expression was assessed according to the ΔΔCq-method (135). This methodological approach has also been described in an original research article (1).

2.3.5 Protein extraction

Protein was extracted from cultured cells using RIPA buffer (Thermo Scientific, Rockford, USA) supplemented with protease and phosphatase inhibitor (PhosphoStop; both Roche Applied Science, Vienna, Austria). After snap-freezing the cells in liquid nitrogen, lysis buffer was added and cells were scraped off and incubated on ice for 20 min. For protein extraction from tissue, collected samples were submerged in liquid nitrogen and subsequently pulverized with a hammer. Lysis buffer was added and homogenized samples were incubated on ice for at least one hour. Lysates were then centrifuged at 15,000×g, 15 min, 4°C, and protein concentrations of the supernatants were determined with Pierce BCA Protein Assay Kit (Thermo Scientific).

2.3.6 Western blotting

For Western blot analysis, protein lysates were supplemented with 6x Laemmli buffer containing β-mercaptoethanol and denatured at 95°C for 5 min. Proteins were separated on 4-12% Tris-Glycine gels (Thermo Scientific) and blotted onto polyvinylidene difluoride membranes (Bio-Rad) using the wet transfer system (100 V, 75 min, 4°C). Membranes were blocked in Tris-buffered saline/Tween 20 buffer (TBST; 154 mM NaCl, 10 mM Tris-HCl pH 7.4, 0.1% (v/v) Tween 20) containing 5% non-fat dry milk for one hour at room temperature. Primary antibodies were then applied overnight at 4°C: COX-2 (ab15191, 1:1000), NF-κB (CST 4764, 1:1000), STAT3 (CST 4904, 1:1000), p(Tyr705)-STAT3 (CST 9145, 1:1000), pERK1/2 (CST 9101, 1:1000), ERK1/2 (CST 4695, 1:1000), α-tubulin (CST 2125, 1:1000), β-actin (Sigma A5316, 1:7500), or GAPDH (CST 5174, 1:1000). Horseradish peroxidase-conjugated secondary antibody (goat anti-mouse, Jackson ImmunoResearch #115-036-062, 1:5000; or goat anti-rabbit, Jackson ImmunoResearch #111-036-045, 1:5000) was then applied for one hour at room temperature. Detection was performed on a ChemiDoc Touch Imaging System using Clarity Western ECL Blotting Substrate (both Bio-Rad). Immunoblot images were analyzed with Image Lab 5.2 software (Bio-Rad).

Stripping of membranes was performed by incubation in 62.5 mM Tris-HCl buffer (pH 6.8) containing 2% SDS and 100 mM β-mercaptoethanol at 50°C for 30 min. Membranes were then washed four times 15 min in TBST and subsequently reblocked and reprobed.

2.3.7 Cytokine arrays

Cytokine expression in tumor tissue was measured using the ProcartaPlex Mouse Essential Th1/Th2 and Panel 2 Multiplex Immunoassays (affymetrix eBioscience, Vienna, Austria) according to the manufacturer's instructions.

2.3.8 Immunohistochemistry

Paraffin-embedded sections of mouse colon were cut (5 µm) and deparaffinized. Sections were then microwaved for 2 x 5 min in citrate buffer (10 mM sodium citrate,

pH 6.0) for antigen retrieval, and processed by ABC method according to the manufacturer's protocol (Vectastain ABC kit; Vector Laboratories, Burlingname, CA, USA). The following antibodies were used: COX-2 (ab15191, 1:2000) and STAT3 (CST 4904, 1:500). Antibody binding was visualized with ImmPACT NovaRed (Vector Laboratories) and sections were counterstained with hematoxylin. Images were taken with a high resolution digital camera (Olympus DP 50) and analyzed by Cell^A imaging software (Olympus, Vienna, Austria). Only contrast and brightness of images were adjusted.

2.3.9 Liquid chromatography-mass spectrometry (LC-MS/MS)

Analysis of mouse tumor tissue to detect prostanoids and endocannabinoids was performed using liquid chromatography-electrospray ionization-tandem mass spectrometry (LC-ESI-MS/MS). In both cases, the LC-MS/MS system consisted of a hybrid triple quadrupole linear ion trap mass spectrometer 5500 QTrap (Sciex, Darmstadt, Germany) equipped with a Turbo-V-source operating in negative ESI mode, an Agilent 1200 binary pump, a degasser (Agilent, Waldbron, Germany), and an HTC Pal autosampler (Chromtech, Idstein, Germany).

For the analysis of prostanoids, tissue pieces of approximately 10 mg were spiked with the respective isotopically labeled internal standards, mixed with 200 µl PBS, 100 µl EDTA solution (0.15 M), 600 µl ethyl acetate and homogenized using a swing mill (Retsch, Haan, Germany) with 4 zirconium oxide grinding balls for each sample (25 Hz for 2.5 minutes). The organic phase was removed, and the extraction repeated with 600 µl ethyl acetate. The organic fractions were combined and evaporated at a temperature of 45°C under a gentle stream of nitrogen. The residues were reconstituted with 50 µl of acetonitrile/water/formic acid (20:80:0.0025, v/v) in glass vials. The chromatographic separation was carried out using a Synergi Hydro-RP column (150 × 2 mm I.D., 4-µm particle size and 80 Å pore size from Phenomenex, Aschaffenburg, Germany). A linear gradient was employed at a flow rate of 300 µl/min. The mobile phase A was water/formic acid (100:0.0025, v/v) and mobile phase B was acetonitrile/formic acid (100:0.0025, v/v). The total run time was 16 min and injection volume 20 µl. Retention times of TXB_2, $PGF_{2\alpha}$, PGE_2 and PGD_2 were 7.8 min, 8.1 min, 8.5 min and 8.9 min, respectively.

The precursor-to-product ion transitions used for quantification were m/z 351.1 → m/z 315.0 for PGE_2 and PGD_2, m/z 353.1 →m/z 291.0 for $PGF_{2\alpha}$ and m/z 369.1 →m/z 169.1 for TXB_2.

For the analysis of endocannabinoids, tissue pieces of approximately 10 mg were spiked with the respective isotopically labeled internal standards, mixed with 50 µL PBS, 50 µL ethyl acetate/n-hexan (9:1, v/v) and homogenized using a swing mill (Retsch, Haan, Germany) with 4 zirconium oxide grinding balls for each sample (25 Hz for 2.5 minutes). The organic phase was removed, and the extraction repeated with 150 µl extraction solvent. The organic fractions were combined and evaporated at a temperature of 45°C under a gentle stream of nitrogen. The residues were reconstituted with 50 µl of acetonitrile in glass vials. HPLC analysis was done under gradient conditions using a Luna C18 column (150 mm L × 2 mm ID, 5 µm particle size, Phenomenex, Aschaffenburg, Germany). The total run time was 12 min and injection volume 10 µl. Retention times of AEA, 2-AG, 1-AG, PEA and OEA were 10.2 min, 10.6 min, 10.8 min, 10.9 min and 11.2 min, respectively. Precursor-to-product ion transitions of m/z 346→259 for AEA, m/z 298→268 for PEA, m/z 377→303 for 2-AG and 1-AG and m/z 324→86 for OEA were used for quantification.

2.3.10 Isolation of recruited leukocytes and flow cytometry

A previously described protocol for the isolation of leukocytes from murine colon (136) was slightly adapted. Tumors were excised from the colon of $GPR55^{-/-}$ mice and wild-type littermates that had been subjected to the protocol of CAC (Figure 2). Next, tumors were cut into small pieces with a scalpel and washed with HBSS (containing 20 mM HEPES and P/S) 4 x 10 min at room temperature. Intraepithelial immunocytes were extracted by incubation with HBSS containing 10 mM EDTA, 2.5% FBS, and P/S for 4 x 20 min at 37°C on a rotating device. The tissue was washed with RPMI and digested with RPMI supplemented with 5% FBS, 10 mM HEPES, P/S, and 200 U/ml collagenase type II for one hour at 37°C (all Life Technologies). Isolated cells were passed through a 40 µm cell strainer, washed with PBS once, and leukocytes were stained for flow cytometry. Cells were stained with the following antibodies (all BD, Vienna, Austria), diluted in antibody diluent (Dako, Glostrup, Denmark), for one hour at 4°C: CD45-APC (1:200, clone: 30-F11),

CD3e-BV510 (1:100, clone 145-2C11), CD4-PE-Cy7 (1:500, clone RM4-5), CD8a-APC-H7 (1:100, clone 53-6.7), CD11b-FITC (1:200, clone M1/70), Ly6G-BV421 (1:500, clone 1A8), Ly6C-PE-Cy7 (1:200, clone AL-21), CD16/32 (1:100, clone 2.4G2). Samples were analyzed on a BD FACS Canto II flow cytometer. Analysis was done with FlowJo 4.0 software. This method has also been reported in the original research article that resulted from this work (1).

2.3.11 DNA demethylation

Demethylation of genomic DNA in colon cancer cell lines was performed as previously described (1,137). Cells were seeded in 6 well-plates in a way that they would be confluent four days later. After allowing them to adhere for 24 hours, the medium was exchanged to medium containing 1 or 10 µM 5-Aza-2'-deoxycytidine ("5-Aza"; Sigma). Cells were incubated for 72 hours and the medium was replaced daily. Cells incubated under the same conditions without 5-Aza treatment served as control. DNA was then extracted using Gentra Puregene Cell Kit (Qiagen).

2.3.12 Bisulfite conversion and sequencing

1000 ng of DNA were bisulfite converted using the EpiTect Bisulfite Kit (Qiagen). For the amplification of three regions of interest within the *GPR55* gene that had been determined from the methylation data obtained from CRC patients, i.e. chr2:231789465 in the gene body ("body"), chr2:231789465 in the 5'-untranslated region ("5'-UTR"), and chr2:231790813 upstream of the transcription start site ("TSS"), primers were designed using Methyl Primer Express (Life Technologies) with hg19 as a reference. Primer sequences are listed in **Table 1**.

Table 1 *Sequences of primers for amplification of regions of interest of* GPR55*.* Table was adapted from (1).

Name	Sequence	Size (bp)
GPR55_body_BS2_F	ATTTGGGGTTTTTTTTGTAGTTTTT	280
GPR55_body_BS2_R	AAAATTCAAAACCAAAACTTTCTTC	
GPR55_UTR_BS1_F	GAGTTTGGGTTTTTAGGTTTTTTTT	388
GPR55_UTR_BS1_R	TTATACACACCTATCCCAACTCAAC	
GPR55_TSS1500_BS2_F	GTTGGGAGGGTTGAGATTTATT	231
GPR55_TSS1500_BS2_R	AAAAACCCAAAAATAATTTCTATTCCTATA	

The regions of interest were amplified using the HotStar Taq® Mix Kit (Qiagen). Briefly, 25-70 ng of bisulfite converted DNA were mixed with 6 µl of HotStar Taq® Master Mix, 0.5 µl primers (10 µM), and nuclease-free water to a final volume of 12 µL. After an initial denaturation step at 95°C for 15 min, the samples were run for 40 cycles at 95°C for 45 sec, 57°C for 45 sec and 72°C for 45 sec, followed by an elongation step at 72°C for 7 min. Amplicons were then sequenced using the BigDye® Terminator v3.1 Cycle Sequence Kit (Life Technologies). Briefly, 0.5 µl of undiluted PCR products were mixed with 8 µl nuclease-free water, 0.5 µl BigDye® Terminator v3.1 Sequencing Buffer (5x), 0.5 µl BigDye® ready reaction mix and 0.5 µl primer (10µM). The samples were run with the following program: 25 cycles at 96°C for 30 sec, 50°C for 15 sec and 60°C for 4 min. The sequencing reactions were purified using Sephadex G50 Superfine (Sigma) and sequenced on an ABI 3130xl Genetic Analyzer. Sequences were analyzed using the SeqScape software (Life Technologies) and CpG methylation was calculated as a function of the area under the curve of the C and T traces.

2.4 Statistical analysis

Statistical analysis of *in vivo* and *in vitro* experiments was performed with GraphPad Prism 4.0 (GraphPad Software, La Jolla, CA, USA). The level of significance between two treatment groups was assessed by two-tailed unpaired student's t-test and Welch's correction was applied if variances were unequal. Comparison of more than two treatment groups was done by one-way ANOVA and Tukey's posthoc test.

Statistical analysis of DNA methylation data was performed by L. Stirling as reported in detail elsewhere (132). Briefly, a regularized t-test was conducted using the limma package in R. P-values were adjusted for multiple-testing using the false-discovery method.

3. RESULTS

Since parts of this thesis have previously been published as an original research article in the International Journal of Cancer (1), this section has been partially adapted from there and similarities with regards to content and wording are to be expected.

3.1 GPR55 promotes CRC

3.1.1 Genetic deletion of GPR55 reduces colonic tumor burden in mice

To assess whether GPR55 plays a tumor-promoting or suppressing role in colorectal carcinogenesis, GPR55$^{-/-}$ mice and wild-type littermates were subjected to a model of inflammation-driven tumorigenesis, i.e. CAC, a well-established murine CRC model (134,138,139). In this model, tumor formation is initiated through the application of the carcinogen AOM, and tumor growth is driven by inflammatory processes caused by DSS applied in the drinking water (see **Figure 1**). Subjecting GPR55$^{-/-}$ mice and wild-type littermates to this model of CAC revealed that genetic ablation of GPR55 resulted in mice presenting with ~50% less tumors (7.6 ± 4.7 vs. 16.4 ± 8.7), as shown in **Figure 5** A. This reduction in total tumor number was reflected by a decrease in tumors of all sizes (**Figure 5** B). For this analysis, tumors were classified into groups according to their size which was determined by measuring the largest and the smallest horizontal diameter (area=width × length). GPR55$^{-/-}$ mice showed reduced tumor numbers in all categories compared to wild-type littermates, i.e. <2 mm² (1.1 ± 0.2 vs. 3.5 ± 0.6), <5 mm² (3.5 ± 0.5 vs. 5.5 ± 0.6), <10 mm² (2.0 ± 0.3 vs. 4.0 ± 0.5), <20 mm² (0.8 ± 0.2 vs. 1.4 ± 0.2), and >20 mm² (0.2 ± 0.1 vs. 0.3 ± 0.1). Accordingly, total tumor areas were also reduced by ~50% (43.7 ± 36.8 vs. 90.4 ± 62.0) in GPR55$^{-/-}$ mice (**Figure 5** C). These data have been reported in a similar fashion elsewhere (1).

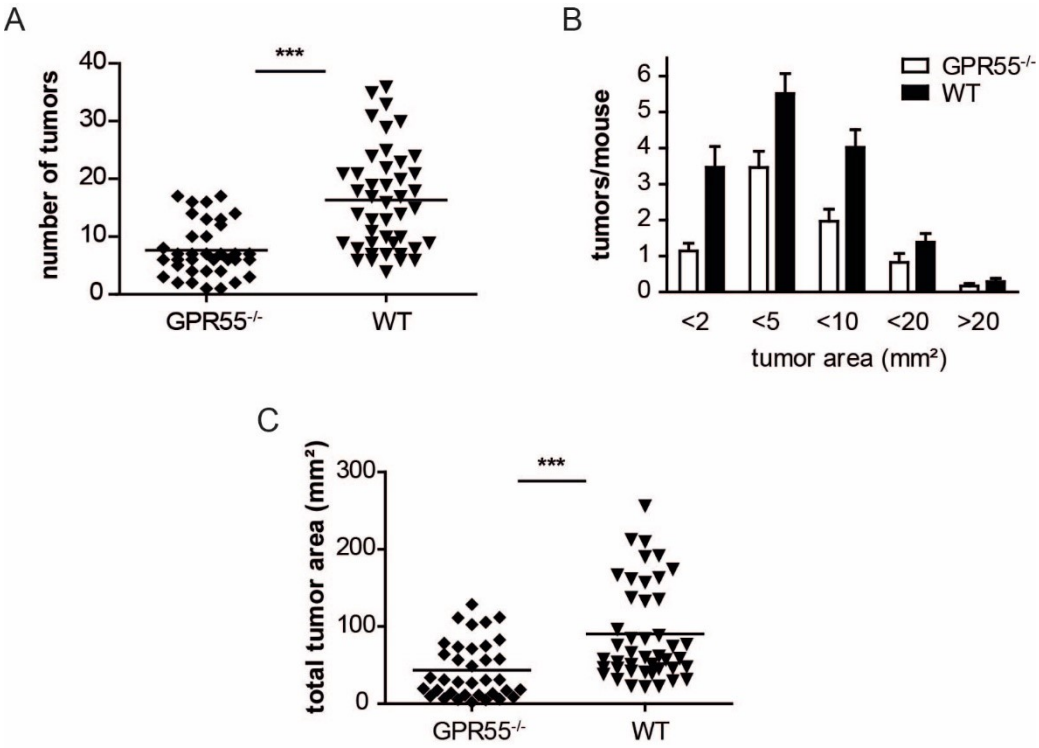

Figure 5. *Loss of GPR55 reduces tumor burden in mice.*
(**A**) In a model of CAC, GPR55$^{-/-}$ mice (n=36) had significantly less tumors than their wild-type littermates (WT, n=44). (**B**) Analysis of the tumors by size revealed that GPR55$^{-/-}$ mice (white bars) showed reduced numbers of tumors of all sizes compared to wild-type littermates (WT, black bars). (**C**) Total tumor areas were also significantly reduced in GPR55$^{-/-}$ mice. (**A**-**C**) The experiment was performed three times in total, with male and female mice, and data were combined. (**A**, **C**) Symbols depict data from individual mice, and bars show the mean. *** $p<0.001$ (**B**) Data are shown as mean + SEM. This figure has been adapted from (1).

3.1.2 Pharmacological inhibition of GPR55 reduces colonic tumor burden

To assess whether the results obtained from genetic deletion of GPR55 could be mimicked with a pharmacological approach, CD1 mice were subjected to the protocol of CAC and, additionally, treated with the GPR55 antagonist CID16020046, or vehicle control (see **Figure 3**). Evaluation of tumor burden showed that CID16020046 treated mice had ~30% less tumors (12.6 ± 2.7 vs. 17.7 ± 4.2), and, accordingly, ~40% smaller total tumor areas (82.1 ± 31.7 vs. 144.5 ± 44.5) compared to vehicle treated mice. These results were also reported here (1).

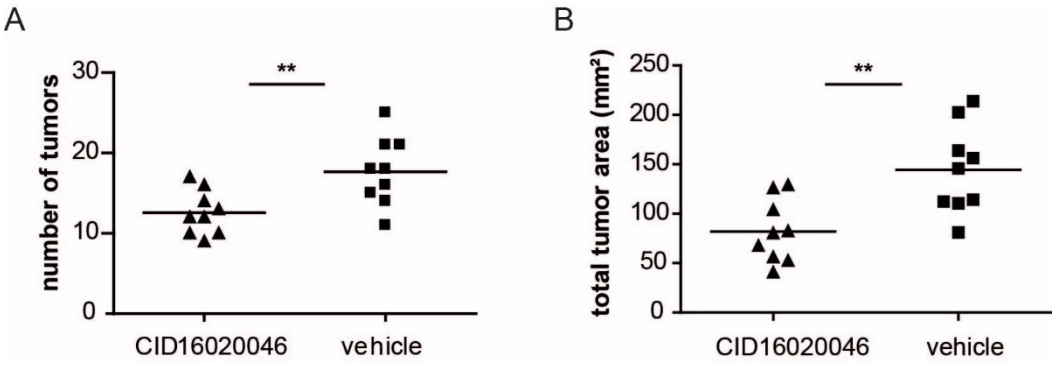

Figure 6. *CID16020046 reduces colonic tumor burden in CD1 mice.*
Male CD1 mice were subjected to the protocol of CAC and treated with either 5 mg/kg CID16020046 (16x, i.p.) or vehicle control (n=9 for both groups). Tumor numbers (**A**) and tumor areas (**B**) were reduced significantly in CID16020046 treated mice. Symbols depict data obtained from single mice, bars are the means. ** $p<0.01$ Figure adapted from (1).

3.1.3 GPR55 promotes CRC independently of its role in inflammation

Since GPR55 has been shown to promote intestinal inflammation (83) and the above described model relies on inflammation as a driving force of tumor growth, we next investigated whether GPR55 also promoted CRC in an inflammation-independent model. Therefore, $GPR55^{-/-}$ mice and wild-type littermates were subjected to a protocol of spontaneous tumor progression where tumor growth is driven by repeated administration of AOM (see **Figure 4**). Evaluation of tumor burden 8 months after the last AOM injection showed that $GPR55^{-/-}$ mice had ~50% less tumors (2.8 ± 1.0 vs. 5.6 ± 3.2) and ~80% smaller total tumor areas (11.9 ± 8.1 vs. 64.5 ± 58.9) compared to wild-type littermates (**Figure 7**). These results have previously been published (1).

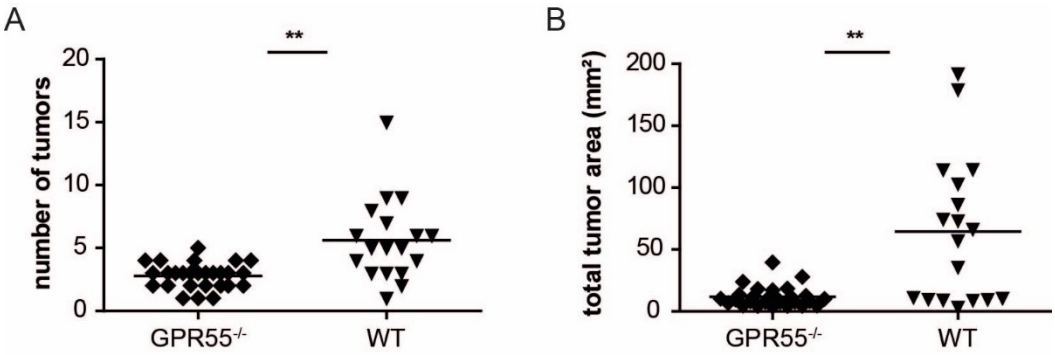

Figure 7. *Loss of GPR55 reduces colonic tumor burden in a model of spontaneous tumor progression.*
Tumor numbers (**A**) and tumor areas (**B**) were significantly reduced in GPR55$^{-/-}$ mice (n=27) compared to wild-type littermates (WT, n=18). Male and female mice were used for this experiment. Data show values obtained from individual mice and bars are the means. ** p<0.01 Figure adapted from (1).

3.1.4 GPR55 expression correlates with disease-free survival in CRC patients

For human cross validation, a publicly available data set of gene expression in CRC patients was analyzed. Although there was no correlation between GPR55 expression and overall survival, a significant association between high GPR55 mRNA expression and reduced relapse-free survival was found (**Figure 8**).

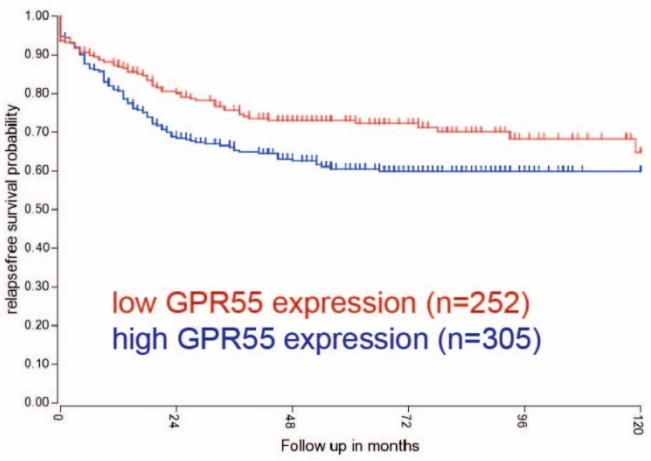

Figure 8. *High GPR55 expression is associated with reduced relapse-free survival.*
The publicly available clinical CRC expression data set R2 was analyzed (n=557). A significant (p=0.016) association between high GPR55 expression and shortened

relapse-free survival was found. Data were provided by M. Pichler and published previously (1).

Taken together, data obtained from the different mouse models of CRC as well as the survival analysis of CRC patients suggest that GPR55 plays a tumor-promoting role in colon carcinogenesis.

3.2 GPR55 actions are not mediated by epithelial cells

3.2.1 GPR55 agonism/antagonism does not affect cell proliferation

Recent studies on other types of cancer indicate that GPR55 plays a tumor-promoting role to some extent by increasing proliferation of cancer cells through the LPI/GPR55-axis (reviewed in (123)). Therefore, six commercially available CRC cell lines were examined for GPR55 expression. As shown in **Figure 9** A, all cell lines expressed GPR55 mRNA with SW480 cells expressing ~50-fold more mRNA than DLD-1, HCT116, HT29, SW620, or CaCo-2.

Treatment with the endogenous GPR55 agonist LPI, however, did not increase cell proliferation of HCT116 or SW480 cells. Antagonism of GPR55 with CID16020046 did not alter cell proliferation in these cell lines either (**Figure 9** B, C). These findings have been reported previously (1).

Additionally, GPR55-related signaling pathways were examined. Treatment with LPI (concentrations from 0.1 to 10 µM for 1-30 min) or CID16020046 (0.1 to 10 µM for 10-30 min), however, did not alter expression levels of phosphorylated p38, AKT, STAT3 or ERK1/2 in native colon cancer cells. Furthermore, β-catenin translocation and Ca^{2+} release from intracellular stores after LPI treatment were analyzed but no effects were observed (data not shown).

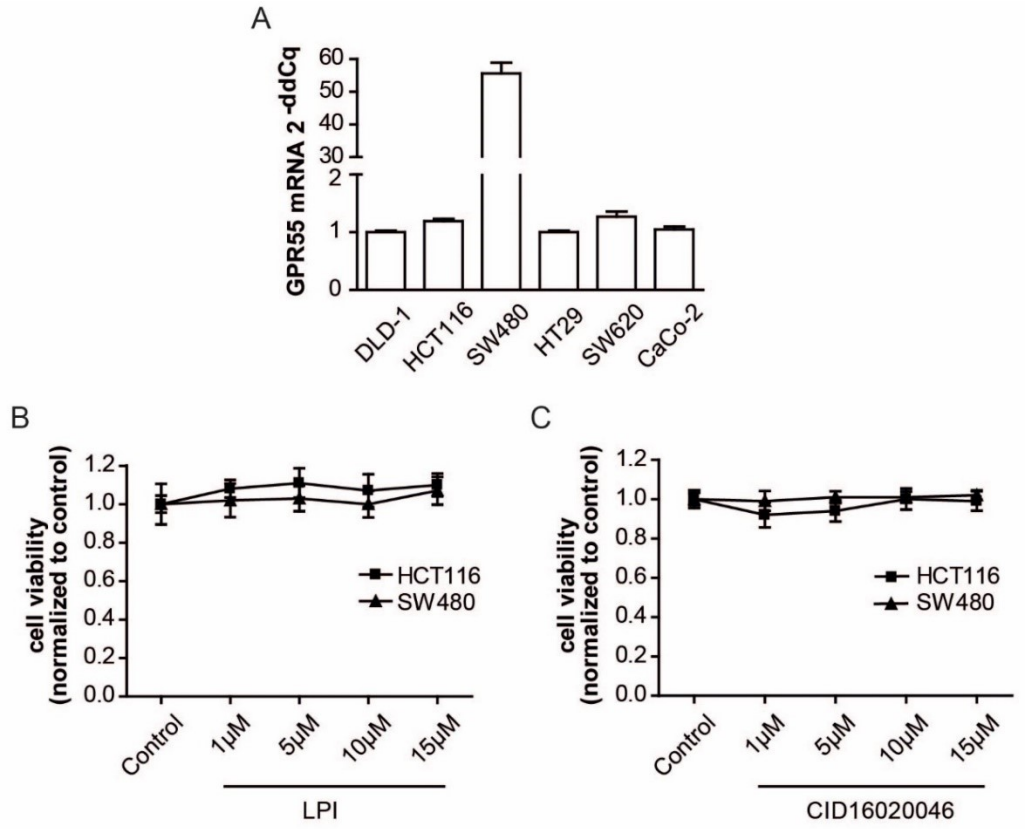

Figure 9. *CRC cell lines express GPR55 but cell proliferation is not altered by GPR55 activation or antagonism.*
(**A**) SW480 cells expressed ~50-fold more GPR55 mRNA than DLD-1, HCT116, HT29, SW620, or CaCo-2 cells. mRNA levels were assessed in three different biological replicates of the cells, each thawed from the nitrogen stock separately. Data are shown as mean + SD. *GAPDH* was used as reference gene. (**B**, **C**) HCT116 and SW480 cells were treated with the indicated concentrations of LPI (**B**) or CID16020046 (**C**) and cell viability was examined but no differences were noted. Assays were performed at least five times. Figure adapted from (1).

3.2.2 Stable overexpression of GPR55 in HCT116 and SW480 cells

Since no effect of GPR55 activation or antagonism could be observed in native CRC cell lines, GPR55 was stably overexpressed in HCT116 and SW480 cells. This way, GPR55 mRNA expression was increased 1000-fold in HCT55 cells, and 24-fold in SW55 cells. As a result, SW55 cells showed significantly increased proliferation compared to SW480 cells. HCT55 cells showed the same trend but did not reach statistical significance (**Figure 10** A, B). Concomitantly, SW55 cells showed increased levels of ERK1/2-phosphorylation compared to SW480 cells. HCT55

cells, again, showed the same trend but expression levels were not statistically different from HCT116 cells (**Figure 10** C, D).

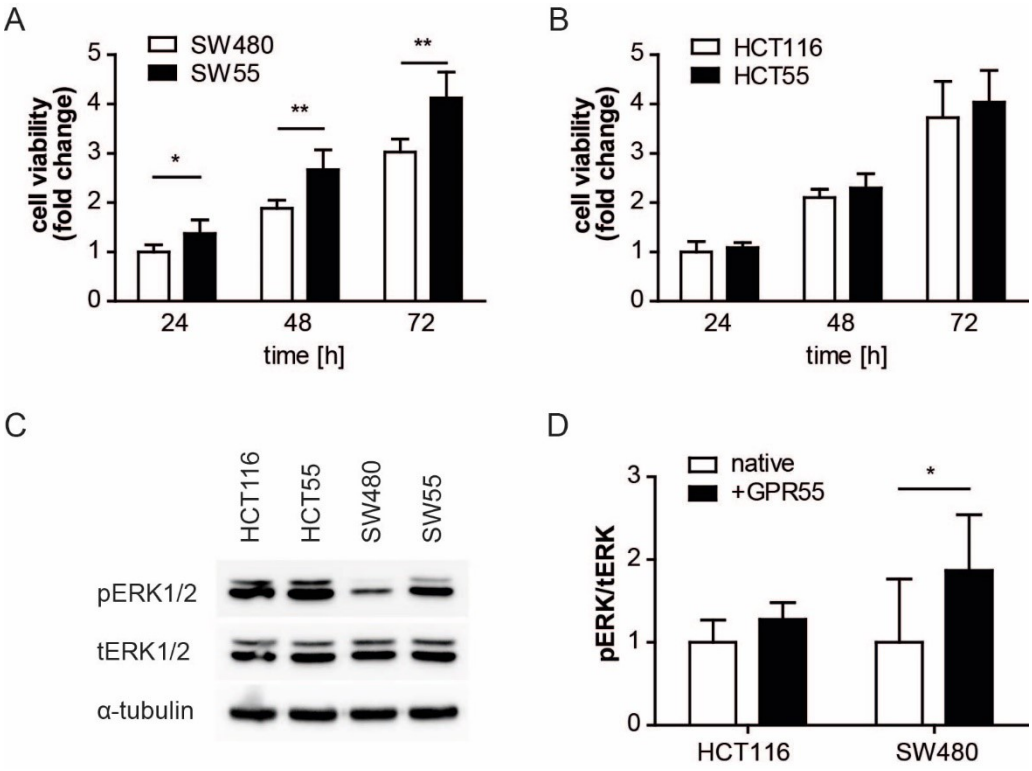

Figure 10. *GPR55 overexpression leads to a growth advantage and increases ERK1/2-phosphorylation.*
(**A**, **B**) Cell viability was increased in GPR55-overexpressing cells compared to native SW480 or HCT116 cells. Data are shown as mean + SD from at least five independent experiments performed in sextuplicates. * $p<0.05$, ** $p<0.01$ (**C**, **D**) ERK1/2-phosphorylation was increased in GPR55-overexpressing cells. A representative Western blot is shown in (**C**). (**D**) Data from three independent experiments are shown as mean + SD. * $p<0.05$

GPR55-overexpressing cells were then treated with LPI and ERK1/2-phosphorylation was examined via Western blotting. Indeed, pERK1/2 expression was increased by ~70% in HCT55 cells, and ~260% in SW55 cells after treatment with 1 µM LPI for 10 min (**Figure 11** A). Treatment of native HCT116 or SW480 cells with LPI, on the other hand, had no effect on ERK1/2-phosphorylation (data not shown).

In accordance with this observation, ERK1/2-phosphorylation was also altered in GPR55-overexpressing cells after treatment with the GPR55 antagonist CID16020046, but not in native HCT116 or SW480 cells. In HCT55 cells, pERK1/2 expression was reduced by ~35%, and in SW55 cells by ~50% after treatment with 10 µM for 30 min (**Figure 11** B).

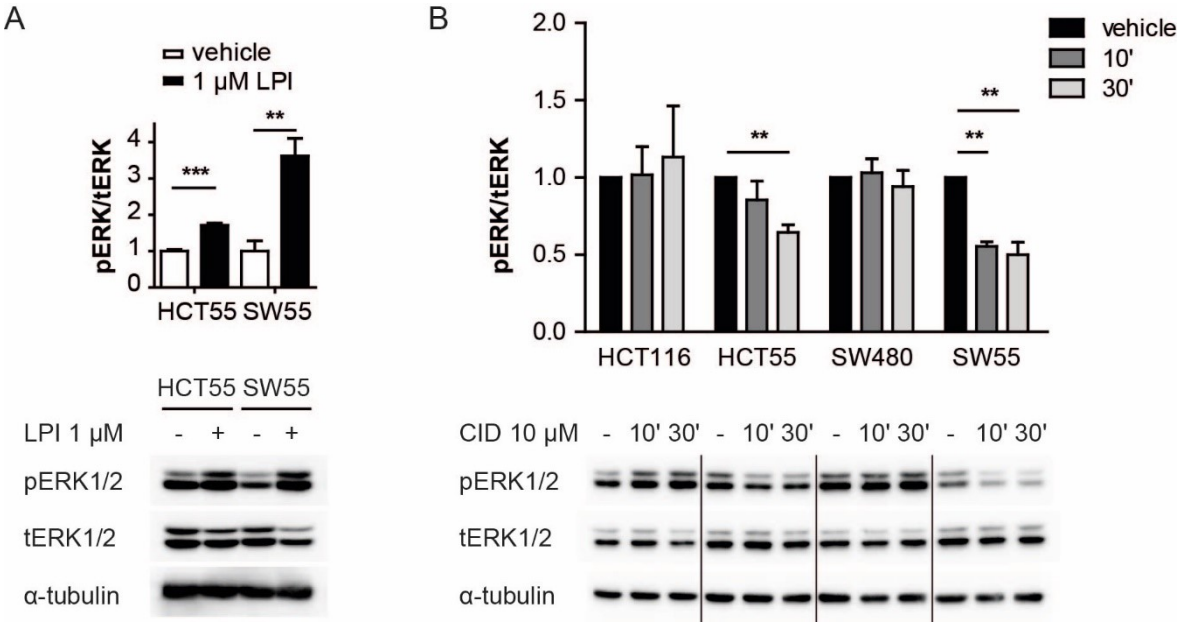

Figure 11. *ERK1/2-phosphorylation is altered in GPR55-overexpressing cells after LPI or CID16020046 treatment.*
(**A**) HCT55 and SW55 cells were treated with 1 µM LPI or vehicle control for 10 min at room temperature. A representative blot of three independent experiments is shown. Bars are means + SD. (**B**) HCT116, HCT55, SW480, and SW55 cells were treated with 10 µM CID16020046 for 10 or 30 min, or with vehicle control. In GPR55-overexpressing cells, a decrease in pERK1/2 levels was observed after CID16020046 (CID) treatment whereas this effect was absent in native HCT116 and SW480 cells. A representative blot of three independent experiments is shown. ** $p<0.01$, *** $p<0.001$

3.2.3 Xenografts of HCT116 cells in SCID mice

Human colon cancer xenografts were grown from HCT116 cells in SCID mice. Treatment with CID16020046 (GPR55 antagonist), WIN55,212-2 (CB_1/CB_2 agonist), JWH133 (CB_2 agonist), or combinations thereof, however, had no effect on tumor growth compared to vehicle treatment (**Figure 12**).

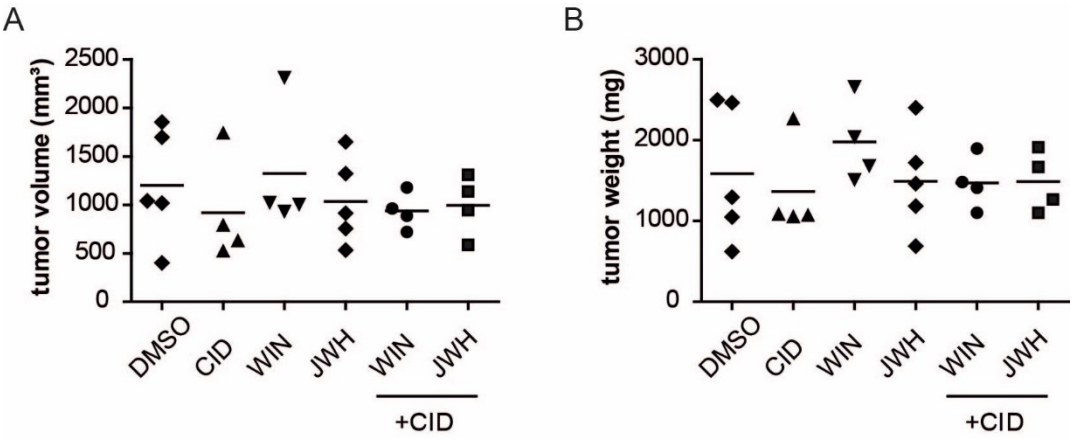

Figure 12. *Tumor xenografts in SCID mice.*
Treatment of colon cancer xenografts with CID16020046 ("CID", 20 mg/kg/day), WIN55,212-1 ("WIN", 1 mg/kg/day), JWH133 ("JWH", 1 mg/kg/day), or combinations thereof (WIN + CID, JWH + CID) did not result in significant differences regarding (**A**) tumor volume or (**B**) tumor weight compared to vehicle (DMSO) treatment. n=4-5 per group

3.3 GPR55 modulates the tumor microenvironment

Since experiments performed with CRC cell lines did not reveal the mechanism underlying the tumor-promoting function of GPR55, tissue collected from murine CAC (see **Figure 5**) was analyzed next. Results detailed in this section have partly been reported previously (1).

3.3.1 COX-2 is expressed at lower levels in GPR55$^{-/-}$ tumors

Analysis of tumor and non-tumor tissue as well as colon tissue collected from healthy control mice revealed that COX-2 is up-regulated in non-tumor tissue, which can be regarded as inflamed tissue because of the exposure of the mice to DSS. In tumor tissue, COX-2 expression was found to be even higher at both mRNA and protein level (**Figure 13** A, B). Comparison of COX-2 levels in tumors of GPR55$^{-/-}$ and wild-type mice revealed that protein levels were lower in GPR55$^{-/-}$ tumors as observed through Western blotting as well as immunohistochemical staining (**Figure 13** C, D).

For qRT-PCR *Hprt* was used as housekeeping gene after it was identified as being stably expressed across the different tissues that were analyzed. On protein level, GAPDH was stably expressed across different tissues, but β-actin showed more stability in comparing tumors of GPR55$^{-/-}$ and wild-type mice.

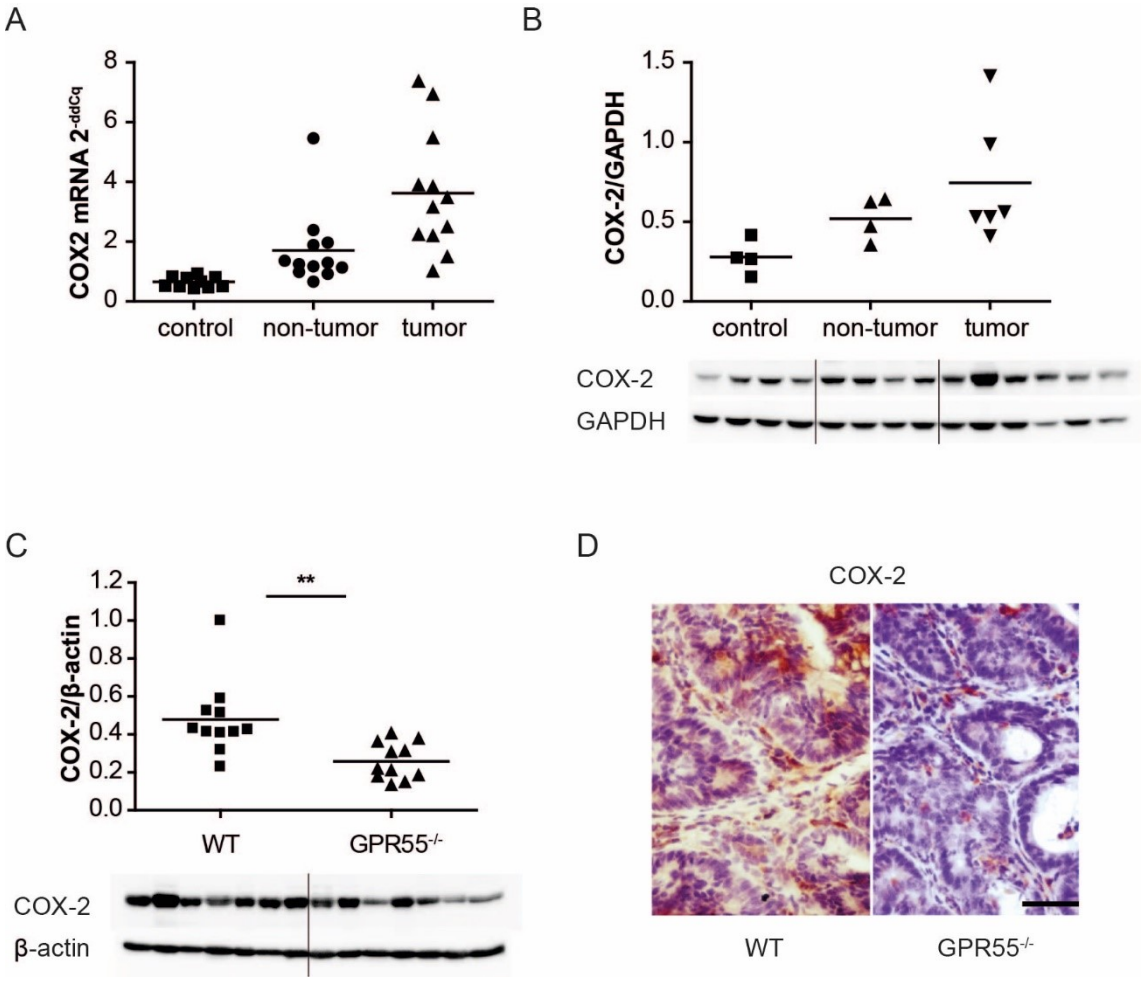

Figure 13. *Tumors of GPR55$^{-/-}$ mice show reduced COX-2 expression.*
(**A**) In wild-type mice, COX-2 mRNA was up-regulated in non-tumor and tumor tissue compared to healthy control tissue. Housekeeping gene: *Hprt*. n=10-12 (**B**) COX-2 protein levels were also increased in non-tumor and tumor tissue compared to control tissue. The corresponding Western blot is shown. n=4-6 (**C**) COX-2 protein levels were lower in tumors of GPR55$^{-/-}$ mice compared to tumors of wild-type littermates (WT). A representative Western blot is shown. n=11 (**D**) Sections of colonic tumors were stained for COX-2 (brown color). Expression levels were lower in tumors of GPR55$^{-/-}$ mice. Representative images are shown (scale bar, 50 µm). Data points show values obtained from tissue collected from individual mice, bars are the means. ** $p<0.01$ Figure adapted from (1).

3.3.2 STAT3 expression is altered in GPR55$^{-/-}$ tumors

Further analysis of collected tumor tissue showed that STAT3 signaling was altered in tumors of GPR55$^{-/-}$ mice. STAT3 activation through Tyr705-phosphorylation was reduced in GPR55$^{-/-}$ tumors but did not reach statistical significance. Total protein levels of STAT3, however, were significantly reduced in tumors of GPR55$^{-/-}$ mice as assessed by Western blotting (**Figure 14** A). This finding was confirmed by histological staining of colonic sections (**Figure 14** B).

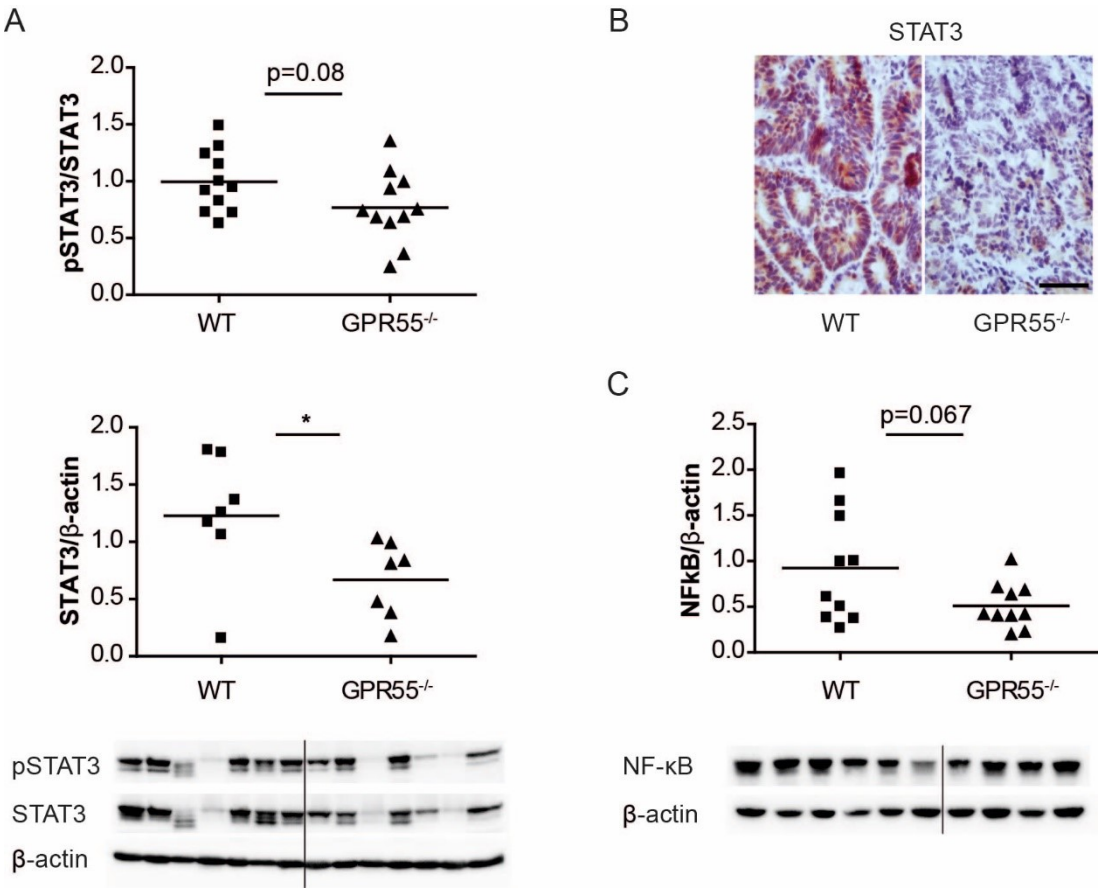

Figure 14. *STAT3 expression is reduced in tumors of GPR55$^{-/-}$ mice.*
(**A**) Compared to tumors of wild-type (WT) mice, tumors of GPR55$^{-/-}$ mice showed reduced expression of STAT3 protein levels. The degree of STAT3-phosphorylation was reduced in GPR55$^{-/-}$ mice but statistical significance was not achieved (upper panel). The amount of total STAT3, however, was significantly lower in tumors of GPR55$^{-/-}$ mice (lower panel). (**B**) Staining of colonic tumor sections for STAT3 (brown color) confirmed reduced protein levels in GPR55$^{-/-}$ tumors. Representative images are shown (scale bar, 50 µm). (**C**) NF-κB expression was also reduced in tumors of GPR55$^{-/-}$ without reaching statistic significance. Data points show values obtained from tissue collected from individual mice, bars represent the mean value.

Representative Western blots are shown. n=7-11, * $p<0.05$. Figure adapted from (1).

Additionally, NF-κB expression was found to be slightly reduced in tumors of GPR55$^{-/-}$ mice (**Figure 14** C). The degree of NF-κB activation through phosphorylation of the p65 subunit, however, did not differ between tumors of GPR55$^{-/-}$ mice and wild-type littermates (data not shown).

3.3.3 Differential expression of cytokines in tumors of GPR55$^{-/-}$ mice

Cytokine levels in tumor tissue were assessed using a multiplex ELISA. Four cytokines were found to be differentially expressed in tumors of GPR55$^{-/-}$ mice. IL-5, IL-10, and IL-12 levels were elevated compared to tumors of wild-type littermates whereas the presence of myeloid cells-recruiting chemokine monocyte chemoattractrant protein-1 (MCP-1/CCL2) was decreased (**Figure 15**). Other cytokines that were analyzed, but did not show differential expression, included interferon γ, IL-1β, IL-17A, IL-4, IL-6, C-X-C motif chemokine ligand 1 and 2 (CXCL1 and CXCL2), macrophage inflammatory protein 1 α and β, and tumor necrosis factor α (data not shown).

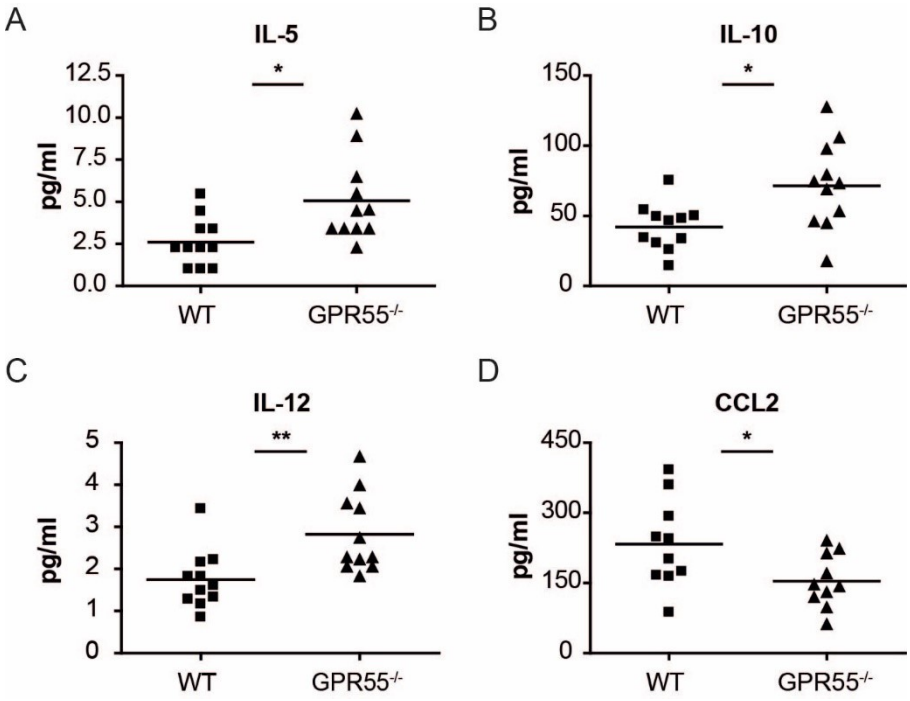

Figure 15. *Differential cytokine production in tumors of GPR55$^{-/-}$ mice.*
IL-5 (**A**), IL-10 (**B**), and IL-12 (**C**) expression was increased in tumors of GPR55$^{-/-}$ mice compared to wild-type littermates (WT) whereas CCL2 expression was decreased (**D**). Data points show values obtained from individual mice, bars are the means. n=11, * $p<0.05$, ** $p<0.01$. Figure adapted from (1).

3.3.4 Reduced expression of prostanoids in GPR55$^{-/-}$ tumors

Since tumors of GPR55$^{-/-}$ mice showed reduced COX-2 expression, down-stream effector molecules of COX-2 were analyzed by mass spectrometry. Indeed, thromboxane A_2 (as determined through the measurement of the primary metabolite thromboxane B_2 (TXB_2)) and prostaglandin $F_{2\alpha}$ ($PGF_{2\alpha}$) were found to be expressed at lower levels in tumors of GPR55$^{-/-}$ mice (**Figure 16**). These results have also been published here (1). Prostaglandin E_2 and D_2 levels were also assessed but the content of the samples was so high that all measured values were above the calibration curve and, therefore, could not be analyzed. Additionally, 6-keto-prostaglandin 1α was measured, but there was no difference between tumors of wild-type and GPR55$^{-/-}$ mice (data not shown).

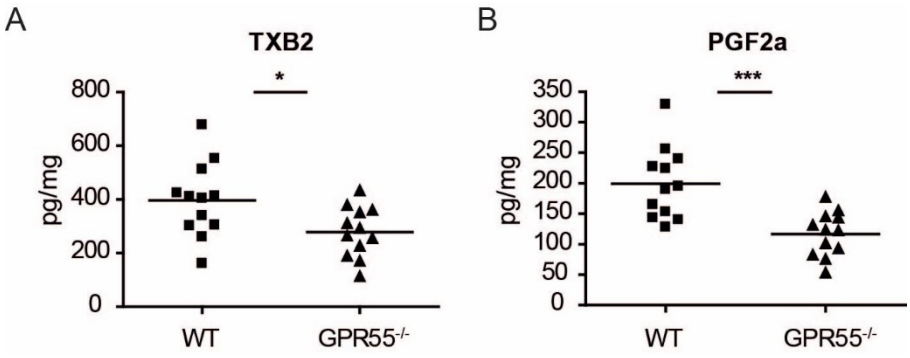

Figure 16. *Reduced expression of prostanoids TXB_2 and $PGF_{2\alpha}$ in tumors of $GPR55^{-/-}$ mice.*
Mass spectrometry revealed that TXB_2 (**A**) and $PGF_{2\alpha}$ (**B**) were expressed at lower levels in tumors of $GPR55^{-/-}$ mice than in tumors of wild-type littermates (WT). Data were provided by N. Ferreirós and have also been reported here (1). Data points show prostanoid content of tumor tissue collected from individual mice. n=12 *p<0.05, *** p<0.001

3.3.5 Reduced levels of endocannabinoids in $GPR55^{-/-}$ tumors

Furthermore, levels of endocannabinoids and related lipids were assessed in tumor tissue as well as in healthy control tissue collected from $GPR55^{-/-}$ mice and wild-type littermates. In accordance with previous reports on human CRC biopsies (98,99), endocannabinoids AEA and 2-AG were expressed at very low levels in healthy colonic tissue, but expression was strongly increased in tumors of wild-type mice (**Figure 17**). In tumors of $GPR55^{-/-}$ mice, however, AEA and 2-AG levels were strongly reduced compared to tumors of wild-type mice, and the amount of compound detected was almost reduced to control tissue levels. The same was true for endocannabinoid-like compounds OEA and 1-AG. PEA was also expressed at lower levels in tumors of $GPR55^{-/-}$ mice. In accordance with endocannabinoid levels assessed from human CRC biopsies (98), 2-AG levels were about two orders of magnitude higher than AEA levels in both control and tumor tissue of wild-type mice corroborating that the *in vivo* model used here is an appropriate model to study endocannabinoids in CRC.

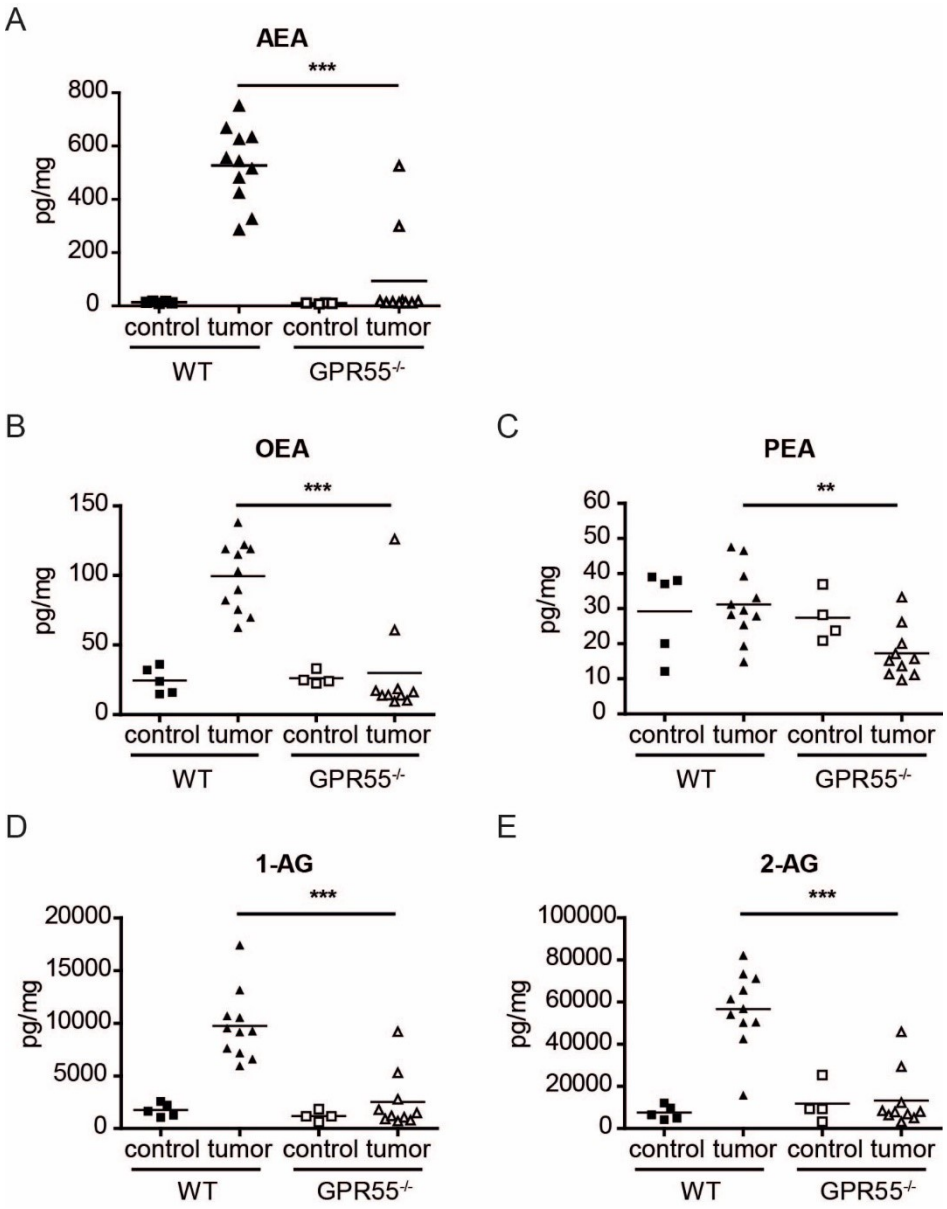

Figure 17. *Levels of endocannabinoids and related compounds are altered in tumors of GPR55$^{-/-}$ mice.*

Mass spectrometry analysis of healthy control colonic tissue (n=4-5) and tumor tissue (n=10-11) revealed that *N*-acylethanolamines AEA (**A**), OEA (**B**), and PEA (**C**) were expressed at lower levels in tumors of GPR55$^{-/-}$ mice compared to tumors of wild-type littermates (WT). Monoacylglycerols 1-AG (**D**) and 2-AG (**E**) expression levels were also strongly reduced in tumors of GPR55$^{-/-}$ mice. (**A**-**E**) Data were provided by N. Ferreirós and show concentrations measured in tissue samples obtained from single mice. ** $p<0.01$, *** $p<0.001$

3.3.6 Leukocyte populations are altered in tumors of GPR55$^{-/-}$ mice

Since the analysis of the tumor tissue collected from GPR55$^{-/-}$ mice and wild-type littermates revealed differential cytokine expression as well as altered expression of COX-2 and STAT3, the leukocyte populations recruited into the tumors were investigated next. A recent publication reported that one of the cytokines reduced in GPR55$^{-/-}$ tumors, i.e. CCL2, contributes to carcinogenesis in CAC through the recruitment of myeloid-derived suppressor cells (MDSCs) (140). MDSCs in turn have been reported to contribute to colonic tumor growth via the inhibition of T cells (141). Therefore, flow cytometric analysis was targeted at identifying these distinct subsets of leukocytes in tumors of GPR55$^{-/-}$ mice and wild-type littermates that had been subjected to the model of CAC (as outlined in **Figure 2**). Indeed, as shown in **Figure 18**, a subset of CD11b^{+} cells, i.e. Ly6C^{hi}Ly6G^{-} cells, reported to be monocytic MDSCs (140,141), were significantly less abundant in tumors of GPR55$^{-/-}$ mice. Importantly, total amounts of CD11b^{+} cells were not altered between tumors of GPR55$^{-/-}$ mice and wild-type littermates, suggesting that the observed effect was not due to “per se” reduced infiltration of leukocytes in tumors of GPR55$^{-/-}$ mice.

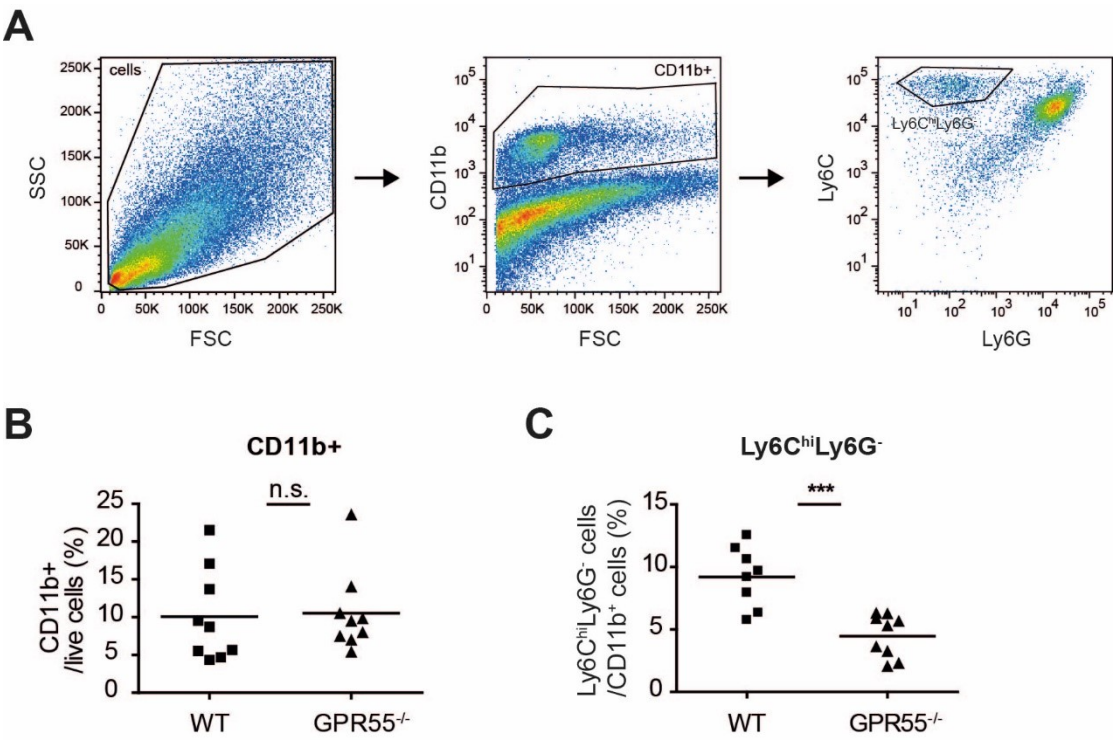

Figure 18. *Reduced recruitment of Ly6C^{hi}Ly6G^{-} cells in tumors of GPR55$^{-/-}$ mice.* (**A**) Gating strategy for MDSCs: after exclusion of cell debris from the FSC/SSC plot, CD11b^{+} cells were further analyzed for their Ly6C and Ly6G expression. (**B**) No

difference in CD11b$^+$ cells was observed between tumors of wild-type (WT) and GPR55$^{-/-}$ mice. n.s.= not significant (**C**) The population of Ly6C^{hi}Ly6G$^-$CD11b$^+$ cells, however, was strongly reduced in tumors of GPR55$^{-/-}$ mice. Each data point represents the leukocytes extracted from the pooled tumors of one individual mouse, bars are the means. *** p<0.001 n=9 per group. Figure adapted from (1).

Furthermore, tumors of GPR55$^{-/-}$ mice displayed strongly enriched numbers of CD3$^+$ leukocytes (**Figure 19**). Subsequent analysis of the CD3$^+$ population revealed an increase in both CD4$^+$ and CD8$^+$ T cells in these tumors. Taken together, the data indicate that systemic genetic disruption of GPR55 alters the composition of CAC tumors leading to a rather tumor-rejecting microenvironment. A schematic overview of how altered leukocyte populations and mediators assessed in this study may contribute to the observed reduction in tumor burden of GPR55$^{-/-}$ mice is given in **Figure 20**. These data have also been reported here (1).

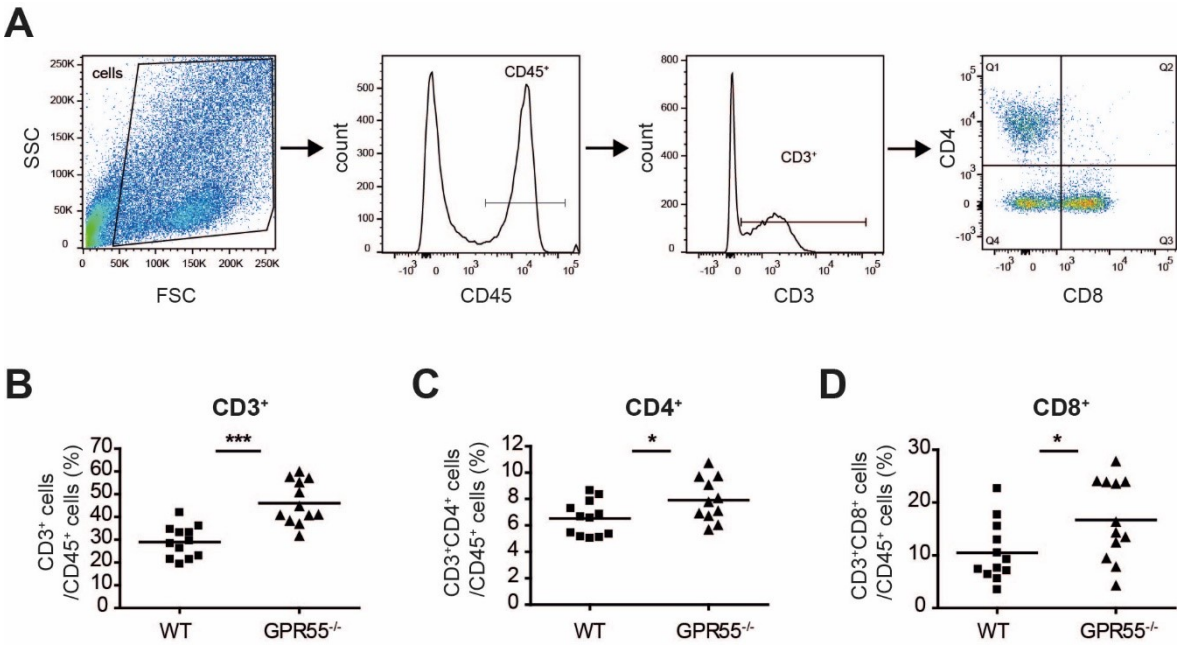

Figure 19. *Tumors of GPR55$^{-/-}$ mice show increased infiltration of CD3$^+$ cells.* (**A**) Gating strategy for T cells: following the exclusion of cell debris, CD45$^+$ and CD3$^+$ leukocytes were analyzed for their CD4 (Q1) and CD8 (Q3) expression. (**B**) Tumors of GPR55$^{-/-}$ mice showed strongly increased numbers of CD3$^+$ leukocytes compared to tumors of wild-type littermates (WT). This increase was further translated into the enhanced presence of CD4$^+$ (**C**) and CD8$^+$ (**D**) T cells in tumors of GPR55$^{-/-}$ mice. (**B**-**D**) Each data point represents the leukocytes extracted from

the pooled tumors of one individual mouse, bars are the means. * p<0.05, ***p<0.001, n=12 per group. Figure adapted from (1).

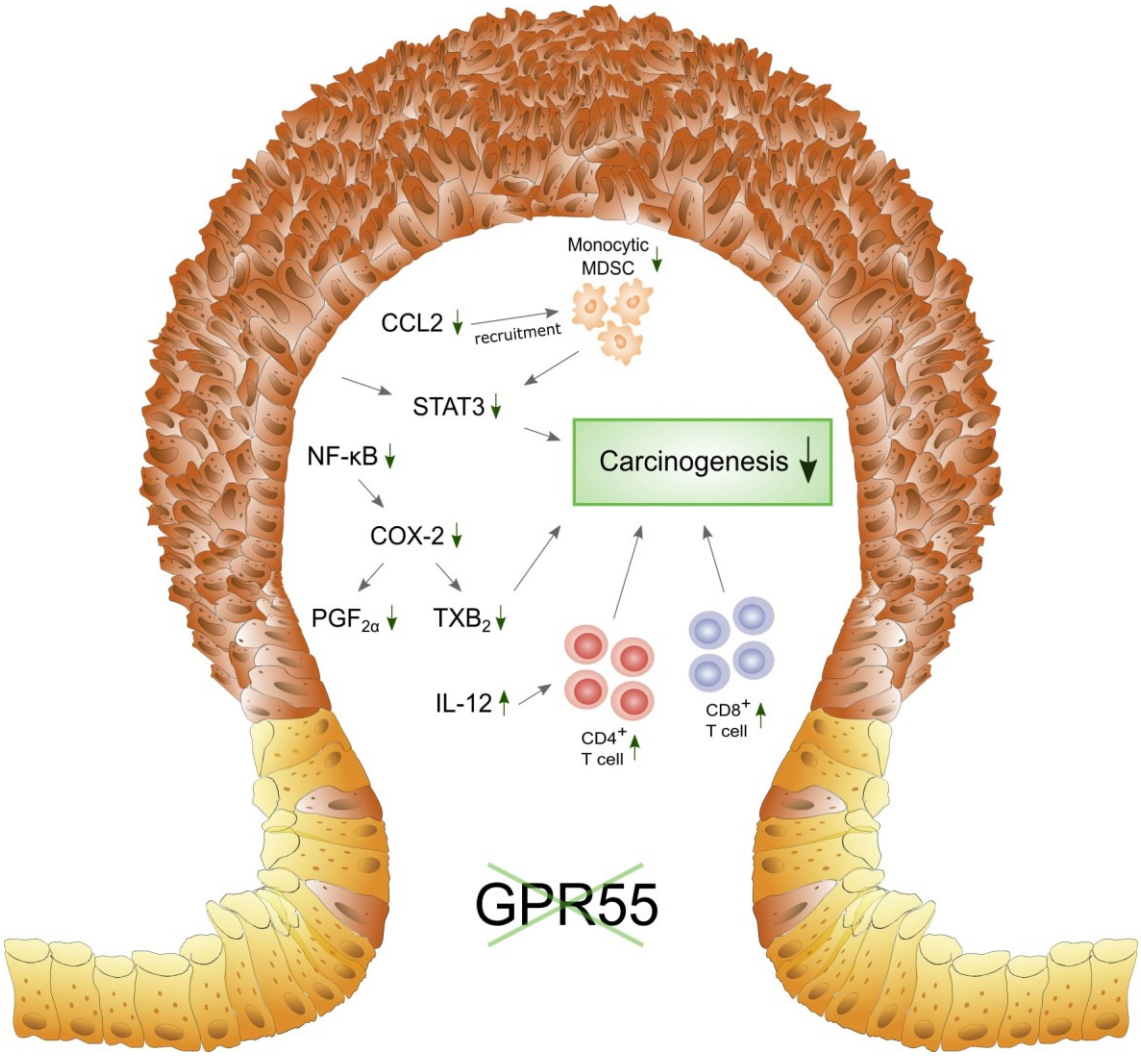

Figure 20. *Deletion of GPR55 alters the tumor microenvironment in murine CAC.* This scheme summarizes the various alterations identified between tumors of GPR55$^{-/-}$ mice and wild-type littermates that could account for the reduced colon carcinogenesis observed in GPR55$^{-/-}$ mice. Changes in leukocyte populations and mediators caused by genetic disruption of GPR55 are indicated by green arrows. Firstly, reduced numbers of monocytic myeloid-derived suppressor cells (MDSC) were observed, which is likely a consequence of reduced CCL2 expression (140). Therefore, STAT3 expression in turn could be diminished partly by reduced CCL2-MDSC signaling (140), although the role of other cells, e.g. neoplastic cells, cannot be excluded (142). Secondly, reduced expression levels of transcription factor NF-κB and COX-2 as well as of its effector molecules $PGF_{2\alpha}$ and TXB_2 were observed. Both prostanoids have been shown to promote carcinogenesis (143,144). Thirdly,

recruitment of both T helper cells ($CD4^+$) and cytotoxic T cells ($CD8^+$) was enhanced in tumors of $GPR55^{-/-}$ mice. Increased infiltration of T cells has been shown to be associated with a favorable clinical outcome in CRC (145) and might thus also contribute to reduced carcinogenesis in this model. This figure and its legend have been reproduced from (1) with permission of Wiley.

3.4 CB_1 is a tumor-suppressor and has opposing effects to GPR55

3.4.1 $CB_1^{-/-}$ mice have a higher tumor burden than wild-type littermates

CB_1 has been shown to play a tumor-suppressing role in a genetic mouse model of intestinal cancer (101) where polyps develop mainly in the small intestine (*Apc*$^{min/+}$ mice). To examine whether CB_1 would also be protective in CRC, $CB_1^{-/-}$ mice and wild-type littermates were subjected to the AOM+DSS-induced model of CAC (see **Figure 1**) as well as the model of spontaneous tumor progression (see **Figure 4**). As shown in **Figure 21**, it was observed that $CB_1^{-/-}$ mice developed significantly more tumors and, accordingly, had larger tumor areas than wild-type littermates in both models of colon cancer. In the CAC model, $CB_1^{-/-}$ mice had ~3.3 times more tumors than wild-type littermates (10.9 ± 4.2 vs. 3.3 ± 1.3) and tumor areas were increased ~2.4-fold (62.0 ± 45.4 vs. 26.3 ± 16.7). In the model of spontaneous tumor progression, $CB_1^{-/-}$ mice showed ~1.5-fold higher tumor numbers (5.0 ± 0.8 vs. 3.4 ± 1.0) and ~1.9-fold (30.0 ± 8.0 vs. 16.1 ± 6.4) increased tumor areas.

These data confirm the tumor-suppressing role of CB_1 in intestinal cancer and suggest that CB_1 plays a contrary role to GPR55. The results have also been reported here (1).

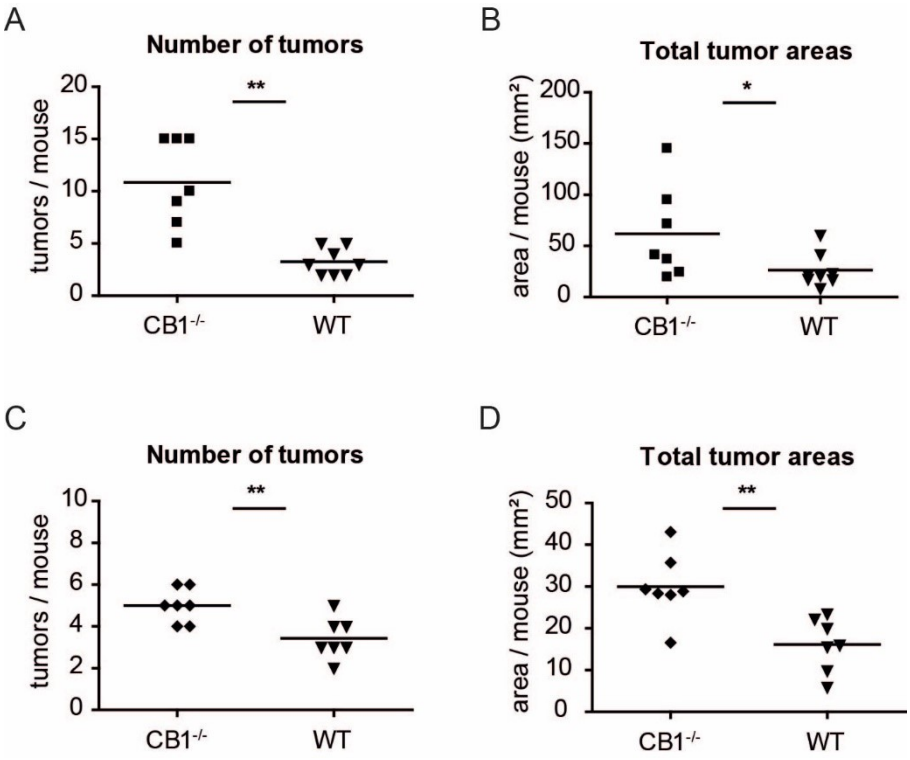

Figure 21. *CB_1 plays a tumor-suppressing role in murine models of CRC.*
(**A**, **B**) $CB_1^{-/-}$ mice (n=7) and wild-type littermates (WT, n=8) were subjected to the model of CAC. $CB_1^{-/-}$ mice developed more tumors and, accordingly, had larger tumor areas. Because of the high mortality in male $CB_1^{-/-}$ mice after application of DSS, only female mice were used for this experiment. (**C**, **D**) Male $CB_1^{-/-}$ mice (n=7) and wild-type littermates (n=7) were subjected to the protocol of spontaneous tumor progression. Again, $CB_1^{-/-}$ mice had more tumors and increased total tumor areas. Data show values obtained from individual mice, bars are the means. * $p<0.05$, **$p<0.01$ Figure has been adapted from (1).

3.4.2 CB_1 opposes the role of GPR55 in murine CRC

To further analyze the contrary roles of CB_1 and GPR55 in CRC, double knockout mice ($CB_1^{-/-}GPR55^{-/-}$) and wild-type littermates were subjected to the protocol of CAC. As shown in **Figure 22**, there was no statistically significant difference in tumor burden between $CB_1^{-/-}GPR55^{-/-}$ mice and wild-type littermates, i.e. neither in tumor numbers (9.6 ± 4.1 vs. 6.5 ± 4.3) nor in tumor areas (46.0 ± 28.35 vs. 29.9 ± 23.9). These data suggest that the tumor-promoting role of GPR55 is indeed opposed by the tumor-suppressing role of CB_1.This has also been reported previously (1).

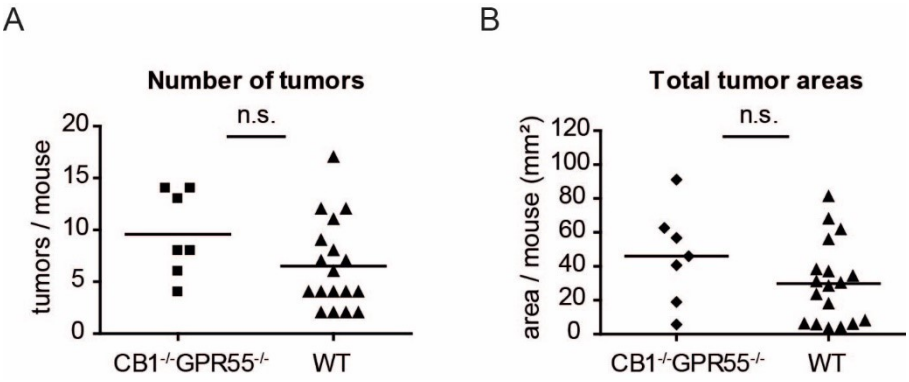

Figure 22. *CB_1 appears to oppose the tumor-promoting role of GPR55.*
CAC was induced in CB_1/GPR55 double knockout mice ($CB_1^{-/-}GPR55^{-/-}$, n=7) and wild-type littermates (n=18). Tumor burden, i.e. tumor numbers (**A**) and total tumor areas (**B**), was not significantly (n.s.) different between the two groups. Data points are values obtained from individual mice, and bars are the means. Figure adapted from (1).

3.5 Differential regulation of CB_1 and GPR55

3.5.1 CB_1 and GPR55 mRNA expression are differentially regulated

Wang *et al*. (101) had reported that the tumor-suppressing function of CB_1 was diminished in neoplastic tissue because of the down-regulation of the receptor as compared to adjacent control tissue. Following up on this finding, expression levels of CB_1 and GPR55 mRNA were analyzed in tissue collected from the murine model of CAC. qRT-PCR revealed that CB_1 mRNA levels were indeed strongly down-regulated in tumor tissue compared to healthy control colon. In colonic non-tumor tissue, i.e. tissue that did not exhibit neoplastic lesions but was nevertheless affected by the multiple exposure to DSS, CB_1 expression was increased as compared to healthy colon. This regulatory pattern of CB_1 mRNA expression was found in both wild-type mice as well as $GPR55^{-/-}$ mice. CB_1 levels were also comparable between healthy colon tissue of wild-type and $GPR55^{-/-}$ mice (**Figure 23** A). On the contrary, GPR55 mRNA levels were decreased in non-tumor tissue and increased in tumor tissue compared to colon tissue of healthy control mice (**Figure 23** B). Additionally, we analyzed mRNA expression levels in a cohort of 86 CRC patients (132). In accordance with a previous report (101), we found a strong

down-regulation of CB_1 in tumors as compared to control tissue. Interestingly, however, CB_1 mRNA levels increased again with disease severity (**Figure 23** C). GPR55 levels, on the other hand, decreased with increasing tumor stage (**Figure 23** D). Taken together, the data indicate a differential regulation for the transcription of CB_1 and GPR55 in CRC. These findings have also been reported here (1).

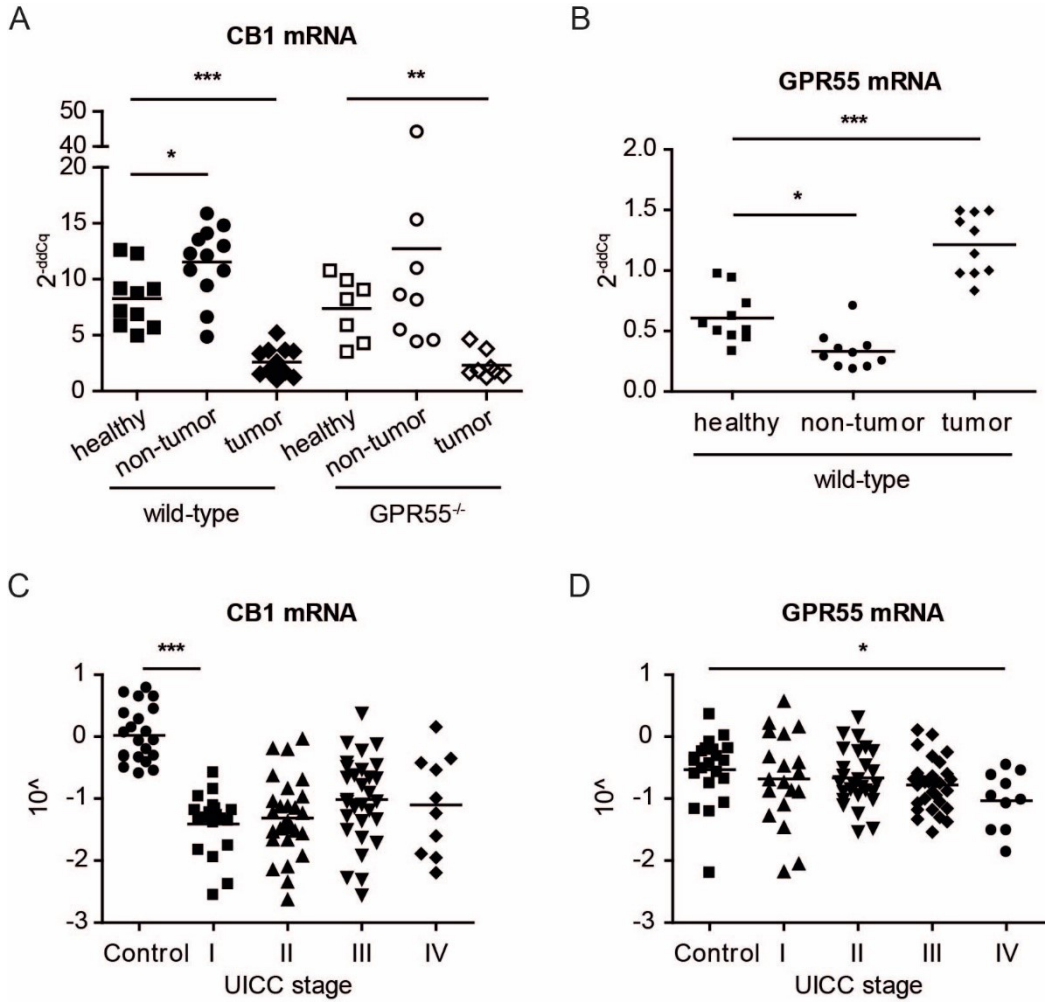

Figure 23. *Differential regulation of CB_1 and GPR55 mRNA.*
(**A**, **B**) CB_1 and GPR55 mRNA expression levels were assessed in healthy colonic tissue of control mice (n=10) and in tumor and non-tumor tissue of mice that had been subjected to the AOM+DSS-induced model of CAC (n=10-12). mRNA levels were assessed with qRT-PCR with *Hprt* as reference gene. (**A**) CB_1 was found to be up-regulated in non-tumor tissue and down-regulated in tumor tissue compared to healthy colon tissue. This regulatory pattern was observed in both wild-type (filled symbols) and $GPR55^{-/-}$ mice (empty symbols). (**B**) GPR55 mRNA, in contrast, was down-regulated in non-tumor tissue compared to healthy control colon whereas it was up-regulated in tumors. (**C**, **D**) mRNA expression levels in tumors of CRC patients (n=86) and adjacent control tissue (n=21) were determined by RNAseq

(132). Tumors were TNM staged according to the guidelines of the Union international contre le cancer (UICC). (**C**) CB_1 mRNA was strongly down-regulated in tumors but increased with disease severity. (**D**) GPR55 mRNA, in contrast, decreased with stage. (**A**-**D**) Statistical analysis was done by one-way ANOVA followed by Tukey's posthoc test. Data points show values obtained from individual mice (**A**, **B**) or patient samples (**C**, **D**), and bars represent the mean values. * $p<0.05$, ** $p<0.01$, *** $p<0.001$ RNAseq raw data were provided by the OncoTrack consortium. The figure has been adapted from (1).

3.5.2 Epigenetic changes in *CNR1* and *GPR55* in CRC patients

A possible explanation for the aforementioned down-regulation of CB_1 expression in tumor tissue compared to control tissue was given by Wang *et al*. – epigenetic hypermethylation of the *CNR1* promoter resulted in reduced transcription in their patient cohort (101). To further elucidate these findings, the methylation status of *CNR1* and *GPR55* was assessed in our cohort of CRC patients. Indeed, *CNR1* was found to have a CpG island-associated promoter (**Figure 24** A) that was characterized by low DNA methylation in healthy colonic mucosa, i.e. the fraction of methylated cells ("β") was <0.11 in all CpG's in the promoter region in the control samples. In tumor samples, however, six analyzed CpG's were significantly hypermethylated ($\Delta\beta>0.04$, $p<0.01$). These CpG's are located at -755 to +268 with regard to the transcription start site (hg19 coordinates 88875844 to 88875398). Additionally, differences at CpG's within the 5'-untranslated region (5'-UTR) and the gene body were observed. These CpG's are not part of CpG islands but rather located in open sea regions. In control samples, these regions were characterized by much higher methylation ($\beta>0.54$). In tumor samples, however, ten CpG's were substantially hypomethylated in this region ($\Delta\beta=0.04$-0.32, $p<0.001$). This phenotype is consistent with the idea that *CNR1* is actively transcribed in both CRC and healthy controls, but that transcription is being nuanced toward down-regulation in CRC samples. In contrast, *GPR55* does not have CpG islands and exhibited a rather global decrease in methylation (**Figure 24** B). Four of the analyzed CpGs were significantly less methylated in tumor samples as compared to control tissue ($\Delta\beta=0.03$-0.07, $p<0.01$). These observations have also been reported previously (1).

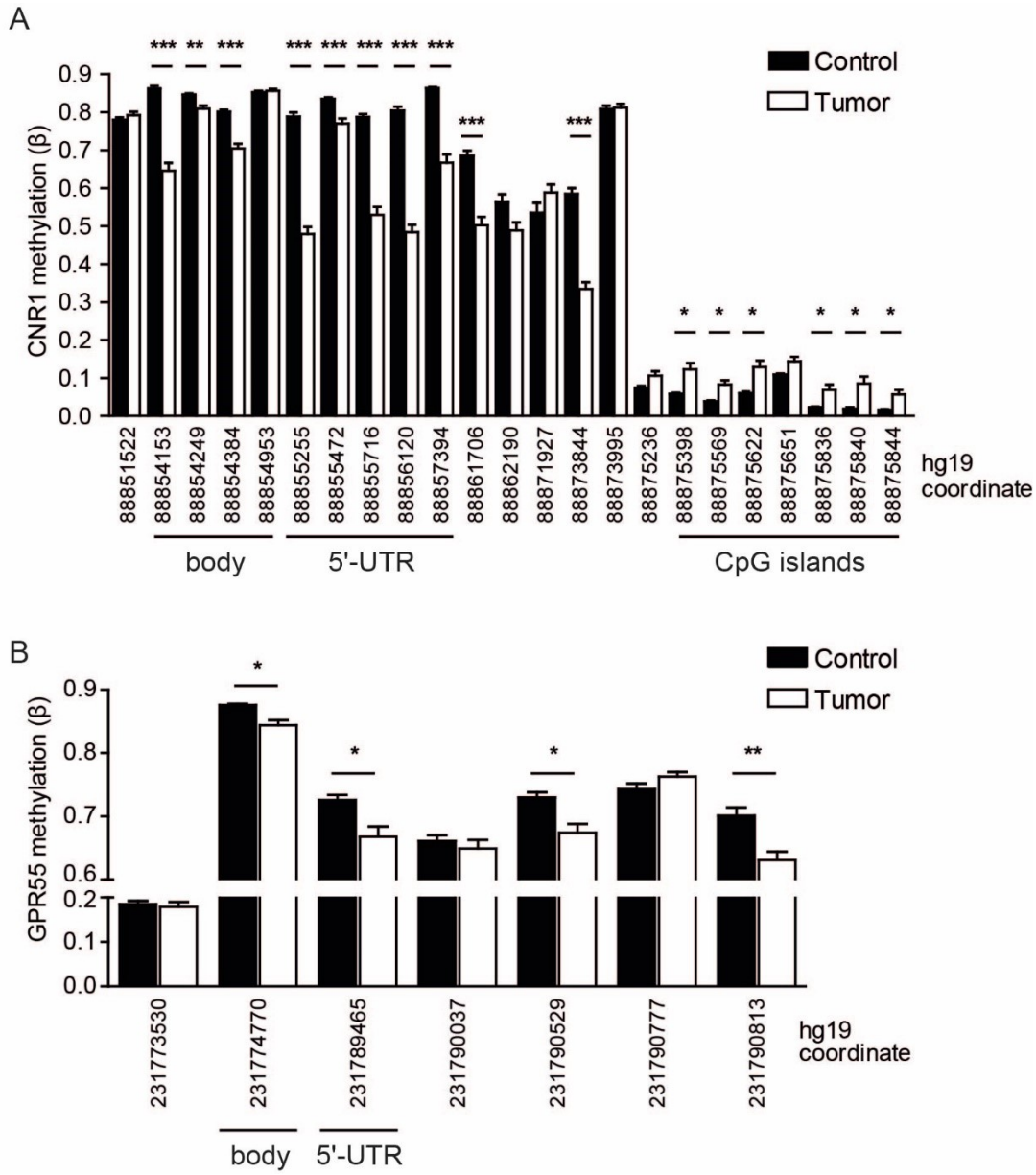

Figure 24. *Methylation of* CNR1 *and* GPR55 *is differentially regulated in CRC patients.*

The methylation status of *CNR1* and *GPR55* DNA was assessed in tumor samples (n=81, white bars) and in adjacent control tissue (n=67, black bars). Each set of bars shows the mean + SEM degree of methylation in one CpG. The hg19 coordinate of each CpG is indicated by the x-axis label. Raw data were provided by L. Stirling, who also performed the statistical analysis as reported in detail elsewhere (132). (**A**) In tumor samples, *CNR1* methylation was increased at CpG islands surrounding the promoter region, whereas it was decreased at CpG's located in the body of the gene. (**B**) *GPR55* lacks CpG islands and rather exhibited a global decrease in methylation in tumor samples. Four CpG's including the one located in the body of the gene showed significantly decreased methylation. * $p<0.01$, ** $p<0.001$, *** $p<0.0001$ The figure and its legend have been adapted from (1).

3.5.3 DNA hypomethylation increases GPR55 expression levels

To examine the effect of epigenetic demethylation on the expression of GPR55, six colon cancer cell lines were treated with the demethylating agent 5-Aza-dC. The methylation status of GPR55 was then assessed in three regions of interest of interest (gene body, 5'-UTR, and upstream of the transcription start site) using bisulfite sequencing. *GPR55* was heavily methylated in untreated colon cancer cell lines (**Figure 25** A). SW480 cells, however, showed a slightly lower degree of methylation at CpG's in the gene body and the 5'-UTR compared to the other cell lines. Intriguingly, SW480 cells also expressed ~55-fold more GPR55 mRNA (see **Figure 9** A). Treatment with 5-Aza-dC caused a reduction of methylation in 4 out of 6 examined cell lines, i.e. DLD-1, HCT116, SW620, and HT29 cells. The methylation status of SW480 and CaCo-2 cells was not altered after treatment with the demethylating agent.

Concomitantly with the decrease in methylation, an increase in GPR55 mRNA expression was observed in DLD-1, HCT116, SW620, and HT29 cells (**Figure 25** B). In SW480 and Caco-2 cells unaltered degrees of methylation after the treatment with 5-Aza-dC resulted in unchanged GPR55 expression levels. Alterations in epigenetic methylation thus seem to have an effect on GPR55 mRNA expression.

Bisulfite sequencing was performed in cooperation with E. Heitzer and R. Graf from the Institute of Human Genetics (Medical University of Graz). The data obtained from these experiments have been reported in a similar fashion in the original research article that originated from this study (1).

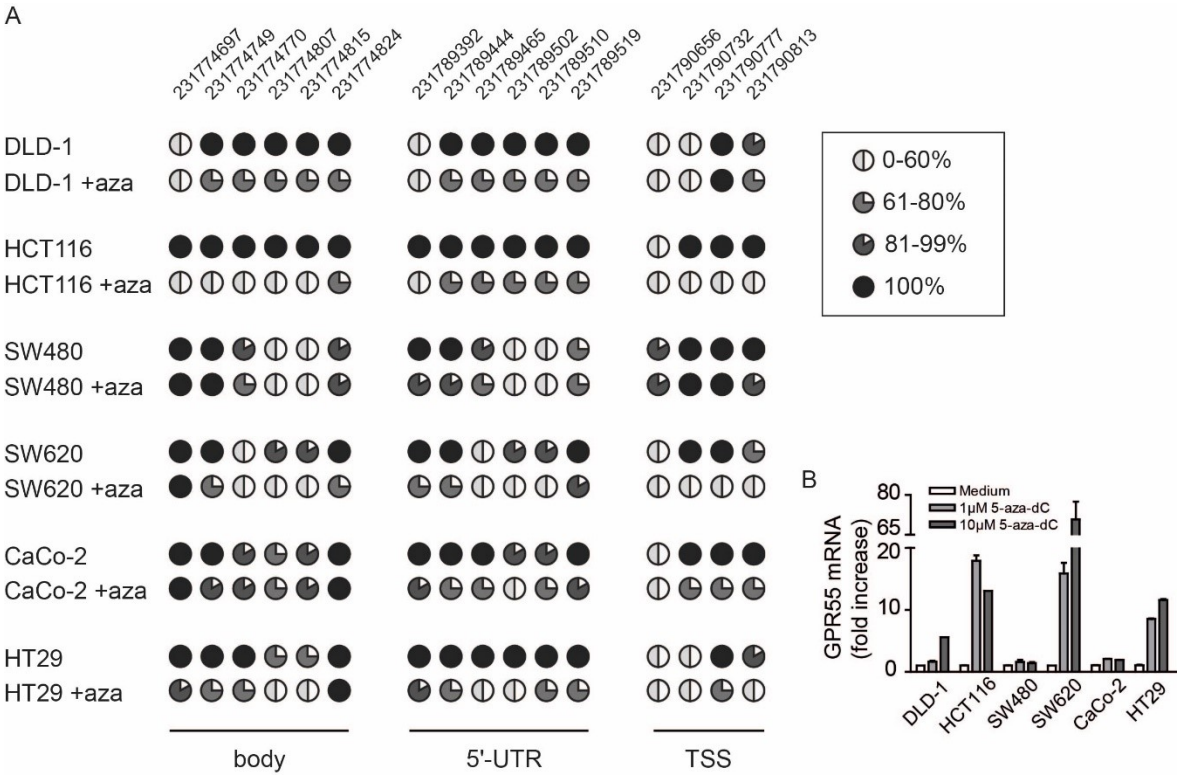

Figure 25. *Epigenetic changes in* GPR55 *in colon cancer cell lines.*
(**A**) The methylation status of *GPR55* was assessed in three regions of interest that have been determined from the data obtained from CRC patients: one in the gene body, one in the 5'-UTR, and one upstream of the transcription start site (TSS). In each region of interest four to six CpG's were analyzed (hg19 coordinate as indicated on top). Pie charts represent the amount of methylation in a single CpG as assessed by bisulfite sequencing. *GPR55* was heavily methylated in all colon cancer cell lines (upper rows). Treatment with 5-Aza-dC (aza) reduced epigenetic methylation in DLD-1, HCT116, SW620, and HT29 cells. (**B**) Accordingly, GPR55 mRNA levels were increased in those four cell lines after treatment with 5-Aza-dC but not in SW480 and CaCo-2 cells. Data shown are means + SEM of three independent experiments, reference gene: *HPRT1*. The figure has been adapted from (1).

4. DISCUSSION

Cannabinoids are currently used in medicine for pain relief after spastic attacks in multiple sclerosis, stimulation of appetite in HIV/aids patients, and for the reduction of nausea and vomiting induced by chemotherapy (146). Over the last years, however, a plethora of preclinical studies have been published that report possible anti-tumorigenic properties of cannabinoids and related substances. Several recent review articles summarize these findings, thereby highlighting the great potential of cannabinoids in the treatment of cancer (8,15,115,147–158). The majority of authors conclude that experimental evidence obtained from cell-based assays is very promising, i.e. cannabinoids show anti-proliferative, pro-apoptotic, anti-angiogenic, anti-migratory, and anti-invasive properties *in vitro*. Data from *in vivo* models are more scarce and paint a rather complicated picture leading the authors to conclude that the complexity of the endocannabinoid system needs to be further elucidated, before the therapeutic potential of medical marijuana can be fully exploited.

Until a few years ago, the endocannabinoid system was defined as comprising the two cannabinoid receptors CB_1 and CB_2, certain endocannabinoids (e.g. AEA and 2-AG), as well as the endocannabinoid synthesizing and degrading enzymes. Recent discoveries of receptors responsive to cannabinoids whose endogenous ligands, however, are not cannabinoids have challenged the perception of the endocannabinoid system being a confined system. Endocannabinoid-like compounds (i.e. mediators belonging to the same chemical class as the endocannabinoids with targets other than $CB_{1/2}$) have also been discovered and the term “endocannabinoidome” has been coined to describe the whole entity (12). It has become evident that our understanding of this complex system has to increase drastically before its great therapeutic potential can be exploited. Accordingly, the aim of this thesis was to elucidate the role of the atypical cannabinoid receptor GPR55 and to further investigate the role of classical cannabinoid receptor CB_1 in colorectal carcinogenesis.

4.1 GPR55 exerts its tumor-promoting function via modulation of the tumor microenvironment

To assess whether GPR55 plays a tumor-promoting or suppressing role in CRC, the AOM+DSS-driven model of CAC was applied to GPR55$^{-/-}$ mice and wild-type littermates. Genetic deletion of GPR55 resulted in a significantly reduced tumor burden in the colon, i.e. GPR55$^{-/-}$ mice had less tumors and, accordingly, smaller total tumor areas. To examine whether the results obtained after genetic ablation of GPR55 could be mimicked with a pharmacological approach, CD1 mice were subjected to the protocol of AOM+DSS-induced CAC and given CID16020046 or vehicle control. In this experiment, CD1 mice were the preferred strain of mice because they are more susceptible to the AOM+DSS model than C57BL/6 mice (159) meaning that the rate of non-responders, i.e. mice that do not develop any tumors, and the mortality caused by the protocol is greatly reduced in CD1 mice. Pharmacological inhibition of GPR55 gave similar results to the afore mentioned experiment with GPR55$^{-/-}$ mice, i.e. CID16020046 treated mice had lower tumor numbers and smaller tumor areas than vehicle treated mice. Since GPR55 has been reported to play a pro-inflammatory role in mouse models of colitis (83) and DSS-induced inflammation drives tumor growth in the CAC model, GPR55$^{-/-}$ mice and wild-type littermates were also subjected to a model of CRC that is independent of inflammation, i.e. the AOM-induced model of spontaneous tumor progression. Here, GPR55$^{-/-}$ mice again presented with less tumors and had smaller tumor areas than wild-type littermates. Thus, it can be concluded that GPR55 plays a tumor-promoting role in murine CRC.

To elucidate the mechanism by which GPR55 exerts its tumor-promoting function, *in vitro* experiments with colon cancer cell lines were performed. The endogenous GPR55 ligand LPI has been established to promote tumorigenesis by activating signaling cascades related to cell proliferation, migration, and survival (123). Recent work of our group had already revealed that GPR55 enhanced the migration and adhesion of colon cancer cells (125), but its role in cell proliferation had not yet been investigated. Therefore, cell viability assays were performed with two colon cancer cell lines, one with high GPR55 mRNA expression (SW480 cells) and one with low GPR55 mRNA expression (HCT116 cells). Interestingly, however, no effect of

GPR55 activation with LPI or antagonism with CID16020046 on cell proliferation was found in either cell line. Additionally, several GPR55-related signaling pathways were examined, but no effect of agonism or antagonism on signaling molecules could be detected. A possible explanation for these findings could lie in the purported cross-regulation of CB_1 and GPR55, i.e. GPR55 signaling was found to be inhibited when CB_1 and GPR55 were co-expressed in HEK293 cells (43). HCT116 and SW480 cells express both receptors and thus it is possible that GPR55 signaling is inhibited in the presence of CB_1. Therefore, GPR55 was stably over-expressed in HCT116 and SW480 cells and cell viability assays revealed that this, indeed, led to a growth advantage of GPR55 over-expressing cells compared to native cells. Concomitantly, both HCT55 and SW55 had increased basal expression levels of phosphorylated ERK1/2 compared to their native counterparts. Treatment with LPI (1 µM) further increased ERK1/2-phosphorylation in both over-expressing cell lines. Interestingly, however, cell viability was still not enhanced by LPI in these cell lines (data not shown), although the activation of signaling cascades was apparent. Treatment with CID16020046 decreased basal expression levels of phosphorylated ERK1/2 in HCT55 and SW55 cells, but not in HCT116 and SW480 cells. These data suggest that GPR55 can only be manipulated pharmacologically when it is expressed several fold higher than CB_1. Whether CB_1 actually inhibits GPR55 signaling in native colon cancer cells, however, still needs to be established.

To further elucidate the tumor-promoting role of GPR55 in CRC, tumor tissue collected from the AOM+DSS-induced model of CAC was analyzed. As summarized in **Figure 20**, several alterations were observed between tumors of $GPR55^{-/-}$ mice and wild-type littermates that, together, could be responsible for the differences in tumor burden in the two experimental groups. In fact, tumors of $GPR55^{-/-}$ mice exhibited modifications in the tumor microenvironment that constituted of altered leukocyte populations and a concomitantly reduced expression of tumor-promoting factors. For instance, reduced expression of the myeloid cell-recruiting chemokine CCL2 was observed. Deletion of CCL2 has been reported to reduce the recruitment of myeloid-derived suppressor cells (MDSCs) in colitis-associated CRC (140). In line with this finding, reduced numbers of monocytic MDSCs were observed in $GPR55^{-/-}$ tumors. MDSCs suppress immune responses mediated by $CD4^+$ and $CD8^+$ T cells by inhibiting T cell proliferation, migration and function (160). Increased

numbers of both $CD4^+$ and $CD8^+$ T cells were found to be present in tumors of $GPR55^{-/-}$ mice which could be a consequence of reduced amounts of MDSCs in the tumor microenvironment. Importantly, $CD3^+$ lymphocytes have been shown to be beneficial in CRC patients since increased numbers of $CD3^+$ cells were associated with an increased disease-free survival (145). Furthermore, it was observed that COX-2, a promising target in the prevention of CRC (97,161) and shown to be up-regulated in tumors of the CAC model compared to non-tumor and healthy colonic tissue, was expressed at lower levels in tumors of $GPR55^{-/-}$ mice as compared to tumors of wild-type littermates. Subsequent analysis of COX-2-derived mediators revealed that, indeed, $PGF_{2\alpha}$ and TXB_2, which have both been attributed tumor-promoting functions (143,144) were also expressed at lower levels in $GPR55^{-/-}$ tumors. Additionally it was found that STAT3 signaling, which has been established to drive colon carcinogenesis (91,142), was reduced in tumors of $GPR55^{-/-}$ mice, which could partly be due to diminished CCL2-MDSC signaling (140). Cytokine analysis further revealed increased levels of IL-5, IL-10, and IL-12 in tumors of $GPR55^{-/-}$ mice, which might be caused by increased numbers of T cells present in these tumors (97). While the role of IL-5 in CRC has not been fully clarified yet, clinical trials using recombinant human IL-10 (ClinicalTrials.gov identifier: NCT02009449) and IL-12 (NCT01417546) in solid tumors including CRC are currently ongoing. Taken together, the data obtained from the tumor tissue analysis suggest that genetic deletion of GPR55 modulates the tumor microenvironment and shapes it towards tumor rejection.

Further evidence for the involvement of GPR55 in the modulation of the tumor microenvironment rather than a straight-forward role in cell proliferation is provided by the xenograft experiment that was performed. HCT116 cells, which are colorectal carcinoma cells of epithelial origin, were grafted into immunodeficient SCID mice. Antagonism of GPR55 with CID16020046, however, did not reduce tumor growth in this model. In light of the observations described above, i.e. that GPR55 agonism and antagonism had no effect on the proliferation of cultured HCT116 cells, this finding supports the notion that GPR55 does not exert its tumor-promoting function in CRC via epithelial cells. On the contrary, it could even be argued that the ineffectiveness of CID16020046 in the xenograft model was due to the absence of functional T lymphocytes in SCID mice (162). In line with this, WIN 55,212-2 (a non-

selective $CB_{1/2}$ agonist) and JWH133 (a CB_2-selective agonist) had previously been reported to have more pronounced anti-tumor effects on xenografts in immunocompetent mice than on those generated in immunodeficient mice (54). Accordingly, these results would confirm that GPR55 exerts its function by shaping the tumor microenvironment through alterations in recruited leukocyte populations.

This conclusion is further supported by the analysis of the tumor distribution in the CAC model of $GPR55^{-/-}$ mice and wild-type littermates. As detailed in **Figure 5 B**, tumors of all sizes were present in lower numbers in $GPR55^{-/-}$ mice than in wild-type mice. If GPR55 were to mainly affect cell proliferation, one would expect knockout mice to present with smaller tumors rather than less tumors which would result in a shift of the distribution to the left, i.e. an increase in smaller tumors and a decrease in larger tumors compared to wild-types (134). Since, instead, a decrease in tumors of all sizes is observed it can again be postulated that genetic ablation of GPR55 results in a rather tumor-rejecting microenvironment leading to a better clearance of beginning tumors. Interestingly, similar observations have also been made when $GPR55^{-/-}$ mice and wild-type littermates were subjected to a model of skin cancer, the only other *in vivo* cancer model with $GPR55^{-/-}$ mice reported to date (120). Here, $GPR55^{-/-}$ mice also had significantly less papillomas and carcinomas than the wild-types but there was no difference in the size of tumors between the two groups (120).

4.2 CB_1 has an opposing role to GPR55 in CRC

CB_1 has been reported to act as tumor-suppressor in a genetic mouse model of intestinal cancer since the genetic deletion of CB_1 in $Apc^{Min/+}$ mice caused a strong increase in polyps of the small intestine and a moderate increase in polyps of the colon (101). To assess whether CB_1 would also act as tumor-suppressor in chemically induced models of CRC, $CB_1^{-/-}$ mice and wild-type littermates were subjected to the AOM+DSS-induced model of CAC as well as the model of spontaneous tumor progression. Indeed, genetic deletion of CB_1 led to an increased tumor burden in both experimental models, i.e. $CB_1^{-/-}$ mice had more tumors than

wild-type littermates and accordingly, larger total tumor areas were detected. These findings, therefore, corroborate the observations made by Wang and colleagues (101).

Since CB_1 and GPR55 appear to have opposing roles in CRC, i.e. CB_1 seems to act as tumor-suppressor whereas GPR55 seems to act as tumor-promoter, a CB_1/GPR55 double knockout mouse was created. When subjected to the AOM+DSS-induced model of CAC, no differences in tumor burden were found between CB_1/GPR55 double knockout mice and wild-type littermates thereby confirming that CB_1 and GPR55 regulate colon carcinogenesis in an opposing manner.

4.3 CB_1 and GPR55 are differentially regulated in CRC

Previous publications had reported that the tumor-suppressing function of CB_1 might be lost in tumor tissue because of translational silencing of the receptor (101,102,163). Therefore, receptor expression was analyzed in tumor and non-tumor tissue collected from mice that had been subjected to the CAC model. Additionally, receptor expression was analyzed in colonic tissue of healthy control mice. While CB_1 appeared up-regulated in inflamed, non-tumor tissue and down-regulated in tumor lesions, GPR55 was found to be down-regulated in non-tumor tissue and up-regulated in tumors when compared to healthy control colon. These findings reveal a differential regulation of CB_1 and GPR55 and corroborate the hypothesis that colonic tumor growth is facilitated by the absence of tumor-suppressing CB_1 and the presence of tumor-promoting GPR55.

Importantly, the same regulatory pattern of CB_1 expression was observed in the tissues of both wild-type and $GPR55^{-/-}$ mice. This finding is particularly noteworthy because it shows that the genetic ablation of GPR55 per se had no effects on CB_1 expression. Accordingly, it is thus feasible that the above described effects on colon carcinogenesis in $GPR55^{-/-}$ mice are indeed caused by the absence of GPR55, rather than resulting from compensatory effects exerted by CB_1.

Since the reason for the down-regulation of CB_1 expression in tumors of CRC patients has been shown to be a result of epigenetic hypermethylation of the *CNR1* promoter (101), the methylation status of *GPR55* and *CNR1* was assessed in a cohort of 86 CRC patients. In accordance with previous reports (101), DNA methylation analysis revealed a strong increase in methylation of CpG's located in the CpG islands of *CNR1* in CRC samples compared to control tissue. Contrarily, a decrease in methylation of *GPR55* was found in tumor samples. Alterations in DNA methylation are ubiquitous in human cancers, with promoter CpG islands often showing hypermethylation that occurs in the context of a global decrease in methylation (164). Increased promoter cytosine methylation has been established to silence gene expression. *CNR1* promoter hypermethylation, therefore, is very likely to contribute to colon carcinogenesis through silencing of tumor-suppressing CB_1. GPR55 on the other hand does not have CpG islands in the promoter region and is, perhaps, subject to the genome-wide hypomethylation frequently observed in cancer (165).

In accordance with the observed promoter hypermethylation, mRNA expression analysis revealed a strong down-regulation of CB_1 in CRC samples compared to control tissue. Interestingly, however, CB_1 expression levels were found to increase with disease severity, i.e. from UICC stage I to stage IV. GPR55 expression, in contrast, decreased with CRC stage in this cohort. These findings differ from other studies which stated that GPR55 mRNA expression was increased in several human tumors, e.g. pancreatic neoplasias and glioblastomas, as compared to the control tissues (121). GPR55 expression levels, however, have also been shown to correlate with aggressiveness (121) and, indeed, high GPR55 expression was associated with a significantly reduced disease-free survival in CRC, confirming the tumor-promoting role of GPR55 in CRC.

CB_1 and GPR55, thus, seem to be subject to differential regulation and appear to play contrary roles in CRC. It could, therefore, be hypothesized that the homeostatic balance of the intestine under physiologic conditions (14,166) is maintained by the ~5-fold higher expression levels of CB_1 compared to GPR55 mRNA in healthy human colonic tissue (compare controls in **Figure 23 C** with controls in **Figure 23 D**). Under pathological conditions, epigenetic hypermethylation of the *CNR1*

promoter causes a drastic down-regulation of CB_1, leaving GPR55 to be expressed at severalfold higher levels than CB_1 in CRC tumors (compare stage I data in **Figure 23 C** with stage I data in **Figure 23 D**). Bearing in mind that GPR55 signaling was shown to be inhibited in the presence of CB_1 (43), one could further reason that the tumor-promoting properties of GPR55 are suppressed in the healthy colon by the strong abundance of CB_1. In tumor tissue, however, the ratio of CB_1 over GPR55 mRNA levels is inversed and GPR55 could thus possibly show increased activity even though the expression of the receptor itself is barely altered. Whether data obtained on mRNA level can also be observed on protein level and whether this proposed mechanism is indeed true still remains to be elucidated.

4.4 GPR55 and the endocannabinoid system in CRC

GPR55 has been reported to be responsive to certain cannabinoids (27), but its endogenous ligand was found to be LPI (33), a non-cannabinoid lipid. Therefore, GPR55 is currently considered an atypical cannabinoid receptor or part of the extended endocannabinoid system, the "endocannabinoidome" (12,25). In the gastrointestinal tract, the endocannabinoid system is thought to play a role in maintaining homeostasis since endocannabinoids are synthesized rapidly on demand (166,167). Endocannabinoids were found to be expressed at much higher levels in human CRC tissue (98,99) as well as in precancerous lesions in a murine model (107) as compared to healthy colonic tissue. Pharmacological inhibition of FAAH, i.e. the primary AEA-degrading enzyme, reduced the development of precancerous lesions, and furthermore, this effect was also mimicked by the non-selective, synthetic CB_1/CB_2 agonist HU210 (107). It was therefore concluded, that endogenous cannabinoids have anti-tumor properties (98,107,168). In the present study, it was indeed observed that the levels of endocannabinoids AEA and 2-AG were strongly increased in tumors of wild-type mice compared to healthy control colon. Endocannabinoid-like substances OEA and 1-AG were also strongly over-expressed in these tumors. In tumors of $GPR55^{-/-}$ mice, however, expression levels of AEA, OEA, PEA, 1-AG, and 2-AG were significantly lower than in tumors of wild-type mice. In fact, in $GPR55^{-/-}$ mice the expression levels of all measured

compounds were barely increased in tumor tissue compared to healthy colon. A possible explanation for this finding could be that endocannabinoids and related substances are either produced at a lesser extent or metabolized more rapidly in tumors of GPR55$^{-/-}$ mice. Increased degradation of endocannabinoids could be facilitated by classical endocannabinoid-degrading enzymes, i.e. FAAH for AEA and MGL for 2-AG; or through pathways involving oxidation and subsequent synthesis to prostamides and prostaglandin glycerol esters, which serve as precursors for prostaglandins (9,12,155,169). Since assessing enzyme activities, however, was not the focus of this project, this reasoning is rather speculative.

4.5 Conclusion

In conclusion, data presented in this thesis suggest that GPR55 plays an opposing role to CB_1 in colon carcinogenesis with GPR55 acting as tumor-promoter and CB_1 as tumor-suppressor. The absence of GPR55 was found to modulate the tumor microenvironment towards a tumor-rejecting phenotype. Additionally, GPR55 appears to play a role in the regulation of expression levels of endocannabinoids and related substances in colonic tumors. These findings highlight the importance of research needed on the entire “endocannabinoidome” rather than just the classical components of the endocannabinoid system before targeting this system for future therapy of colorectal cancer.

5. REFERENCES

1. Hasenoehrl C, Feuersinger D, Sturm EM, Bärnthaler T, Heitzer E, Graf R, et al. G protein-coupled receptor GPR55 promotes colorectal cancer and has opposing effects to cannabinoid receptor 1. Int J Cancer. 2017;accepted August 22, 2017.

2. Gaoni Y, Mechoulam R. Isolation, Structure, and Partial Synthesis of an Active Constituent of Hashish. J Am Chem Soc. 1964 Apr;86(8):1646–7.

3. Matsuda LA, Lolait SJ, Brownstein MJ, Young AC, Bonner TI. Structure of a cannabinoid receptor and functional expression of the cloned cDNA. Nature. 1990 Aug 9;346(6284):561–4.

4. Munro S, Thomas KL, Abu-Shaar M. Molecular characterization of a peripheral receptor for cannabinoids. Nature. 1993 Sep 2;365(6441):61–5.

5. Sugiura T, Kondo S, Sukagawa A, Nakane S, Shinoda A, Itoh K, et al. 2-Arachidonoylglycerol: a possible endogenous cannabinoid receptor ligand in brain. Biochem Biophys Res Commun. 1995 Oct 4;215(1):89–97.

6. Howlett AC, Barth F, Bonner TI, Cabral G, Casellas P, Devane WA, et al. International Union of Pharmacology. XXVII. Classification of cannabinoid receptors. Pharmacol Rev. 2002 Jun;54(2):161–202.

7. Pacher P, Kunos G. Modulating the endocannabinoid system in human health and disease - Successes and failures. FEBS J. 2013;280(9):1918–43.

8. Pisanti S, Picardi P, D'Alessandro A, Laezza C, Bifulco M. The endocannabinoid signaling system in cancer. Trends Pharmacol Sci. 2013;34(5):273–82.

9. Lu HC, Mackie K. An introduction to the endogenous cannabinoid system. Biol Psychiatry. 2016;79(7):516–25.

10. Pertwee RG, Howlett AC, Abood ME, Alexander SPH, Di Marzo V, Elphick MR, et al. International Union of Basic and Clinical Pharmacology . LXXIX . Cannabinoid Receptors and Their Ligands : Beyond CB 1 and CB 2. Pharmacol Rev. 2010;62(4):588–631.

11. Fonseca BM, Costa MA, Almada M, Correia-da-Silva G, Teixeira NA. Endogenous cannabinoids revisited: a biochemistry perspective. Prostaglandins Other Lipid Mediat. 2013 Apr;102–103(228):13–30.

12. Di Marzo V, Piscitelli F. The Endocannabinoid System and its Modulation by Phytocannabinoids. Neurotherapeutics. 2015;12(4):692–8.

13. Grabner GF, Zimmermann R, Schicho R, Taschler U. Monoglyceride lipase as a drug target: At the crossroads of arachidonic acid metabolism and endocannabinoid signaling. Pharmacol Ther. 2017;

14. Hasenoehrl C, Taschler U, Storr M, Schicho R. The gastrointestinal tract - a central organ of cannabinoid signaling in health and disease. Neurogastroenterol Motil. 2016 Aug 26;28(12):1765–80.

15. Maccarrone M, Bab I, Bíró T, Cabral GA, Dey SK, Di Marzo V, et al. Endocannabinoid signaling at the periphery: 50 years after THC. Trends Pharmacol Sci. 2015;36(5):277–96.

16. Wang D, Dubois RN. Eicosanoids and cancer. Nat Rev Cancer. 2010 Mar;10(3):181–93.

17. Fezza F, Bari M, Florio R, Talamonti E, Feole M, Maccarrone M. Endocannabinoids, related compounds and their metabolic routes. Molecules. 2014 Oct 24;19(11):17078–106.

18. Di Marzo V. The endocannabinoid system: Its general strategy of action, tools for its pharmacological manipulation and potential therapeutic exploitation. Pharmacol Res. 2009;60(2):77–84.

19. Zygmunt PM, Petersson J, Andersson DA, Chuang H, Sørgård M, Di Marzo

V, et al. Vanilloid receptors on sensory nerves mediate the vasodilator action of anandamide. Nature. 1999 Jul 29;400(6743):452–7.

20. Toth A, Blumberg PM, Boczan J. Anandamide and the Vanilloid Receptor (TRPV1). In: Vitamins and hormones. 2009. p. 389–419.

21. O'Sullivan SE. An update on PPAR activation by cannabinoids. Br J Pharmacol. 2016 Jun;173(12):1899–910.

22. Hasenoehrl C, Storr M, Schicho R. Cannabinoids for treating inflammatory bowel diseases: where are we and where do we go? Expert Rev Gastroenterol Hepatol. 2017;11(4):329–37.

23. Esposito G, Filippis D De, Cirillo C, Iuvone T, Capoccia E, Scuderi C, et al. Cannabidiol in inflammatory bowel diseases: a brief overview. Phytother Res. 2013 May;27(5):633–6.

24. Ryberg E, Larsson N, Sjögren S, Hjorth S, Hermansson N-O, Leonova J, et al. The orphan receptor GPR55 is a novel cannabinoid receptor. Br J Pharmacol. 2007;152:1092–101.

25. Lauckner JE, Jensen JB, Chen H-YY, Lu H-CC, Hille B, Mackie K. GPR55 is a cannabinoid receptor that increases intracellular calcium and inhibits M current. Proc Natl Acad Sci U S A. 2008 Feb 19;105(7):2699–704.

26. Waldeck-Weiermair M, Zoratti C, Osibow K, Balenga N, Goessnitzer E, Waldhoer M, et al. Integrin clustering enables anandamide-induced Ca2+ signaling in endothelial cells via GPR55 by protection against CB1-receptor-triggered repression. J Cell Sci. 2008;121:1704–17.

27. Sharir H, Console-Bram L, Mundy C, Popoff SN, Kapur A, Abood ME. The endocannabinoids anandamide and virodhamine modulate the activity of the candidate cannabinoid receptor GPR55. J Neuroimmune Pharmacol. 2012;7:856–65.

28. McPartland JM, Matias I, Di Marzo V, Glass M. Evolutionary origins of the

endocannabinoid system. Gene. 2006 Mar 29;370:64–74.

29. Henstridge CM. Off-target cannabinoid effects mediated by GPR55. Pharmacology. 2012;89:179–87.

30. Noguchi K, Ishii S, Shimizu T. Identification of p2y9/GPR23 as a Novel G Protein-coupled Receptor for Lysophosphatidic Acid, Structurally Distant from the Edg Family. J Biol Chem. 2003 Jul 3;278(28):25600–6.

31. Kotarsky K, Boketoft A, Bristulf J, Nilsson NE, Norberg A, Hansson S, et al. Lysophosphatidic acid binds to and activates GPR92, a G protein-coupled receptor highly expressed in gastrointestinal lymphocytes. J Pharmacol Exp Ther. 2006 Aug;318(2):619–28.

32. Kotsikorou E, Madrigal KE, Hurst DP, Sharir H, Lynch DL, Heynen-Genel S, et al. Identification of the GPR55 Agonist Binding Site Using a Novel Set of High-Potency GPR55 Selective Ligands. Biochemistry. 2011 Jun 28;50(25):5633–47.

33. Oka S, Nakajima K, Yamashita A, Kishimoto S, Sugiura T. Identification of GPR55 as a lysophosphatidylinositol receptor. Biochem Biophys Res Commun. 2007 Nov 3;362(4):928–34.

34. Oka S, Toshida T, Maruyama K, Nakajima K, Yamashita A, Sugiura T. 2-Arachidonoyl-sn-glycero-3-phosphoinositol: A possible natural ligand for GPR55. J Biochem. 2009;145(1):13–20.

35. Henstridge CM, Balenga NA, Ford LA, Ross RA, Waldhoer M, Irving AJ. The GPR55 ligand L-alpha-lysophosphatidylinositol promotes RhoA-dependent Ca2+ signaling and NFAT activation. FASEB J. 2009;23:183–93.

36. Yamashita A, Oka S, Tanikawa T, Hayashi Y, Nemoto-Sasaki Y, Sugiura T. The actions and metabolism of lysophosphatidylinositol, an endogenous agonist for GPR55. Prostaglandins Other Lipid Mediat. 2013;107:103–16.

37. Sawzdargo M, Nguyen T, Lee DK, Lynch KR, Cheng R, Heng HHQ, et al.

Identification and cloning of three novel human G protein-coupled receptor genes GPR52, GPR53 and GPR55: GPR55 is extensively expressed in human brain. Mol Brain Res. 1999;64:193–8.

38. Balenga NA, Aflaki E, Kargl J, Platzer W, Schröder R, Blättermann S, et al. GPR55 regulates cannabinoid 2 receptor-mediated responses in human neutrophils. Cell Res. 2011;21(10):1452–69.

39. Kargl J, Brown AJ, Andersen L, Dorn G, Schicho R, Waldhoer M, et al. A selective antagonist reveals a potential role of G protein-coupled receptor 55 in platelet and endothelial cell function. J Pharmacol Exp Ther. 2013;346:54–66.

40. Henstridge CM, Balenga NA, Kargl J, Andradas C, Brown AJ, Irving AJ, et al. Minireview: recent developments in the physiology and pathology of the lysophosphatidylinositol-sensitive receptor GPR55. Mol Endocrinol. 2011 Nov;25(11):1835–48.

41. Schicho R, Storr M. A potential role for GPR55 in gastrointestinal functions. Curr Opin Pharmacol. 2012;12(6):653–8.

42. Anavi-Goffer S, Baillie G, Irving AJ, Gertsch J, Greig IR, Pertwee RG, et al. Modulation of L-alpha-Lysophosphatidylinositol/GPR55 Mitogen-activated Protein Kinase (MAPK) Signaling by Cannabinoids. J Biol Chem. 2012;287(1):91–104.

43. Kargl J, Balenga N, Parzmair GP, Brown AJ, Heinemann A, Waldhoer M. The cannabinoid receptor CB1 modulates the signaling properties of the lysophosphatidylinositol receptor GPR55. J Biol Chem. 2012;287:44234–48.

44. Martínez-Pinilla E, Reyes-Resina I, Oñatibia-Astibia A, Zamarbide M, Ricobaraza A, Navarro G, et al. CB1 and GPR55 receptors are co-expressed and form heteromers in rat and monkey striatum. Exp Neurol. 2014;261:44–52.

45. Moreno E, Andradas C, Medrano M, Caffarel MM, Pérez-Gómez E, Blasco-Benito S, et al. Targeting CB2-GPR55 receptor heteromers modulates cancer cell signaling. J Biol Chem. 2014;289:21960–72.

46. Balenga N, Martinez-Pinilla E, Kargl J, Schröder R, Peinhaupt M, Platzer W, et al. Heteromerization of GPR55 and cannabinoid CB 2 receptors modulates signalling. Br J Pharmacol. 2014;171:5387–406.

47. Gasperi V, Dainese E, Oddi S, Sabatucci A, Maccarrone M. GPR55 and its interaction with membrane lipids: comparison with other endocannabinoid-binding receptors. Curr Med Chem. 2013;20(i):64–78.

48. Sharir H, Abood ME. Pharmacological characterization of GPR55, a putative cannabinoid receptor. Pharmacol Ther. 2010;126(3):301–13.

49. Yang H, Zhou J, Lehmann C. GPR55 – a putative “type 3” cannabinoid receptor in inflammation. J Basic Clin Physiol Pharmacol. 2016;27(3):297–302.

50. Kotsikorou E, Sharir H, Shore DM, Hurst DP, Lynch DL, Madrigal KE, et al. Identification of the GPR55 antagonist binding site using a novel set of high-potency GPR55 selective ligands. Biochemistry. 2013;52:9456–69.

51. Kleberg K, Hassing HA, Hansen HS. Classical endocannabinoid-like compounds and their regulation by nutrients. BioFactors. 2014;40(4):363–72.

52. Burstein S. The elmiric acids: biologically active anandamide analogs. Neuropharmacology. 2008 Dec;55(8):1259–64.

53. Zhang X, Maor Y, Wang JF, Kunos G, Groopman JE. Endocannabinoid-like N-arachidonoyl serine is a novel pro-angiogenic mediator. Br J Pharmacol. 2010;160:1583–94.

54. Blázquez C, Carracedo A, Barrado L, Real PJ, Fernández-Luna JL, Velasco G, et al. Cannabinoid receptors as novel targets for the treatment of melanoma. FASEB J. 2006;20(14):2633–5.

55. Russo EB. Taming THC: Potential cannabis synergy and phytocannabinoid-terpenoid entourage effects. Br J Pharmacol. 2011;163(7):1344–64.

56. Dócs K, Mészár Z, Gonda S, Kiss-Szikszai A, Holló K, Antal M, et al. The ratio of 2-AG to its isomer 1-AG as an intrinsic fine tuning mechanism of CB1 receptor activation. Front Cell Neurosci. 2017;11(39):1–13.

57. Lutz B, Marsicano G, Maldonado R, Hillard CJ. The endocannabinoid system in guarding against fear, anxiety and stress. Nat Rev Neurosci. 2015 Nov 20;16(12):705–18.

58. Cabral GA, Ferreira GA, Jamerson MJ. Endocannabinoids and the Immune System in Health and Disease. In: Endocannabinoids, Handbook of Experimental Pharmacology. 2015. p. 185–211.

59. Coutts AA, Irving AJ, Mackie K, Pertwee RG, Anavi-Goffer S. Localisation of cannabinoid CB(1) receptor immunoreactivity in the guinea pig and rat myenteric plexus. J Comp Neurol. 2002 Jul 8;448(4):410–22.

60. Wright K, Rooney N, Feeney M, Tate J, Robertson D, Welham M, et al. Differential Expression of Cannabinoid Receptors in the Human Colon: Cannabinoids Promote Epithelial Wound Healing. Gastroenterology. 2005;129(2):437–53.

61. Duncan M, Davison JS, Sharkey KA. Review article: endocannabinoids and their receptors in the enteric nervous system. Aliment Pharmacol Ther. 2005 Oct 15;22(8):667–83.

62. Cani PD, Plovier H, Hul M Van, Geurts L, Delzenne NM, Druart C, et al. Endocannabinoids — at the crossroads between the gut microbiota and host metabolism. Nat Publ Gr. 2016;12(3):133–43.

63. Lee Y, Jo J, Chung HY, Pothoulakis C, Im E. Endocannabinoids in the gut. Am J Physiol - Gastrointest Liver Physiol. 2016;311(4):G655–66.

64. DiPatrizio N V. Endocannabinoids in the Gut. Cannabis Cannabinoid Res.

2016;1(1):67–77.

65. Izzo AA, Sharkey KA. Cannabinoids and the gut: New developments and emerging concepts. Pharmacol Ther. 2010;126(1):21–38.

66. Sharkey KA, Wiley JW. The Role of the Endocannabinoid System in the Brain–Gut Axis. Gastroenterology. 2016;151(2):252–66.

67. Cosnes J, Gowerrousseau C, Seksik P, Cortot A. Epidemiology and natural history of inflammatory bowel diseases. Gastroenterology. 2011;140(6):1785–94.

68. Engel MA, Neurath MF. New pathophysiological insights and modern treatment of IBD. J Gastroenterol. 2010;45(6):571–83.

69. D'Argenio G, Valenti M, Scaglione G, Cosenza V, Sorrentini I, Di Marzo V. Up-regulation of anandamide levels as an endogenous mechanism and a pharmacological strategy to limit colon inflammation. FASEB J. 2006;20:568–70.

70. Kimball ES, Schneider CR, Wallace NH, Hornby PJ. Agonists of cannabinoid receptor 1 and 2 inhibit experimental colitis induced by oil of mustard and by dextran sulfate sodium. Am J Physiol Gastrointest Liver Physiol. 2006;291(2):G364–71.

71. Storr MA, Keenan CM, Emmerdinger D, Zhang H, Yüce B, Sibaev A, et al. Targeting endocannabinoid degradation protects against experimental colitis in mice: Involvement of CB1 and CB2 receptors. J Mol Med. 2008 Aug;86(8):925–36.

72. Salaga M, Mokrowiecka A, Zakrzewski PK, Cygankiewicz A, Leishman E, Sobczak M, et al. Experimental colitis in mice is attenuated by changes in the levels of endocannabinoid metabolites induced by selective inhibition of fatty acid amide hydrolase (FAAH). J Crohn's Colitis. 2014;8(9):998–1009.

73. Alhouayek M, Lambert DM, Delzenne NM, Cani PD, Muccioli GG. Increasing

endogenous 2-arachidonoylglycerol levels counteracts colitis and related systemic inflammation. FASEB J. 2011;25(8):2711–21.

74. Storr MA, Keenan CM, Zhang H, Patel KD, Makriyannis A, Sharkey KA. Activation of the cannabinoid 2 receptor (CB2) protects against experimental colitis. Inflamm Bowel Dis. 2009;15(11):1678–85.

75. Jamontt JM, Molleman A, Pertwee RG, Parsons ME. The effects of d9-tetrahydrocannabinol and cannabidiol alone and in combination on damage, inflammation and in vitro motility disturbances in rat colitis. Br J Pharmacol. 2010;160(3):712–23.

76. Schicho R, Storr M. Topical and systemic cannabidiol improves trinitrobenzene sulfonic acid colitis in mice. Pharmacology. 2012;89:149–55.

77. Borrelli F, Aviello G, Romano B, Orlando P, Capasso R, Maiello F, et al. Cannabidiol, a safe and non-psychotropic ingredient of the marijuana plant Cannabis sativa, is protective in a murine model of colitis. J Mol Med. 2009;87(11):1111–21.

78. Pagano E, Capasso R, Piscitelli F, Romano B, Parisi OA, Finizio S, et al. An orally active Cannabis extract with high content in cannabidiol attenuates chemically-induced intestinal inflammation and hypermotility in the mouse. Front Pharmacol. 2016;7(341):1–12.

79. de Filippis D, Esposito G, Cirillo C, Cipriano M, de Winter BY, Scuderi C, et al. Cannabidiol reduces intestinal inflammation through the control of neuroimmune axis. PLoS One. 2011;6(12):1–8.

80. Borrelli F, Fasolino I, Romano B, Capasso R, Maiello F, Coppola D, et al. Beneficial effect of the non-psychotropic plant cannabinoid cannabigerol on experimental inflammatory bowel disease. Biochem Pharmacol. 2013;85(9):1306–16.

81. Romano B, Borrelli F, Fasolino I, Capasso R, Piscitelli F, Cascio M, et al. The

cannabinoid TRPA1 agonist cannabichromene inhibits nitric oxide production in macrophages and ameliorates murine colitis. Br J Pharmacol. 2013 May;169(1):213–29.

82. De Petrocellis L, Ligresti A, Moriello AS, Allarà M, Bisogno T, Petrosino S, et al. Effects of cannabinoids and cannabinoid-enriched Cannabis extracts on TRP channels and endocannabinoid metabolic enzymes. Br J Pharmacol. 2011 Aug;163(7):1479–94.

83. Stancic A, Jandl K, Hasenoehrl C, Reichmann F, Marsche G, Schuligoi R, et al. The GPR55 antagonist CID16020046 protects against intestinal inflammation. Neurogastroenterol Motil. 2015;27(10):1432–45.

84. Borrelli F, Romano B, Petrosino S, Pagano E, Capasso R, Coppola D, et al. Palmitoylethanolamide, a naturally occurring lipid, is an orally effective intestinal anti-inflammatory agent. Br J Pharmacol. 2015;172:142–58.

85. Sasso O, Migliore M, Habrant D, Armirotti A, Albani C, Summa M, et al. Multitarget fatty acid amide hydrolase/cyclooxygenase blockade suppresses intestinal inflammation and protects against nonsteroidal anti-inflammatory drug-dependent gastrointestinal damage. FASEB J. 2015 Jun 1;29(6):2616–27.

86. Alhouayek M, Bottemanne P, Subramanian K V., Lambert DM, Makriyannis A, Cani PD, et al. N-acylethanolamine-hydrolyzing acid amidase inhibition increases colon N-palmitoylethanolamine levels and counteracts murine colitis. FASEB J. 2015;29(2):650–61.

87. Alhouayek M, Muccioli GG. The endocannabinoid system in inflammatory bowel diseases: From pathophysiology to therapeutic opportunity. Trends Mol Med. 2012;18(10):615–25.

88. Izzo AA, Sharkey KA. Cannabinoids and the gut: new developments and emerging concepts. Pharmacol Ther. 2010 Apr;126(1):21–38.

89. Terzić J, Grivennikov S, Karin E, Karin M. Inflammation and colon cancer. Gastroenterology. 2010 Jun;138(6):2101–2114.e5.

90. Lakatos P-L, Lakatos L. Risk for colorectal cancer in ulcerative colitis: changes, causes and management strategies. World J Gastroenterol. 2008 Jul 7;14(25):3937–47.

91. Grivennikov S, Karin E, Terzic J, Mucida D, Yu G-Y, Vallabhapurapu S, et al. IL-6 and Stat3 are required for survival of intestinal epithelial cells and development of colitis-associated cancer. Cancer Cell. 2009 Feb 3;15(2):103–13.

92. Karin M, Greten FR. NF-kappaB: linking inflammation and immunity to cancer development and progression. Nat Rev Immunol. 2005 Sep 20;5(10):749–59.

93. Rustgi AK. The genetics of hereditary colon cancer. Genes Dev. 2007 Oct 15;21(20):2525–38.

94. Kuipers EJ, Grady WM, Lieberman D, Seufferlein T, Sung JJ, Boelens PG, et al. Colorectal cancer. Nat Rev Dis Prim. 2015;1:15065.

95. Siegel R, Desantis C, Jemal A. Colorectal Cancer Statistics, 2014. CA Cancer J Clin. 2014;64(1):104–17.

96. Le DT, Uram JN, Wang H, Bartlett BR, Kemberling H, Eyring AD, et al. PD-1 Blockade in Tumors with Mismatch-Repair Deficiency. N Engl J Med. 2015;372(26):2509–20.

97. Peddareddigari VG, Wang D, Dubois RN. The tumor microenvironment in colorectal carcinogenesis. Cancer Microenviron. 2010;3(1):149–66.

98. Ligresti A, Bisogno T, Matias I, De Petrocellis L, Cascio MG, Cosenza V, et al. Possible endocannabinoid control of colorectal cancer growth. Gastroenterology. 2003;125(3):677–87.

99. Chen L, Chen H, Li Y, Li L, Qiu Y, Ren J. Endocannabinoid and ceramide

levels are altered in patients with colorectal cancer. Oncol Rep. 2015;34:447–54.

100. Ye L, Zhang B, Seviour EG, Tao K xiong, Liu X hua, Ling Y, et al. Monoacylglycerol lipase (MAGL) knockdown inhibits tumor cells growth in colorectal cancer. Cancer Lett. 2011;307(1):6–17.

101. Wang D, Wang H, Ning W, Backlund MG, Dey SK, DuBois RN. Loss of cannabinoid receptor 1 accelerates intestinal tumor growth. Cancer Res. 2008 Aug 1;68(15):6468–76.

102. Cianchi F, Papucci L, Schiavone N, Lulli M, Magnelli L, Vinci MC, et al. Cannabinoid receptor activation induces apoptosis through tumor necrosis factor alpha-mediated ceramide de novo synthesis in colon cancer cells. Clin Cancer Res. 2008;14:7691–700.

103. Jung CK, Kang WK, Park JM, Ahn HJ, Kim SW, Oh ST, et al. Expression of the cannabinoid type I receptor and prognosis following surgery in colorectal cancer. Oncol Lett. 2013;5:870–6.

104. Gustafsson SB, Palmqvist R, Henriksson ML, Dahlin AM, Edin S, Jacobsson SOP, et al. High tumour cannabinoid CB 1 receptor immunoreactivity negatively impacts disease-specific survival in stage II microsatellite stable colorectal cancer. PLoS One. 2011;6(8):e23003.

105. Bedoya F, Rubio JC, Morales-Gutierrez C, Abad-Barahona A, Lora Pablos D, Meneu JC, et al. Single nucleotide change in the cannabinoid receptor-1 (CNR1) gene in colorectal cancer outcome. Oncology. 2009;76(6):435–41.

106. Martínez-Martínez E, Gómez I, Martín P, Sánchez A, Román L, Tejerina E, et al. Cannabinoids receptor type 2, CB2, expression correlates with human colon cancer progression and predicts patient survival. Oncoscience. 2015;2(2):131–41.

107. Izzo AA, Aviello G, Petrosino S, Orlando P, Marsicano G, Lutz B, et al.

Increased endocannabinoid levels reduce the development of precancerous lesions in the mouse colon. J Mol Med. 2008;86:89–98.

108. Aviello G, Romano B, Borrelli F, Capasso R, Gallo L, Piscitelli F, et al. Chemopreventive effect of the non-psychotropic phytocannabinoid cannabidiol on experimental colon cancer. J Mol Med. 2012;90(8):925–34.

109. Romano B, Borrelli F, Pagano E, Cascio MG, Pertwee RG, Izzo AA. Inhibition of colon carcinogenesis by a standardized Cannabis sativa extract with high content of cannabidiol. Phytomedicine. 2014;21(5):631–9.

110. Borrelli F, Pagano E, Romano B, Panzera S, Maiello F, Coppola D, et al. Colon carcinogenesis is inhibited by the TRPM8 antagonist cannabigerol, a Cannabis-derived non-psychotropic cannabinoid. Carcinogenesis. 2014;35(12):2787–97.

111. Kargl J, Haybaeck J, Stančić A, Andersen L, Marsche G, Heinemann A, et al. O-1602, an atypical cannabinoid, inhibits tumor growth in colitis-associated colon cancer through multiple mechanisms. J Mol Med. 2013;91:449–58.

112. Santoro A, Pisanti S, Grimaldi C, Izzo A a, Borrelli F, Proto MC, et al. Rimonabant inhibits human colon cancer cell growth and reduces the formation of precancerous lesions in the mouse colon. Int J Cancer. 2009;125:996–1003.

113. Thapa D, Kang Y, Park P-H, Noh SK, Lee YR, Han SS, et al. Anti-tumor Activity of the Novel Hexahydrocannabinol Analog LYR-8 in Human Colorectal Tumor Xenograft Is Mediated through the Inhibition of Akt and Hypoxia-Inducible Factor-1α Activation. Biol Pharm Bull. 2012;35(6):924–32.

114. Izzo AA, Muccioli GG, Ruggieri MR, Schicho R. Endocannabinoids and the Digestive Tract and Bladder in Health and Disease. In: Pertwee RG, editor. Handbook of Experimental Pharmacology. Endocannab. Springer International Publishing Switzerland; 2015. p. 423–47.

115. Velasco G, Sánchez C, Guzmán M. Towards the use of cannabinoids as antitumour agents. Nat Rev Cancer. 2012;12(6):436–44.

116. Greenhough A, Patsos H a., Williams AC, Paraskeva C. The cannabinoid Δ9-tetrahydrocannabinol inhibits RAS-MAPK and PI3K-AKT survival signalling and induces BAD-mediated apoptosis in colorectal cancer cells. Int J Cancer. 2007;121:2172–80.

117. Pellerito O, Notaro A, Sabella S, De Blasio A, Vento R, Calvaruso G, et al. WIN induces apoptotic cell death in human colon cancer cells through a block of autophagic flux dependent on PPARgamma down-regulation. Apoptosis. 2014;19:1029–42.

118. Fredriksson R, Lagerstrom MC, Lundin LG, Schioth HB. The G-protein-coupled receptors in the human genome form five main families. Phylogenetic analysis, paralogon groups, and fingerprints. Mol Pharmacol. 2003 Jun;63(6):1256–72.

119. Juneja J, Casey PJ. Role of G12 proteins in oncogenesis and metastasis. Br J Pharmacol. 2009 Sep;158(1):32–40.

120. Pérez-Gómez E, Andradas C, Flores JM, Quintanilla M, Paramio JM, Guzmán M, et al. The orphan receptor GPR55 drives skin carcinogenesis and is upregulated in human squamous cell carcinomas. Oncogene. 2012;32(20):2534–42.

121. Andradas C, Caffarel MM, Pérez-Gómez E, Salazar M, Lorente M, Velasco G, et al. The orphan G protein-coupled receptor GPR55 promotes cancer cell proliferation via ERK. Oncogene. 2010;30:245–52.

122. Hu G, Ren G, Shi Y. The putative cannabinoid receptor GPR55 promotes cancer cell proliferation. Oncogene. 2011;30:139–41.

123. Falasca M, Ferro R. Role of the lysophosphatidylinositol/GPR55 axis in cancer. Adv Biol Regul. 2016;60:88–93.

124. Piñeiro R, Maffucci T, Falasca M. The putative cannabinoid receptor GPR55 defines a novel autocrine loop in cancer cell proliferation. Oncogene. 2011;30:142–52.

125. Kargl J, Andersen L, Hasenöhrl C, Feuersinger D, Stancic A, Fauland A, et al. GPR55 promotes migration and adhesion of colon cancer cells indicating a role in metastasis. Br J Pharmacol. 2016;173(1):142–54.

126. Hofmann NA, Yang J, Trauger SA, Nakayama H, Huang L, Strunk D, et al. The GPR 55 agonist, L-α-lysophosphatidylinositol, mediates ovarian carcinoma cell-induced angiogenesis. Br J Pharmacol. 2015;172(16):4107–18.

127. Sutphen R, Xu Y, Wilbanks GD, Fiorica J, Grendys EC, LaPolla JP, et al. Lysophospholipids are potential biomarkers of ovarian cancer. Cancer Epidemiol Biomarkers Prev. 2004 Jul;13(7):1185–91.

128. Ford LA, Roelofs AJ, Anavi-Goffer S, Mowat L, Simpson DG, Irving AJ, et al. A role for L-α-lysophosphatidylinositol and GPR55 in the modulation of migration, orientation and polarization of human breast cancer cells. Br J Pharmacol. 2010 Jun;160(3):762–71.

129. Andradas C, Blasco-Benito S, Castillo-Lluva S, Dillenburg-Pilla P, Diez-Alarcia R, Juanes-Garcia A, et al. Activation of the orphan receptor GPR55 by lysophosphatidylinositol promotes metastasis in triple-negative breast cancer. Oncotarget. 2016 Jun 21;7(30):47565–75.

130. Huang L, Ramirez JC, Frampton G a, Golden LE, Quinn MA, Pae HY, et al. Anandamide exerts its antiproliferative actions on cholangiocarcinoma by activation of the GPR55 receptor. Lab Invest. 2011 Jul;91(7):1007–17.

131. Leyva-Illades D, DeMorrow S. Orphan G protein receptor GPR55 as an emerging target in cancer therapy and management. Cancer Manag Res. 2013;5:147–55.

132. Schütte M, Risch T, Abdavi-Azar N, Boehnke K, Schumacher D, Keil M, et al. Molecular dissection of colorectal cancer in pre-clinical models identifies biomarkers predicting sensitivity to EGFR inhibitors. Nat Commun. 2017;8:14262.

133. Mortazavi A, Williams BA, McCue K, Schaeffer L, Wold B. Mapping and quantifying mammalian transcriptomes by RNA-Seq. Nat Methods. 2008;5(7):621–8.

134. Neufert C, Becker C, Neurath MF. An inducible mouse model of colon carcinogenesis for the analysis of sporadic and inflammation-driven tumor progression. Nat Protoc. 2007;2:1998–2004.

135. Pfaffl MW. A new mathematical model for relative quantification in real-time RT-PCR. Nucleic Acids Res. 2001 May 1;29(9):e45.

136. Stančić A, Jandl K, Hasenöhrl C, Reichmann F, Marsche G, Schuligoi R, et al. The GPR55 antagonist CID16020046 protects against intestinal inflammation. Neurogastroenterol Motil. 2015;27(10):1432–45.

137. Heitzer E, Artl M, Filipits M, Resel M, Graf R, Weißenbacher B, et al. Differential survival trends of stage II colorectal cancer patients relate to promoter methylation status of PCDH10, SPARC, and UCHL1. Mod Pathol. 2014;27(6):906–15.

138. De Robertis M, Massi E, Poeta ML, Carotti S, Morini S, Cecchetelli L, et al. The AOM/DSS murine model for the study of colon carcinogenesis: From pathways to diagnosis and therapy studies. J Carcinog. 2011 Mar 24;10:9.

139. Tanaka T, Kohno H, Suzuki R, Yamada Y, Sugie S, Mori H. A novel inflammation-related mouse colon carcinogenesis model induced by azoxymethane and dextran sodium sulfate. Cancer Sci. 2003;94(11):965–73.

140. Chun E, Lavoie S, Michaud M, Gallini CA, Kim J, Soucy G, et al. CCL2 Promotes Colorectal Carcinogenesis by Enhancing Polymorphonuclear

Myeloid-Derived Suppressor Cell Population and Function. Cell Rep. 2015;12(2):244–57.

141. Katoh H, Wang D, Daikoku T, Sun H, Dey SK, DuBois RN. CXCR2-Expressing Myeloid-Derived Suppressor Cells Are Essential to Promote Colitis-Associated Tumorigenesis. Cancer Cell. 2013;24(5):631–44.

142. Sanchez-Lopez E, Flashner-Abramson E, Shalapour S, Zhong Z, Taniguchi K, Levitzki A, et al. Targeting colorectal cancer via its microenvironment by inhibiting IGF-1 receptor-insulin receptor substrate and STAT3 signaling. Oncogene. 2015;35(July):1–11.

143. Li H, Liu K, Boardman LA, Zhao Y, Wang L, Sheng Y, et al. Circulating Prostaglandin Biosynthesis in Colorectal Cancer and Potential Clinical Significance. EBioMedicine. 2015;2(2):165–71.

144. Keightley MC, Sales KJ, Jabbour HN. PGF2alpha-F-prostanoid receptor signalling via ADAMTS1 modulates epithelial cell invasion and endothelial cell function in endometrial cancer. BMC Cancer. 2010;10:488.

145. Galon J, Costes A, Sanchez-Cabo F, Kirilovsky A, Mlecnik B, Lagorce-Pagès C, et al. Type, Density, and Location of Immune Cells Within Human Colorectal Tumors Predict Clinical Outcome. Science (80-). 2006;313(5795):1960–4.

146. Vemuri VK, Makriyannis A. Medicinal Chemistry of Cannabinoids. Clin Pharmacol Ther. 2015;97(6):553–8.

147. Velasco G, Sánchez C, Guzmán M. Anticancer mechanisms of cannabinoids. Curr Oncol. 2016;23(March):S23–32.

148. Hall W, Christie M, Currow D. Cannabinoids and cancer: causation, remediation, and palliation. Lancet Oncol. 2005;6(1):35–42.

149. Chakravarti B, Ravi J, Ganju RK. Cannabinoids as therapeutic agents in cancer: current status and future implications. Oncotarget. 2014;5(15):5852–

72.

150. Abrams DI, Guzman M. Cannabis in Cancer Care. Clin Pharmacol Ther. 2015;97(6):575–86.

151. Fowler CJ. Delta 9 -Tetrahydrocannabinol and Cannabidiol as Potential Curative Agents for Cancer : A Critical Examination of the Preclinical Literature. Clin Pharmacol Ther. 2015;97(6):587–96.

152. Kramer JL. Medical Marijuana for Cancer. Cancer J Clin. 2015;65(2):109–22.

153. Ramer R, Hinz B. New Insights into antimetastatic and antiangiogenic effects of cannabinoids. Vol. 314, International Review of Cell and Molecular Biology. Elsevier Ltd; 2015. 43-116 p.

154. McAllister SD, Soroceanu L, Desprez PY. The Antitumor Activity of Plant-Derived Non-Psychoactive Cannabinoids. J Neuroimmune Pharmacol. 2015;10:255–67.

155. Flygare J, Sander B. The endocannabinoid system in cancer — Potential therapeutic target? Semin Cancer Biol. 2008;18:176–89.

156. Velasco G, Hernandez-Tiedra S, Davila D, Lorente M. The use of cannabinoids as anticancer agents. Prog Neuro-Psychopharmacology Biol Psychiatry. 2016;64:259–66.

157. Birdsall SM, Birdsall TC, Tims LA. The Use of Medical Marijuana in Cancer. Curr Oncol Rep. 2016;18(7).

158. Pyszniak M, Tabarkiewicz J, Łuszczki JJ. Endocannabinoid system as a regulator of tumor cell malignancy - biological pathways and clinical significance. Onco Targets Ther. 2016;9:4323–36.

159. Suzuki R, Kohno H, Sugie S, Nakagama H, Tanaka T. Strain differences in the susceptibility to azoxymethane and dextran sodium sulfate-induced colon carcinogenesis in mice. Carcinogenesis. 2006;27(1):162–9.

160. Lindau D, Gielen P, Kroesen M, Wesseling P, Adema GJ. The immunosuppressive tumour network: Myeloid-derived suppressor cells, regulatory T cells and natural killer T cells. Immunology. 2013;138(2):105–15.

161. Brown JR, DuBois RN. COX-2: A molecular target for colorectal cancer prevention. J Clin Oncol. 2005;23(12):2840–55.

162. Bosma MJ, Carroll AM. The SCID Mouse Mutant: Definition, Characterization, and Potential Uses. Annu Rev Immunol. 1991 Apr;9(1):323–50.

163. Notarnicola M, Tutino V, De Nunzio V, Dituri F, Caruso M, Giannelli G. Dietary ω-3 Polyunsaturated Fatty Acids Inhibit Tumor Growth in Transgenic ApcMin/+ Mice, Correlating with CB1 Receptor Up-Regulation. Int J Mol Sci. 2017;18(3):485.

164. Jones PA, Baylin SB. The Epigenomics of Cancer. Cell. 2007;128(4):683–92.

165. Ehrlich M. DNA hypomethylation in cancer cells. Epigenomics. 2009;1(2):239–59.

166. Schicho R, Storr M. Alternative targets within the endocannabinoid system for future treatment of gastrointestinal diseases. Can J Gastroenterol. 2011;25(7):377–83.

167. Schicho R, Storr M. Targeting the endocannabinoid system for gastrointestinal diseases: future therapeutic strategies. Expert Rev Clin Pharmacol. 2010;3(2):193–207.

168. Izzo AA, Camilleri M. Cannabinoids in intestinal inflammation and cancer. Pharmacol Res. 2009;60:117–25.

169. Patsos HA, Hicks DJ, Dobson RRH, Greenhough A, Woodman N, Lane JD, et al. The endogenous cannabinoid, anandamide, induces cell death in colorectal carcinoma cells: a possible role for cyclooxygenase 2. Gut. 2005;54:1741–50.